The Journal of Prosthetic Dentistry

Mechanical properties of 3D printed additive manufacturing dental prosthetic materials compared to subtractive and traditional techniques: a systematic review and meta-analysis.

--Manuscript Draft--

Manuscript Number:	
Article Type:	Systematic Review
Keywords:	Systematic review; Additive manufacturing; 3D printing, Prosthetic dentistry; Dental materials
Corresponding Author:	Stefano Pagano, Ph.D. School of Medicine, University of Perugia Perugia, ITALY
First Author:	Chiara Valenti, Dr.
Order of Authors:	Chiara Valenti, Dr.
	Maria Isabella Federici, Dr.
	Francesca Masciotti, Student
	Lorella Marinucci, Researcher
	Iva Xhimitiku, Phd
	Stefano Cianetti, Professor
	Stefano Pagano, Ph.D.
Abstract:	Statement of Problem Three-dimensional (3D) additive manufacturing (AM) printing is a rapidly evolving technology in dentistry, proposed as an alternative to classical subtractive manufacturing (MM) techniques. However there are still concerns about the use of AM technology instead of milling. Purpose A systematic review and meta-analysis was performed to evaluate the mechanical properties of 3D printing AM prosthetic materials compared to MM and traditional techniques. Material and methods Following the PRISMA statement, the electronic search of the literature was conducted using MEDLINE (via PubMed), Scopus and Web of Science. Inclusion criteria were: in vitro studies published in the last 5 years, in English or Italian with 3D AM printed dental prosthetic materials. Quality assessment was based on QATSDD. Data extraction was focused on dental prosthetic materials (ceramics, polymers and metals) and their mechanical properties evaluated: flexural strength (post-manufacturing and post ageing), fracture load, hardness, roughness, removable partial denture (RPD) fit accuracy, trueness (post-manufacturing and post ageing), marginal discrepancy and internal fit. Data considered homogenous were subjected to meta-analysis. Results From a total of 3624 eligible articles, 2855 studies have been selected and 76 studies included after full-text reading. Most of the studies that fit the inclusion criteria printed polymer-based restorative materials and used stereolitography (SLA) and digital light processing (DLP) printing techniques. No significant difference was detected in terms of hardness, roughness and marginal discrepancy between AM and MM technique. Milling techniques showed significantly higher values of flexural strength (Hedge's g = -3.88; 95% CI: -7.20 – -0.58; p = 0.02), also post-ageing (Hedge's g = -3.29; 95% CI: -

6.41 – -0.17; p = 0.04), compared to AM printing. Regarding fracture load, milled prostheses exhibited best values but in a non-significant way. While considering trueness, evaluated through the root main square (RMS) (Hedge's g = 1.12; 95% CI: -0.48 – 2.73; p = 0.17) and internal fit (Hedge's g = 2.29; 95% CI: -0.72 – 5.30; p = 0.14), additive manufactures demonstrated non-statistically significant higher values compared to milled ones.

Conclusions

AM is comparable in terms of mechanical properties to MM, in particular with polymeric materials, the flexural strength of AM-printed prostheses is lower than with conventional and subtractive techniques, as are the parameters of hardness and fracture load, while the marginal discrepancy is essentially comparable to subtractive and conventional techniques. Printing temporary restorations appears to be the best application of 3D AM printing in prosthetic dentistry.

Prof. Dr. Stephen F. Rosenstiel,

Editor-in-Chief

Journal of Prosthetic Dentistry

Dear Editor,

We are enclosing the results of our systematic review about the mechanical properties of 3D printing additive manufacturing entitled "**Mechanical properties of 3D printed additive manufacturing dental prosthetic materials compared to subtractive and traditional techniques: a systematic review and meta-analysis.**" and we hope that you will consider suitable for publication.

The 3D printing with additive manufacturing represents an important innovation in prosthetic dentistry, in term of printing small customized devices quickly and repeatably, maintaining printing accuracy with complex geometries. with less undercuts and post-productions, reducing material waste and costs compared to subtractive milling techniques.

Different problems are still present about its use as a substitute technology for traditional or subtractive methods. In particular, different studies focused on this aspect with different methodology and there are no clear-cut results in the literature. The present review was designed to evaluate the mechanical properties of prosthetic materials (ceramics, metals and polymers) printed with additive manufacturing, in terms of flexural strength (post-manufacturing and post-ageing), fracture load, hardness, roughness, removable partial denture (RPD) fit accuracy, trueness (post-manufacturing and post-ageing), marginal discrepancy and internal fit. In particular these parameters were also compared with results obtained using traditional or subtractive techniques.

The paper, new and original, has been submitted solely to Journal of Prosthetic Dentistry and not currently under consideration for publication elsewhere. All co-authors have read and approved the final draft and, if accepted, it will not be published elsewhere in the same form, in English or in any other language, including electronically. All of the named authors were involved in the work leading to the publication of the paper contributing to: Conceptualization: SP and CV; Data curation: CV and IX; Formal analysis: CV and MIF; Investigation: MIF and MF; Methodology: CV and MIF; Project administration: SC; Software: MF; Supervision: SP and LM; Validation: IX; Visualization: SC; Roles/Writing - original draft: CV and SP; Writing - review & editing: SP and LM.

All authors agree to the submission of the manuscript to Journal of Prosthetic Dentistry and declare any potential conflict of interest.

We thank you for your kind attention.

Yours sincerely,

Dr. Stefano PAGANO

Mechanical properties of 3D printed additive manufacturing dental prosthetic materials compared to subtractive and traditional techniques: a systematic review and meta-analysis.

Chiara Valenti[a], Maria Isabella Federici[b], Francesca Masciotti[c], Lorella Marinucci[d], Iva Xhimitiku[e], Stefano Cianetti[f], Stefano Pagano[g]*

a Dr., Department of Medicine and Surgery, Odontostomatological University Centre, University of Perugia, 06132 Perugia, Italy.

b Dr., Department of Medicine and Surgery, Odontostomatological University Centre, University of Perugia, 06132 Perugia, Italy.

c Student, Department of Medicine and Surgery, Odontostomatological University Centre, University of Perugia, 06132 Perugia, Italy.

d Researcher, Department of Medicine and Surgery, Section of Biosciences and Medical Embryology, University of Perugia, Perugia, Italy.

e Phd, University Centre for space studies and activities (CISAS) " Giuseppe Colombo", University of Padua, 35131, Padua, Italy

f Full Professor, Department of Medicine and Surgery, Odontostomatological University Centre, University of Perugia, 06132 Perugia, Italy.

g Researcher, Department of Medicine and Surgery, Odontostomatological University Centre, University of Perugia, 06132 Perugia, Italy.

* corresponding author: Stefano Pagano, stefano.pagano@unipg.it, +39 0755853514

Mechanical properties of 3D printed additive manufacturing dental prosthetic materials compared to subtractive and traditional techniques: a systematic review and meta-analysis.

ABSTRACT

Statement of Problem. Three-dimensional (3D) additive manufacturing (AM) printing is a rapidly evolving technology in dentistry, proposed as an alternative to classical subtractive manufacturing (MM) techniques. However there are still concerns about the use of AM technology instead of milling.

Purpose. A systematic review and meta-analysis was performed to evaluate the mechanical properties of 3D printing AM prosthetic materials compared to MM and traditional techniques.

Material and methods. Following the PRISMA statement, the electronic search of the literature was conducted using MEDLINE (via PubMed), Scopus and Web of Science. Inclusion criteria were: in vitro studies published in the last 5 years, in English or Italian with 3D AM printed dental prosthetic materials. Quality assessment was based on QATSDD. Data extraction was focused on dental prosthetic materials (ceramics, polymers and metals) and their mechanical properties evaluated: flexural strength (post-manufacturing and post ageing), fracture load, hardness, roughness, removable partial denture (RPD) fit accuracy, trueness (post-manufacturing and post ageing), marginal discrepancy and internal fit. Data considered homogenous were subjected to meta-analysis.

Results. From a total of 3624 eligible articles, 2855 studies have been selected and 76 studies included after full-text reading. Most of the studies that fit the inclusion criteria printed polymer-based restorative materials and used stereolitography (SLA) and digital light processing (DLP) printing techniques. No significant difference was detected in terms of hardness, roughness and marginal discrepancy between AM and MM technique. Milling techniques showed significantly higher values of flexural strength (Hedge's $g = -3.88$; 95% CI: -7.20 – -0.58; $p = 0.02$), also post-ageing (Hedge's $g = -3.29$; 95% CI: -6.41 – -0.17; $p = 0.04$), compared to AM printing.

Regarding fracture load, milled prostheses exhibited best values but in a non-significant way. While considering trueness, evaluated through the root main square (RMS) (Hedge's g = 1.12; 95% CI: -0.48 – 2.73; p = 0.17) and internal fit (Hedge's g = 2.29; 95% CI: -0.72 – 5.30; p = 0.14), additive manufactures demonstrated non-statistically significant higher values compared to milled ones.

Conclusions. AM is comparable in terms of mechanical properties to MM, in particular with polymeric materials, the flexural strength of AM-printed prostheses is lower than with conventional and subtractive techniques, as are the parameters of hardness and fracture load, while the marginal discrepancy is essentially comparable to subtractive and conventional techniques. Printing temporary restorations appears to be the best application of 3D AM printing in prosthetic dentistry.

INTRODUCTION

Three-dimensional (3D) printing is a rapidly evolving technology in dentistry[1] and consists of two different printing techniques: subtractive (CAD-CAM milling, MM) or additive manufacturing (AM) technique. In particular, MM technique is a machining process that starts with a solid block, a plate or a bar, and produces a machined part by removing material with a cutting tool. Depending on the characteristics of the machine, the subtractive cutting movements can be characterized by 3, 4 or 5 degrees of freedom, according to the complexity of the geometries produced. In dentistry, MM is now widely used for the fabrication of prosthetic components in different materials, such as zirconia (ZrO2), cobalt chrome alloy (Co-Cr), titanium (Ti), wax, resin, polymethyl methacrylate (PMMA) or polyetheretherketone (PEEK)[2].

The revolution brought about by the introduction of 3D printing is changing the landscape of modern manufacturing, and the new frontiers of 3D printing consist of AM technology.

AM technique is proposed as an alternative to classical subtractive manufacturing principles and is now being used in a number of different sectors, from industrial to healthcare. AM printing allows small customized devices to be manufactured quickly and repeatably, while maintaining printing accuracy even with complex geometries; it also ensures less undercuts and reduced post-production, thanks to the smooth surface of the printed objects. In addition, less material waste further reduces costs compared to MM[3]. This type of manufacturing allows the realization of complex custom-made parts following the same principle: a digital model is transformed into a physical object three-dimensionally by adding material one layer at a time. So the printing process always starts with a digital 3D model, usually obtained with CAD software, which is processed by further "slicing" software that breaks down the designed object into thin two-dimensional layers and transforms it into a set of machine language instructions so that it can be interpreted and executed by the printer[4]. 3D printers can be classified into seven different groups based on the construction of the layers that make up an item: material extrusion (i.e. fused deposition modelling, FDM), sheet lamination (i.e. LOM and UAM), vat polymerization (i.e. stereolithography, SLA and digital light processing, DLP), powder bed fusion (i.e. selective laser sintering, SLS, direct metal laser sintering DMLS and selective laser melting, SLM), material jetting (MJ), binder jetting (BJ) and direct energy deposition (i.e. LENS and LBMD)[5].

There are still concerns about the use of AM technology compared to milling. In terms of precision, milling is still the most accurate technique today, but to produce small items with more complex shapes, the choice is AM, which can solve the problem of undercuts. On the other hand, the larger the size of the workpiece to be produced, the more cost-effective it is to use milling, because less material has to be removed[6]. However, AM is a technology that is expected to provide major innovations in the healthcare, medical and dental fields. In particular, the integration of AM printing into various sectors of modern dentistry has enabled the manufacture of prosthetic, orthodontic and surgical devices, with different types of materials such as polymers, ceramics and metal alloys, with high biological and mechanical performance, but the accuracy of printed prostheses is affected by the different types of AM printing machines[7,8].

However, further investigations are needed to improve their long-term mechanical performance in order to fully satisfy the requirements of definitive prosthetic restorations. Mechanical properties stability, biocompatibility and the possibility of using the printed manufactures under intraoral conditions for a period longer than 12 months are of extremely relevance[9].

This systematic review aims to investigate and compare the various types of materials used in different 3D printing AM techniques in prosthetic dentistry, evaluating their mechanical properties in terms of: flexural strength (post-manufacturing and post-ageing), fracture load, hardness, roughness, removable partial denture (RPD) fit accuracy, trueness (post-manufacturing and post-ageing), marginal discrepancy and internal fit, and their clinical application, compared to traditional and MM techniques.

MATERIALS AND METHODS

Protocol and registration

The protocol of this review was based on the PRISMA-P systematic review protocols[10] and is available online at: DOI 10.17605/OSF.IO/4CYQH. This systematic review was carried out according to the PRISMA statement[11] and checklist (Supplementary Fig. 1). A PRISMA flow diagram (Fig. 1) was used to represent the included or excluded studies.

This review was conducted based on the following question: “What are the mechanical properties of dental prosthetic materials obtained with AM printing technique, compared to traditional and subtractive methods?". The research team constructed this question according to the PICOS strategy format[12] (Table 1).

Inclusion and exclusion criteria

The eligibility criteria included: *in vitro* studies published in the last 5 years, in English or Italian with 3D AM printed dental prosthetic materials.

Exclusion criteria: *in vivo* clinical studies, qualitative studies, case reports, conferences, commentaries, editorials, surveys, guidelines, reviews and meta-analysis or discussion and opinion pieces; *ex vivo* models and studies on animals, *in vitro* studies with other types of 3D printed dental prosthetic materials and/or non-specified 3D printing AM dental prosthesis materials or investigating materials used in orthodontics and surgery. Studies with no full-text available were also excluded.

Strategy search

The searched databases included MEDLINE (via PubMed), Scopus and Web of Science. Only studies published within the last 5 years (from 12/05/2016 to 12/05/2021) and in English or Italian were considered. The search strategy was outlined based on PubMed MeSH terms and adapted for each database. The search process was performed by two different reviewers (CV and MIF) and is showed in Supplementary Table 1. The electronic searches were followed by a manual search of the reference list of the included articles.

Data collection process: study selection, synthesis, extraction and management

All titles of the articles initially retrieved in the search were selected following the eligibility criteria, and duplicates were eliminated. The selection of the study was performed by three independent reviewers (CV, MIF and FM). The titles were read and those indicating no relevance were excluded. Articles compatible with the inclusion criteria were selected for further examinations and abstracts were screened. The full texts of potentially eligible studies were then reviewed against the inclusion/exclusion criteria independently by the reviewers and any disagreement resolved by consultation with the other authors. The PRISMA flow diagram (Fig.1) was used to report the included and excluded studies.

Three reviewers (CV, MIF and FM) independently extracted data from each article, any discrepancy was identified and resolved through discussion (with a fourth reviewer where necessary). Scientific and technical information were collected into two evidence tables with Microsoft Office Excel, Table 2 including: Author(s) and year of publication, mechanical test types (Flexural strength post-manufacturing and post ageing, fracture load, hardness, roughness, RPD fit accuracy, trueness post-manufacturing and post ageing, marginal discrepancy and internal fit), quality assessment score and funding source(s), and Table 3 including: Author(s) and year of publication, specimen materials and size characteristics (polymers, metals and ceramics), details of the intervention (type of AM technique), control, mechanical properties evaluated and data and principal findings.

Statistical analysis

Since all variables were continuous, they were described in the form of a mean ± standard deviation. Statistical analysis was conducted using the Stata17 statistical software. A 95% confidence interval was used to describe the characteristics of the prostheses produced with AM compared to those produced with milling technique; a $p \leq 0.05$ was considered statistically significant. Since all variables were continuous, Hedges *g* measure was calculated, thus measuring the difference between the experimental group and the control group in terms of standard deviation. The results were also visualized graphically using the forest plots. The heterogeneity of the included studies was assessed by the I^2 statistic: it was considered low with

$I^2 \leq 25\%$, moderate with $25\% < I^2 < 75\%$ and high with $I^2 \geq 75\%$. A fixed-effects model was used for $I^2 = 0\%$, while the statistical analysis was conducted using a random-effects model with $I^2 > 0\%$.

Quality assessment

The quality assessment was performed independently by two reviewer (CV and FM) for each included study using Quality Assessment Tool for Studies with Diverse Designs (QATSDD tool)[13]. A score from 0 (incomplete information) to 3 point (complete information) was given considering the QATSDD, with 14 item for qualitative or quantitative study and 16- item with mixed method, related to: theoretical framework, aims/objectives, setting, sample size, representative sample of target group of a reasonable size, procedure for data collection, rationale for choice of data collection tool(s), detailed recruitment data, statistical assessment of reliability and validity of measurement tool(s) (quantitative only), research question and method of data collection (quantitative only), research question and format and content of data collection tool (qualitative only), research question and method of analysis, analytical method selected, assessment of reliability of analytical process (qualitative only), evidence of user involvement in design, strengths and limitations.

RESULTS

Search results and characteristics of selected articles

The flow diagram of study selection (Fig. 1) shows a total of 3624 potentially eligible articles following the electronic screening strategy search (PubMed n= 2219, Scopus n = 1107, Web of Science n = 298). Duplicates removal led to the elimination of 1036 articles, title/abstract screening was completed on 2588 studies resulting in 2464 non-eligible studies being excluded at this stage and 124 studies progressing to full-text review. Finally, 76 studies were included for full-text data extraction.

Year and country of publication

6 articles were published in 2016[14-19], 9 in 2017[20-28], 12 in 2018[29-40], 17 in 2019[41-57], 22 in 2020[58-79], and 10 publications up to the search date in 2021[80-89]. Table 2 provides details of the year of publication.

34 papers had a setting in Asia, with 13 studies were performed in South Korea[15,17,18, 22,24,31, 53,55,61,68,71,72,78] , 10 in Japan[16,32,42,51,52,65,70,85,87,88],8 in China[27,30,34,39,44,50,80,89] , 2 in Turkey[54,84] and 1 in Lebanon[21]. 26 studies were published in Europe: 9 in Germany[20,57,79,66,73,81-83,86] , 2 in Switzerland[46,62] , 2 in Netherlands[14,23] , 3 in Sweden[37,40,49] , 3 in Spain[29,33,48] , 2 in France[25,69] , 1 in Portugal[58], 1 in Monaco[76] , 1 in Italy[60] , 1 in Croatia[64] and 1 in Norway[35]. The setting of 11 articles was in America, with 10 studies performed in the USA[19,26,38,41,47,56,63,67, 74,75] , 1 in Brazil[77] . While, 2 studies were published in Africa, 1 in Egipt[28] and 1 in Iran[36] and only 3 studies in Oceania, in New Zealand[43,45,59] . Table 2 provides details of the country of publication.

Quality assessment score

According to the 14-item quality assessment tool, all the 76 studies included met the criteria, resulting reliable. The highest score was 41/42 points[67,68,85] and the lowest was 30/42 points[25,40].

AM printing techniques

Considering the AM 3D printing techniques: in 24 studies the authors used SLA technology[14-16,18,21,25,26,39,48-50,53,54,56,67,69,71,73,75,77,78,80,85,89] , in 19 DLP[16,17,19,23,28,30,31,36,45,47,59,61,63,66,68,76,83,85,86] , in 12 SLM[15,20,24,27,33,35,37,38,41,44,60,74] , in 6 SLS[51,52,55,70,72,87] , in 5 FDM[29,30,34,42,65] , in 3 UV light curing[32,64,84] , in 2 direct laser metal sintering (DLMS)[37,43], in 2 PJ[22,88] , in 2 electron beam melting technology (EBM)[33,37], in 2 fused filament fabrication (FFF)[81,82] , in 2 fused layer modeling (FLM)[57,79] , in 1 robocasting[58] , in 1 lithography-based ceramic manufacturing process (LCM)[62], in 1 indirect rapid protoryping[46] , in 1 thermofusion (CX)[16] , in 1 MJ[85] , in 1 direct metal laser melting (DMLM)[37] , in 1 multi-jet modeling (MJM)[16] and only in 1 study the AM technique was not specified[40] . Table 3 details the AM printing techniques.

Material types

From the 76 studies included in this review, 14 studies printed ceramic structures, in particular 9 studies printed zirconia specimen[39,48,50,56,58,62,75,78,80] , 1 study printed lithium[21] and 4 studies alumina[25,54,69,78]. 43 studies printed polymer-based materials[14,16-18,22,23,26,28,31,32,36,42,45-47,49,53,57,59,61,63,64-68,71,73,76,77,79,81-86,88,89] , in particular 6 studies printed PEEK[29,30,34,57,79,82] , 2 studies printed PMMA[17,59] and 3 studies printed PLA[29,30,34]. 23 studies printed metallic alloys: 18 studies printed Co-Cr alloy[15,20,24,27,35,37,38,40,41,43,44,51,52,55,60,72,74,87] , 4 studies printed Titanium[33,37,40,70] and 1 study gold[19]. Table 3 details the type of materials printed.

Mechanical properties evaluated

Regarding the mechanical properties evaluated, 15 studies analyzed flexural strength[25,26,45,50,54,55,59,64,69,72,75,81,82,83,86] with the 3- or 4-point bending test using a universal testing machines. The characteristics of the studies are described in Table 3. For the meta-analysis on flexural strength 5 studies were considered[25,54,59,64,75] and 3 studies on flexural strength post ageing[59,75,86] . MM showed higher values in a statistically significant way compared to AM in terms of flexural strength (Hedge's g = -3.88; 95% CI: -7.20 – -0.58; P= 0.02) (Fig. 2) and flexural strength post ageing (Hedge's g = -3.29; 95% CI: -6.41 – -0.17; P = 0.04) (Fig. 3). The I^2 test showed a high degree of heterogeneity. (Supplementary Fig. 2 and 3)

Fracture load was investigated in 9 studies[45,54,56,57,59,62,69,75,76] and only 4 studies were included in the meta-analysis[56,62,75,76] , considering the force required to create the first fracture.

The characteristics of the studies are described in Table 3. MM techniques exhibited favorable characteristics in terms of fracture load compared to AM, but not in a statistically significant way (Hedge's g = -1.47; 95% CI = -5.41 – 2.47; P = 0.46) (Fig. 4). The I^2 test showed a high degree of heterogeneity (Supplementary Fig. 4).

9 studies analyzed hardness[35,43,54,58,64,69,77,79,81] and only 3 studies that used the same measurement Vickers scale were included in the meta-analysis[35,54,58] . Prpić 2020[64] and Prechtel 2020[79] were excluded because used respectively Brinell and Martens scale and Barazanchi 2019[43] was excluded because did not specify the measurement scale. The characteristics of the studies are described in Table 3. No significant difference was detected when comparing AM and MM techniques in terms of hardness values (Hedges'g = 7.69; 95% CI: -2.07 – 17.46; P = 0.12) (Fig. 5). The I^2 test showed a high degree of heterogeneity (Supplementary Fig. 5).

Surface roughness was investigated on 10 studies[16,35,53,58,65,66,70,77,74,86] and only 2 studies were included in the meta-analysis because considered average roughness (Ra) parameter[35,74]. The characteristics of the studies are described in Table 3. No significant difference was observed between AM and MM (Hedge's g = 3.71; 95% CI: -0.29 – 7.71; P = 0.07) (Fig. 6). The I^2 test showed a high degree of heterogeneity (Supplementary Fig. 6).

5 studies evaluated RPD fit accuracy[20,27,38,44,52] but they were not included in a meta-analysis because the authors evaluated different RPD structures. The characteristics of the studies are described in Table 3.

Trueness was analyzed in 22 studies[14,15,16,26,28,31,32,37,39,42,46,51,53,65,67,71,73,78,80,85,87,88] . 6 studies were included in the meta-analysis because evaluated trueness with the root main square (RMS) formula[39,46,73,78,80,85] and only 2 studies analyzed trueness with RMS formula post-ageing[46,73] . The characteristics of the studies are described in Table 3. AM showed better characteristics in terms of trueness compared to MM but in a non-statistically significant way

(Hedge’s g = 1.12; 95% CI: -0.48 – 2.73; P = 0.17) (Fig. 7), while post ageing no significant difference was detected between AM and MM (Hedge’s g = 3.88; 95% CI = -3.63 – 11.39; P = 0.31) (Figure 8). The I^2 test showed a high degree of heterogeneity (Supplementary Fig. 7 and 8).

20 studies examined marginal discrepancy[17-19,21-24,29,30,41,47,48,50,60,63,67,68,78,80,89] and 7 studies were included in the meta-analysis[19,21,23,30,63,78,89]. Peng 2019[47] and Mai 2017[22] were excluded because did not reported exact data. The characteristics of the studies are described in Table 3. No significant difference was reported in terms of marginal discrepancy between AM and MM (Hedge’s g = 0.85; 95% CI: -0.14 – 1.84; P = 0.09) (Fig. 9). The I^2 test showed a high degree of heterogeneity. (Supplementary Fig. 9).

Internal fit was examined in 23 studies[17,20-24,30,34,36,40,41,44,47-50,63,65,67,68,70,78,89] and 7 studies were included in the meta-analysis[21,22,23,30,47,63,78]. Revilla-Leon 2019[48] was excluded because did not specify internal fit data. The characteristics of the studies are described in Table 3. AM prostheses had better values in terms of internal fit compared to milled ones, but in a non-statistically significant way (Hedge’s g = 2.29; 95% CI: -0.72 – 5.30; P = 0.14) (Fig. 10). The I^2 test showed a high degree of heterogeneity (Supplementary Fig. 10).

The main weakness in terms of bias is linked to the small number of studies considered in each meta-analysis. This means that the funnel plot often presents "uncovered" areas or poor symmetry. The presence of studies widely outside the funnel also confirms what has already emerged from the corresponding forest plots (Supplementary Fig. 2-10)

DISCUSSION

3D AM printing represents an approach to the digitalization of the laboratory process in order to create custom-made items with standardized procedures, simplifying the manufacturing process but, at the same time, providing a final quality comparable to traditional and subtractive techniques. Despite the rapid development of 3D printing in the sanitary sector, the use of this new technology in dentistry is still limited to mainly surgical and orthodontic applications[3] for several reasons, first of all related to the costs of the machinery and the technology itself, but also to the novelty of the technique which is not yet widespread and some discordances and heterogeneous results in the literature, especially in terms of the types of materials and manufactures analyzed (i.e. crowns, bridges, inlays, onlays, denture and frameworks)[90].

This systematic review aimed to carry out an analysis of the mechanical properties, related to clinical application, of dental prosthetic materials from *in vitro* studies comparing AM printing and MM technique. No statistically significant differences were found in terms of hardness, roughness and marginal discrepancy. Considering fracture load, milled prostheses exhibited best values but in a non-significant way. However, a significant difference was observed with the MM technique regarding both flexural strength and flexural strength post ageing. While considering trueness and internal fit AM demonstrated non-statistically significant higher values.

An AM-printed product is constructed by the deposition of consecutive layers, so that certain printing parameters, such as orientation and construction angle, may influence the trueness of the final product[91]. Given the variability in terms of the mechanical tests performed and the composition of the materials selected by the authors, the AM printed structures showed heterogeneous mechanical performances.

Since in the literature many authors have taken conventional and MM techniques as control[2], we decided to focus in this review on the comparison between the data related to these techniques and found that for AM-printed ceramics, the results in terms of flexural strength compared to traditional and MM techniques are discordant. In fact, Li et al.[50] shows no significant difference, Dehurtevent et al.[69] and Revilla-León et al.[75] report an increase in flexural strength, while Ucar et al.[54] and Dehurtevent et al.[25] indicate a reduction in flexural strength. In terms of fracture load, only Revilla-León et al.[75] noted an increase. As far as hardness is concerned, only one study[54] reported an increase for ceramic materials. While roughness is generally increased compared to traditional and MM techniques. The results are discordant both because the authors used different ceramic materials (mostly different product types of zirconia were used), but above all, the variability is linked to the different shapes of the samples: veneers, crowns, inlays or geometrical specimens.

With polymeric materials, however, the flexural strength of AM-printed prostheses is statistically lower than with conventional and MM techniques, as are the parameters of hardness and fracture load[92]. Only one work[83] showed an increase in flexural strength, even post-ageing, while fracture load and hardness were reduced. The marginal discrepancy is basically comparable to MM and conventional techniques with both ceramic and resin materials. This justifies why they are commonly used for temporary crowns and bridges, because rigidity and fracture toughness are not sufficient to support complex masticatory forces[93].

A general increase in fit accuracy was found with the additive technique in RPD clasps, with AM-printed metal materials, although the roughness generally increased. While an increase in hardness was found in only one study[43]. As for the trueness parameter, there is an increase in all types of materials after printing with the AM technique, and the internal fit is also higher than with the MM technique regardless of the material used for AM printing. This is why, to date, the printing of temporary restorations such as crowns and bridges, as well as complete dentures, appears to be the best application of 3D AM printing in prosthetic dentistry[94].

Despite the low risk of bias in the included studies, the results observed in this systematic review must be interpreted carefully. The high heterogeneity in the meta-analysis can be justified because only *in vitro* studies, which can have different methodological procedures, were considered. Therefore, the limitations of this systematic review include the evaluation of only highly heterogeneous *in vitro* studies, even though the inclusion criteria established the highest possible similarity between the included studies. However, more comparative studies are needed, especially considering clinical use.

In only 6 studies dental structures were printed for implant-prosthetic purposes[17,33,40,48,56,67], it would be important and of interest to have more data regarding this field of application. It may also be necessary in the future to compare the data found with further clinical investigations, *in vivo* clinical studies on patients are few[95], as follow-up and large sample sizes are required. It is clear that the biological characteristics of 3D AM-printed materials in human oral tissues is another question to be considered for further research, as *in vitro* works on oral cell populations is lacking in the literature.

Limitations

1. Variability of the sample sizes in different works,
2. Great difference in the type of mechanical tests carried out by the authors,
3. Differences in the type of materials selected to conduct the same test,
4. Shape and size of the additively printed specimens.

CONCLUSIONS

Starting from the limitations of this study, the analysis of the literature on this subject showed a substantial correspondence of the mechanical properties between MM and AM, a sign of the reliability of this new technology in dentistry. The milling technique seems to present better results only in relation to flexural strength and flexural strength post-ageing.

REFERENCES:

1. Tieh MT, Waddell JN, Choi JJE. Optical and mechanical properties of conventional, milled and 3D-printed denture teeth. J Mech Behav Biomed Mater. 2022;126:105061.

2. de Oliveira Limírio JPJ, Gomes JML, Alves Rezende MCR, Lemos CAA, Rosa CDDRD, Pellizzer EP. Mechanical properties of polymethyl methacrylate as a denture base: Conventional versus CAD-CAM resin - A systematic review and meta-analysis of in vitro studies. J Prosthet Dent. 2021;S0022-3913(21)00166-9

3. Tian Y, Chen C, Xu X, et al. A Review of 3D Printing in Dentistry: Technologies, Affecting Factors, and Applications. Scanning. 2021;2021:9950131.

4. Rekow ED. Digital dentistry: The new state of the art - Is it disruptive or destructive?. Dent Mater. 2020;36(1):9-24.

5. Khorsandi D, Fahimipour A, Abasian P, et al. 3D and 4D printing in dentistry and maxillofacial surgery: Printing techniques, materials, and applications. Acta Biomater. 2021;122:26-49.

6. Jockusch J, Özcan M. Additive manufacturing of dental polymers: An overview on processes, materials and applications. Dent Mater J. 2020;39(3):345-354.

7. Gonzalez P, Schwarzer E, Scheithauer U, Kooijmans N, Moritz T. Additive Manufacturing of Functionally Graded Ceramic Materials by Stereolithography. J Vis Exp. 2019;(143):10.3791/57943.

8. Laverty DP, Thomas MBM, Clark P, Addy LD. The Use of 3D Metal Printing (Direct Metal Laser Sintering) in Removable Prosthodontics. Dent Update. 2016;43(9):826-835.

9. Jockusch J, Özcan M. Additive manufacturing of dental polymers: An overview on processes, materials and applications. Dent Mater J. 2020;39(3):345-354.

10. Moher D, Shamseer L, Clarke M, Ghersi D, Liberati A, Petticrew M, Shekelle P, Stewart LA. Preferred Reporting Items for Systematic Review and Meta-Analysis Protocols (PRISMA-P) 2015 statement. Syst Rev. 2015;4(1):1.

11. Page MJ, McKenzie JE, Bossuyt PM, Boutron I, Hoffmann TC, Mulrow CD, et al. The PRISMA 2020 statement: an updated guideline for reporting systematic reviews. BMJ 2021;372:n71.

12. Maia LC, Antonio AG, Systematic reviews in dental research. A guideline, J. Clin. Pediatr. Dent. 2012; 37:117–124.

13. Sirriyeh R, et al. Reviewing studies with diverse designs: the development and evaluation of a new tool. J Eval Clin Pract. 2012;18(4):746–52

14. Alharbi N, Osman R, Wismeijer D. Effects of build direction on the mechanical properties of 3D-printed complete coverage interim dental restorations. J Prosthet Dent. 2016;115(6):760-767.

15. Bae EJ, Jeong ID, Kim WC, Kim JH. A comparative study of additive and subtractive manufacturing for dental restorations. J Prosthet Dent. 2017;118(2):187-193.

16. Ishida Y, Miyasaka T. Dimensional accuracy of dental casting patterns created by 3D printers. Dent Mater J. 2016;35(2):250-256.

17. Park JY, Jeong ID, Lee JJ, Bae SY, Kim JH, Kim WC. In vitro assessment of the marginal and internal fits of interim implant restorations fabricated with different methods. J Prosthet Dent. 2016;116(4):536-542.

18. Kim DY, Jeon JH, Kim JH, Kim HY, Kim WC. Reproducibility of different arrangement of resin copings by dental microstereolithography: Evaluating the marginal discrepancy of resin copings. J Prosthet Dent. 2017;117(2):260-265.

19. Munoz S, Ramos V Jr, Dickinson DP. Comparison of margin discrepancy of complete gold crowns fabricated using printed, milled, and conventional hand-waxed patterns. J Prosthet Dent. 2017;118(1):89-94.

20. Arnold C, Hey J, Schweyen R, Setz JM. Accuracy of CAD-CAM-fabricated removable partial dentures. J Prosthet Dent. 2018;119(4):586-592.

21. Homsy FR, Özcan M, Khoury M, Majzoub ZAK. Marginal and internal fit of pressed lithium disilicate inlays fabricated with milling, 3D printing, and conventional technologies. J Prosthet Dent. 2018;119(5):783-790.

22. Mai HN, Lee KB, Lee DH. Fit of interim crowns fabricated using photopolymer-jetting 3D printing. J Prosthet Dent. 2017;118(2):208-215.

23. Alharbi N, Alharbi S, Cuijpers VMJI, Osman RB, Wismeijer D. Three-dimensional evaluation of marginal and internal fit of 3D-printed interim restorations fabricated on different finish line designs. J Prosthodont Res. 2018;62(2):218-226.

24. Kim DY, Kim JH, Kim HY, Kim WC. Comparison and evaluation of marginal and internal gaps in cobalt-chromium alloy copings fabricated using subtractive and additive manufacturing. J Prosthodont Res. 2018;62(1):56-64.

25. Dehurtevent M, Robberecht L, Hornez JC, Thuault A, Deveaux E, Béhin P. Stereolithography: A new method for processing dental ceramics by additive computer-aided manufacturing. *Dent Mater*. 2017;33(5):477-485.

26. Tahayeri A, Morgan M, Fugolin AP, et al. 3D printed versus conventionally cured provisional crown and bridge dental materials. Dent Mater. 2018;34(2):192-200.

27. Ye H, Ning J, Li M, et al. Preliminary Clinical Application of Removable Partial Denture Frameworks Fabricated Using Computer-Aided Design and Rapid Prototyping Techniques. Int J Prosthodont. 2017;30(4):348-353.

28. Osman RB, Alharbi N, Wismeijer D. Build Angle: Does It Influence the Accuracy of 3D-Printed Dental Restorations Using Digital Light-Processing Technology?. Int J Prosthodont. 2017;30(2):182-188.

29. Molinero-Mourelle P, Canals S, Gómez-Polo M, Solá-Ruiz MF, Del Río Highsmith J, Viñuela AC. Polylactic Acid as a Material for Three-Dimensional Printing of Provisional Restorations. Int J Prosthodont. 2018;31(4):349-350.

30. Liu Y, Ye H, Wang Y, Zhao Y, Sun Y, Zhou Y. Three-Dimensional Analysis of Internal Adaptations of Crowns Cast from Resin Patterns Fabricated Using Computer-Aided Design/Computer-Assisted Manufacturing Technologies. Int J Prosthodont. 2018;31(4):386–393.

31. Sim JY, Jang Y, Kim WC, Kim HY, Lee DH, Kim JH. Comparing the accuracy (trueness and precision) of models of fixed dental prostheses fabricated by digital and conventional workflows. J Prosthodont Res. 2019;63(1):25-30.

32. Tasaka A, Matsunaga S, Odaka K, et al. Accuracy and retention of denture base fabricated by heat curing and additive manufacturing. J Prosthodont Res. 2019;63(1):85-89.

33. Revilla-León M, Ceballos L, Martínez-Klemm I, Özcan M. Discrepancy of complete-arch titanium frameworks manufactured using selective laser melting and electron beam melting additive manufacturing technologies. J Prosthet Dent. 2018;120(6):942-947.

34. Deng K, Chen H, Zhao Y, Zhou Y, Wang Y, Sun Y. Evaluation of adaptation of the polylactic acid pattern of maxillary complete dentures fabricated by fused deposition modelling technology: A pilot study. PLoS One. 2018;13(8):e0201777.

35. Øilo M, Nesse H, Lundberg OJ, Gjerdet NR. Mechanical properties of cobalt-chromium 3-unit fixed dental prostheses fabricated by casting, milling, and additive manufacturing. J Prosthet Dent. 2018;120(1):156.e1-156.e7.

36. Eftekhar Ashtiani R, Nasiri Khanlar L, Mahshid M, Moshaverinia A. Comparison of dimensional accuracy of conventionally and digitally manufactured intracoronal restorations. J Prosthet Dent. 2018;119(2):233-238.

37. Braian M, Jönsson D, Kevci M, Wennerberg A. Geometrical accuracy of metallic objects produced with additive or subtractive manufacturing: A comparative in vitro study. Dent Mater. 2018;34(7):978-993.

38. Soltanzadeh P, Suprono MS, Kattadiyil MT, Goodacre C, Gregorius W. An In Vitro Investigation of Accuracy and Fit of Conventional and CAD/CAM Removable Partial Denture Frameworks. J Prosthodont. 2019;28(5):547-555.

39. Wang W, Yu H, Liu Y, Jiang X, Gao B. Trueness analysis of zirconia crowns fabricated with 3-dimensional printing. J Prosthet Dent. 2019;121(2):285-291.

40. Svanborg P, Eliasson A, Stenport V. Additively Manufactured Titanium and Cobalt-Chromium Implant Frameworks: Fit and Effect of Ceramic Veneering. Int J Oral Maxillofac Implants. 2018;33(3):590-596.

41. Al Maaz A, Thompson GA, Drago C, An H, Berzins D. Effect of finish line design and metal alloy on the marginal and internal gaps of selective laser melting printed copings. J Prosthet Dent. 2019;122(2):143-151.

42. Alsandi Q, Ikeda M, Nikaido T, et al. Evaluation of mechanical properties of new elastomer material applicable for dental 3D printer. J Mech Behav Biomed Mater. 2019;100:103390.

43. Barazanchi A, Li KC, Al-Amleh B, Lyons K, Waddell JN. Adhesion of porcelain to three-dimensionally printed and soft milled cobalt chromium. J Prosthodont Res. 2020;64(2):120-127.

44. Chen H, Li H, Zhao Y, Zhang X, Wang Y, Lyu P. Adaptation of removable partial denture frameworks fabricated by selective laser melting. J Prosthet Dent. 2019;122(3):316-324.

45. Choi JJE, Uy CE, Plaksina P, Ramani RS, Ganjigatti R, Waddell JN. Bond Strength of Denture Teeth to Heat-Cured, CAD/CAM and 3D Printed Denture Acrylics. J Prosthodont. 2020;29(5):415-421.

46. Kalberer N, Mehl A, Schimmel M, Müller F, Srinivasan M. CAD-CAM milled versus rapidly prototyped (3D-printed) complete dentures: An in vitro evaluation of trueness. J Prosthet Dent. 2019;121(4):637-643.

47. Peng CC, Chung KH, Yau HT, Ramos V Jr. Assessment of the internal fit and marginal integrity of interim crowns made by different manufacturing methods. J Prosthet Dent. 2020;123(3):514-522.

48. Revilla-León M, Ceballos L, Özcan M. Implant Prosthodontic Discrepancy of Complete-Arch Co-Cr Implant Frameworks Manufactured Through Selective Laser Melting Additive Manufacturing Technology Using a Coordinate Measuring Machine. Int J Oral Maxillofac Implants. 2019;34(3):698–707.

49. Mahmood DJH, Braian M, Larsson C, Wennerberg A. Production tolerance of conventional and digital workflow in the manufacturing of glass ceramic crowns. Dent Mater. 2019;35(3):486-494.

50. Li R, Wang Y, Hu M, et al. Strength and Adaptation of Stereolithography-Fabricated Zirconia Dental Crowns: An In Vitro Study. Int J Prosthodont. 2019;32(5):439-443.

51. Tasaka A, Shimizu T, Kato Y, et al. Accuracy of removable partial denture framework fabricated by casting with a 3D printed pattern and selective laser sintering. J Prosthodont Res. 2020;64(2):224-230.

52. Tasaka A, Kato Y, Odaka K, et al. Accuracy of Clasps Fabricated with Three Different CAD/CAM Technologies: Casting, Milling, and Selective Laser Sintering. Int J Prosthodont. 2019;32(6):526-529.

53. Shim JS, Kim JE, Jeong SH, Choi YJ, Ryu JJ. Printing accuracy, mechanical properties, surface characteristics, and microbial adhesion of 3D-printed resins with various printing orientations. J Prosthet Dent. 2020;124(4):468-475.

54. Uçar Y, Aysan Meriç İ, Ekren O. Layered Manufacturing of Dental Ceramics: Fracture Mechanics, Microstructure, and Elemental Composition of Lithography-Sintered Ceramic. J Prosthodont. 2019;28(1):e310-e318.

55. Wang H, Lim JY. Metal-ceramic bond strength of a cobalt chromium alloy for dental prosthetic restorations with a porous structure using metal 3D printing. Comput Biol Med. 2019;112:103364.

56. Zandinejad A, Methani MM, Schneiderman ED, Revilla-León M, Bds DM. Fracture Resistance of Additively Manufactured Zirconia Crowns when Cemented to Implant Supported Zirconia Abutments: An in vitro Study. J Prosthodont. 2019;28(8):893-897.

57. Prechtel A, Stawarczyk B, Hickel R, Edelhoff D, Reymus M. Fracture load of 3D printed PEEK inlays compared with milled ones, direct resin composite fillings, and sound teeth. Clin Oral Investig. 2020;24(10):3457-3466.

58. Branco AC, Silva R, Jorge H, et al. Tribological performance of the pair human teeth vs 3D printed zirconia: An in vitro chewing simulation study. J Mech Behav Biomed Mater. 2020;110:103900.

59. Choi JJE, Ramani RS, Ganjigatti R, Uy CE, Plaksina P, Waddell JN. Adhesion of Denture Characterizing Composites to Heat-Cured, CAD/CAM and 3D Printed Denture Base Resins. J Prosthodont. 2021;30(1):83-90.

60. Di Fiore A, Savio G, Stellini E, Vigolo P, Monaco C, Meneghello R. Influence of ceramic firing on marginal gap accuracy and metal-ceramic bond strength of 3D-printed Co-Cr frameworks. J Prosthet Dent. 2020;124(1):75-80.

61. Hsu CY, Yang TC, Wang TM, Lin LD. Effects of fabrication techniques on denture base adaptation: An in vitro study. J Prosthet Dent. 2020;124(6):740-747.

62. Ioannidis A, Bomze D, Hämmerle CHF, Hüsler J, Birrer O, Mühlemann S. Load-bearing capacity of CAD/CAM 3D-printed zirconia, CAD/CAM milled zirconia, and heat-pressed lithium disilicate ultra-thin occlusal veneers on molars. Dent Mater. 2020;36(4):e109-e116.

63. Peng CC, Chung KH, Ramos V Jr. Assessment of the Adaptation of Interim Crowns using Different Measurement Techniques. J Prosthodont. 2020;29(1):87-93.

64. Prpić V, Schauperl Z, Ćatić A, Dulčić N, Čimić S. Comparison of Mechanical Properties of 3D-Printed, CAD/CAM, and Conventional Denture Base Materials. J Prosthodont. 2020;29(6):524-528.

65. Muta S, Ikeda M, Nikaido T, et al. Chairside fabrication of provisional crowns on FDM 3D-printed PVA model. J Prosthodont Res. 2020;64(4):401-407.

66. Li P, Krämer-Fernandez P, Klink A, Xu Y, Spintzyk S. Repairability of a 3D printed denture base polymer: Effects of surface treatment and artificial aging on the shear bond strength. J Mech Behav Biomed Mater. 2021;114:104227.

67. Kim J, Lee DH. Influence of the Postcuring Process on Dimensional Accuracy and Seating of 3D-Printed Polymeric Fixed Prostheses. Biomed Res Int. 2020;2020:2150182.

68. Kim YH, Jung BY, Han SS, Woo CW. Accuracy evaluation of 3D printed interim prosthesis fabrication using a CBCT scanning based digital model. PLoS One. 2020;15(10):e0240508.

69. Dehurtevent M, Robberecht L, Thuault A, et al. Effect of build orientation on the manufacturing process and the properties of stereolithographic dental ceramics for crown frameworks. J Prosthet Dent. 2021;125(3):453-461.

70. Takahashi K, Torii M, Nakata T, Kawamura N, Shimpo H, Ohkubo C. Fitness accuracy and retentive forces of additive manufactured titanium clasp. J Prosthodont Res. 2020;64(4):468-477.

71. You SM, You SG, Kang SY, Bae SY, Kim JH. Evaluation of the accuracy (trueness and precision) of a maxillary trial denture according to the layer thickness: An in vitro study. J Prosthet Dent. 2021;125(1):139-145.

72. Bae EJ, Kim HS, Lim JY. Evaluation of bond strength of porous cobalt-chromium metal and pressed ceramic fabricated by additive manufacturing. J Prosthet Dent. 2020;124(6):808.e1-808.e5.

73. Wemken G, Spies BC, Pieralli S, Adali U, Beuer F, Wesemann C. Do hydrothermal aging and microwave sterilization affect the trueness of milled, additive manufactured and injection molded denture bases?. J Mech Behav Biomed Mater. 2020;111:103975.

74. Revilla-León M, Al-Haj Husain N, Methani MM, Özcan M. Chemical composition, surface roughness, and ceramic bond strength of additively manufactured cobalt-chromium dental alloys. J Prosthet Dent. 2021;125(5):825-831.

75. Revilla-León M, Al-Haj Husain N, Ceballos L, Özcan M. Flexural strength and Weibull characteristics of stereolithography additive manufactured versus milled zirconia. J Prosthet Dent. 2021;125(4):685-690.

76. Reymus M, Fabritius R, Keßler A, Hickel R, Edelhoff D, Stawarczyk B. Fracture load of 3D-printed fixed dental prostheses compared with milled and conventionally fabricated ones: the impact of resin material, build direction, post-curing, and artificial aging-an in vitro study. Clin Oral Investig. 2020;24(2):701-710.

77. Scotti CK, Velo MMAC, Rizzante FAP, Nascimento TRL, Mondelli RFL, Bombonatti JFS. Physical and surface properties of a 3D-printed composite resin for a digital workflow. J Prosthet Dent. 2020;124(5):614.e1-614.e5.

78. Wang W, Sun J. Dimensional accuracy and clinical adaptation of ceramic crowns fabricated with the stereolithography technique. J Prosthet Dent. 2021;125(4):657-663.

79. Prechtel A, Reymus M, Edelhoff D, Hickel R, Stawarczyk B. Comparison of various 3D printed and milled PAEK materials: Effect of printing direction and artificial aging on Martens parameters. Dent Mater. 2020;36(2):197-209.

80. Li R, Chen H, Wang Y, Sun Y. Performance of stereolithography and milling in fabricating monolithic zirconia crowns with different finish line designs. J Mech Behav Biomed Mater. 2021;115:104255.

81. Schönhoff LM, Mayinger F, Eichberger M, Reznikova E, Stawarczyk B. 3D printing of dental restorations: Mechanical properties of thermoplastic polymer materials. J Mech Behav Biomed Mater. 2021;119:104544.

82. Wang Y, Müller WD, Rumjahn A, Schmidt F, Schwitalla AD. Mechanical properties of fused filament fabricated PEEK for biomedical applications depending on additive manufacturing parameters. J Mech Behav Biomed Mater. 2021;115:104250.

83. Keßler a, Hickel R, Ilie N. In vitro investigation of the influence of printing direction on the flexural strength, flexural modulus and fractographic analysis of 3D-printed temporary materials. Dent Mater J. 2021;40(3):641-649.

84. Oğuz Eİ, Kılıçarslan MA, Özcan M, Ocak M, Bilecenoğlu B, Orhan K. Evaluation of Denture Base Adaptation Fabricated Using Conventional, Subtractive, and Additive Technologies: A Volumetric Micro-Computed Tomography Analysis. J Prosthodont. 2021;30(3):257-263.

85. Herpel C, Tasaka A, Higuchi S, et al. Accuracy of 3D printing compared with milling - A multi-center analysis of try-in dentures. J Dent. 2021;110:103681.

86. Wemken G, Burkhardt F, Spies BC, et al. Bond strength of conventional, subtractive, and additive manufactured denture bases to soft and hard relining materials. Dent Mater. 2021;37(5):928-938.

87. Tasaka A, Okano H, Shimizu T, Kato Y, Higuchi S, Yamashita S. Influence of reinforcement bar on accuracy of removable partial denture framework fabricated by casting with a 3D-printed pattern and selective laser sintering. J Prosthodont Res. 2021;65(2):213-218.

88. Tasaka A, Okano H, Odaka K, et al. Comparison of artificial tooth position in dentures fabricated by heat curing and additive manufacturing. Aust Dent J. 2021;66(2):182-187.

89. Wu J, Xie H, Sadr A, Chung KH. Evaluation of Internal Fit and Marginal Adaptation of Provisional Crowns Fabricated with Three Different Techniques. Sensors (Basel). 2021;21(3):740.

90. Kessler A, Hickel R, Reymus M. 3D Printing in Dentistry-State of the Art. Oper Dent. 2020;45(1):30-40.

91. Shim JS, Kim J, Jeong SH et al. Printing accuracy, mechanical properties, surface characteristics, and microbial adhesion of 3D-printed resins with various printing orientations. J. Prosthet. Dent. 2020;124,4: 468-475.

92. Berli C, Thieringer FM, Sharma N, Müller JA et al. Comparing the mechanical properties of pressed, milled, and 3D-printed resins for occlusal devices. J Prosthet Dent. 2020; 124,6:780–786.

93. Zafar MS. Prosthodontic Applications of Polymethyl Methacrylate (PMMA): An Update. Polymers (Basel). 2020;12(10):2299.

94. Giannetti L, Apponi R, Mordini L, Presti S, Breschi L, Mintrone F. The occlusal precision of milled versus printed provisional crowns. J Dent. 2021;117:103924.

95. Della Bona A, Cantelli V, Britto VT, Collares KF, Stansbury JW. 3D printing restorative materials using a stereolithographic technique: a systematic review. Dent Mater. 2021;37(2):336-350

Fundings

This research did not receive any specific grant from funding agencies in the public, commercial, or not-for-profit sectors.

Declarations of interest

None.

Table 1

Research question presented using the PICOS framework.

PI(E)COS	
Population/participants	Prosthetic materials for AM 3D printing (ceramics, polymers and metals)
Intervention (or Exposure)	3D printing additive manufacturing prosthesis
Comparison group	Traditional and subtractive manufacturing (milling technique)
Outcomes	Flexural strength (post-manufacturing and post ageing), fracture load, hardness, roughness, RPD fit accuracy, trueness (post-manufacturing and post ageing), marginal discrepancy and internal fit.
Study design included	In vitro studies

Table 2

Description of the evaluated mechanical properties, quality assessment score and fundings.

Author/s And Year	Flexural Strength	Fracture Load	Hardness	Roughness	RPD Fit Accuracy	RMS/ Trueness	Marginal Discrepancy	Internal Fit	Quality Assessment Score	Fundings
Al Maaz 2019							x	x	36/42	American Academy Of Fixed Prosthodontics
Alharbi 2016						x			31/42	Grant From King Saud University, Riyadh, Kingdom Of Saudi Arabia
Alharbi 2017							x	x	35/42	Supported By A Scholarship Grant Number 2/302626 From King Saud University, Riyadh, Kingdom Of Saudi Arabia.
Alsandi 2019						x			38/42	Grant From The Japan Society For The Promotion Of Science (No. 16H05515).
Arnold 2017					x				33/42	None
Ashtiani 2018								x	37/42	School Of Dentistry, Shahid Beheshti University Of Medical Science, Tehran, Iran.
Bae 2016						x			34/42	None
Bae 2020	x								49/42	Supported By The Basic Science Research Program Through The National Research Foundation (NRF) Of Korea, Funded By The Ministry Of Education (Grant No. 2017R1D1A1B03035688), The Technology Development Program (C0511440) Funded By The Ministry Of Smes And Startups (MSS, Korea), And The National Research Foundation Of Korea (NRF) Grant Funded By The Korea Government (MSIT) (No. 2018R1A5A7023490).
Barazanchi 2019		x							38/42	None

Braian 2018						x			36/42	None
Branco 2020			x	x					40/42	FundaçAo Para A Ciencia E A Tecnologia (FCT), Portugal, For Funding Through Projects 3D-Dentalprint (02/SAICT/2016/023940)
Chen 2019					x				38/42	National Natural Science Foundation Of China, Grant #51705006.
Choi 2019	x	x							38/42	None
Choi 2020	x	x							39/42	None
Dehurtevent 2017	x								30/42	None
Dehurtevent 2020	x	x	x						37/42	None
Deng 2018						x			39/42	Supported By The National Natural Science Foundation Of China (Grant No. 81271181) To YS And The Capital Health Research And Development Of Special (Grant No. 2016-1- 4101) To YSZ.
Fiore 2020							x		38/42	None
Herpel 2021						x			41/42	None
Homsy 2017						x	x	x	37/42	Supported In Part By The National Council For Scientific Research, Beirut, Lebanon.
Hsu 2020						x			39/42	Supported By Grant From The National Taiwan University Hospital, Taipei, Taiwan, Republic Of China (NTUH.106-S3542).
Ioannidis 2020		x							40/42	None
Ishida 2016				x		x			38/42	None
Kalberer 2019						x			37/42	None
Kebler 2021	x								40/42	None
Kim 2016							x		36/42	None
Kim 2017							x	x	33/42	Supported By A Korean University Grant, The Mnistry Of Trade, Industry And Energy (20133110002881), And By SM (Smile Maker) Dental Laboratory.
Kim 2020a						x	x	x	41/42	None

Kim 2020b			x	x	x	41/42	Funded By The Ministry Of Trade,Industry And Energy (MOTIE, Korea).
Li 2019	x			x	x	38/42	Supported By The National Key R&D Program Of China [Grant Number 2018YFB1106900], The National Natural Science Foundation Of China [Grant Number 51475004], And The Capital's Funds For Health Improvement And Research [Grant Number 2018-2-4103].
Li 2020		x				36/42	None
Li 2021			x			37/42	None
Liu 2018				x	x	35/42	National Natural Science Foundation Of China [Grant No. 51475004], Capital's Funds For Health Improvement And Research [Grant No. CHF 2016-1-4101], Project For Culturing Leading Talents In Scientific And Technological Innovation Of Beijing [Grant No. Z171100001117169].
Mahmood 2019					x	40/42	Odontologiskforskningi Region SkåNe, OFRS [Grant Number 509641].
Mai 2017				x	x	37/42	Basic Science Research Program Through The National Research Foundation Of Korea Funded By The Ministry Of Science, Information And Communication Technologies And Future Planning, Grant NRF-2014R1A1A1006073.
Molinero-Mourelle 2018				x		38/42	None
Munoz 2016				x		36/42	None
Muta 2020		x	x		x	40/42	None
Oguz 2021			x			38/42	Supported By Ankara University Scientific Research Projects

										Coordination Unit, Project Number: 18B0234003.
Øilo 2018			x	x					38/42	None
Osman 2017						x			36/42	Scholarship Grant Number 2/302626 From King Saud University, Riyadh, Kingdom Of Saudi Arabia.
Park 2016							x	x	33/42	None
Peng 2019						x	x		37/42	None
Peng 2020							x	x	37/42	Funding In Part By ACP Education Foundation Research Fellowships Program And Department Of Restorative Dentistry, University Of Washington, Grant #63–2073.
Prechtel 2019		x							38/42	None
Prechtel 2020			x						38/42	None
Prpić 2020	x		x						37/42	Supported By The University Of Zagreb Scientific Support “Diagnostic And Therapy Of Craniomandibular Dysfunctions.
Revilla León 2018							x		35/42	Supported By A Research Grant From The Spanish Association For Prosthodontics And Aesthetics.
Revilla-León,2019							x	x	34/42	None
Revilla-León 2020a				x					36/42	None
Revilla-León 2020b	x	x							37/42	None
Reymus 2020		x							32/42	None
Schönhoff 2021	x		x						38/42	Supported By Research Program ZF4052006AW8 (Aifprojekt Gmbh, Berlin, Germany, ZIM-Kooperationsprojekte, Projekttr¨Ager Des Bmwi).
Scotti 2020	x		x	x					39/42	None
Shim 2019	x			x					35/42	None
Sim 2018						x			33/42	None
Soltanzadeh 2018					x				36/42	None
Svanborg								x	30/42	Supported By Grants

2018										From The Adlerbertska Research Foundation, The Sylvan Foundation, The Hjalmar Svenssons Foundation, Wilhelm And Martina Lundgren Foundation, And Dentsply Sirona Implants, IIS Grant I-IS-15-057.
Tahayeri 2017	x					x			32/42	National Institute Of Dental And Craniofacial Research (NIDCR) And The National Institutes Of Health (NIH) (R01DE026170 To LEB), And The Medical Research Foundation Of Oregon (MRF To LEB) And Apprenticeships In Science & Engineering Program At Saturday Academy.
Takahashi 2020				x		x		x	38/42	Supported By JSPS KAKENHI Grant Number 16H05526.
Tasaka 2018						x			33/42	None
Tasaka 2019a						x			33/42	None
Tasaka 2019b					x				35/42	None
Tasaka 2021a						x			36/42	None
Tasaka 2021b						x			36/42	None
Ucar 2019	x	x	x						31/42	None
Wang 2018						x			34/42	None
Wang 2019	x								36/42	Supported By The Technology Development Program Of Ministry Of Smes And Startups (MSS) [C0511440], The Technology Innovation Program Funded By The Ministry Of Trade, Industry & Energy (MOTIE, Korea) [10073062] And The National Research Foundation Of Korea (NRF) Grant Funded By The Korea Government (MSIT)

								[2018R1A5A7023490].
Wang 2020				x	x		38/42	None
Wang 2021	x						32/42	Scholarship From The China Scholarship Countil (Grant Number 201706240007)
Wemken 2020				x				None
Wemken 2021	x						34/42	Material And Financial Support From VOCO, Cuxhaven, Germany (ID 127105).
Wu 2021					x	x	37/42	Supported In Part By The Department Of Restorative Dentistry, University Of Washington [Grant #65-4909 Task 824].
Ye 2017			x				33/42	Supported By The Project For Culturing Leading Talents In Scientific And Technological Innovation Of Beijing (Z171100001117169), The PKU School Of Stomatology For Talented Young Investigators (PKUSS20120210), And The Construction Program For National Key Clinical Speciality From National Health And Familiy Planning Commission Of China (2011).
You 2020				x			36/42	Supported By Korea University Grant (No. K1711261).
Zandinejad 2019		x					34/42	Supported By The International Team For Implantology (ITI) Grant No. 929 2013.

Table 3

Details of the included articles on materials, sample sizes, AM technology used and mechanical properties.

AUTHOR/s AND YEAR	MATERIALS AND SIZE	AM TYPES	CONTROL	MECHANICAL TESTS	DATA AND FINDINGS
			CERAMICS		
Branco 2020	N = 4 crowns Ceramic paste 3 mol % Yttria stabilized with zirconia powder (TZ-3Y-E, Tosoh)	Robocasting	Milling: zirconia powder containing a 3% of an organic binder (TZ-3YB-E, Tosoh)	surface roughness (Ra) with a surface roughness tester (SRT9 of 1,25 mm), Hardness (Vickers test)	Hardness: 1148.8 ± 15.1063; lower than control ($p < 0.001$). Roughness: almost four times higher than control samples (p= 0.002).
Dehurtevent 2020	Crowns Alumina powder (CT1200SG; Almatis) into a photosensitive acrylic resin (C1-alumina; CryoBerylSoftare)	SLA specimens oriented in 3 different planes (ZX, ZY and XY orientation)	None	3-point flexural strength (n= max force: 1kN), Vickers indentation hardness test, fracture toughness with 3-point bend test	Flexural strength: ZY-oriented specimens (409.7 ± 29.6 MPa) significantly higher (p<0.05). Fracture toughness (4.6 ±0.2 MPa.m$^{1/2}$) was higher than ZX-oriented ones (p<0.05).
Dehurtevent 2017	N = 60 rectangular specimens (1.3 × 4 × 22 mm) experimental groups: S80, S75, S70, L80, L75, L70 (C1 - Alumina, CT1200SG, Almatis, PA, USA)	SLA	Milling (In-Ceram AL, Vita Zahnfabrik.)	3-point flexural strengths (100N cell, maximum force of 1kN, constant speed of 0.5 mm/min)	L70 (273.8 ± 41.9 MPa) and S70 (271.7 ± 44.5 MPa) samples flexural strengths were lower than L80 (367.9 ± 52.4 MPa), L75 (363.7 ± 74.6 MPa), and control samples (350.4 ± 49.5 MPa) (p<0.05).
Homsy 2017	N=30 mesio-occlusal inlays lithium disilicate glass-ceramic: e.max Press inlays from 3D printed wax patterns (group CI3DW) and wax plasticized patterns (VisiJet FTX Green; 3D Systems) from scanning of the master and 3D printed wax patterns (group DI3DW).	MICRO-SLA (ProJet 1200; 3D Systems)	conventional impression and manual wax pattern (group CICW) or laboratory scanning; CAD-CAM milling wax blanks (group CIDW) and scanning of the master preparation and CAD-CAM milling (group DIDW)	marginal and internal fit accuracy with replica technique and stereomicroscopy.	Internal fit: 82.9 ± 11.8 µm and 88.8 ± 14.5 µm. Marginal discrepancy: no significant differences among groups CI3DW and DI3DW . The internal discrepancy was larger than the marginal discrepancy within all groups (p<0.001).
Ioannidis 2020	N=20 occlusal veneers (0.5 mm) zirconia (Lithoz,	LCM	Milling: zirconia (Ceramill Zolid FX, Amann Girrbach, Pforzheim,Germany); and heat-pressed lithium	Fracture load necessary to decrease the maximum load by 20% and initiate a crack (F initial) and the load	Fracture load: 1583 ± 542 N. Significant median Finitial values

	Vienna, Austria)		disilicate (IPS e.max Press, Ivoclar Vivadent, Schaan,Liechtenstein).	needed to fracture the specimen (F max). Chewing simulation with cyclic fatigue and temperature variations.	differences between all groups (p <0.0001). The median Fmax values differences were significant between AM and milling (p = 0.0238).
Li 2019	Crowns Zirconia	SLA	None	Flexural strength (universal testing machine), internal and marginal adaptation evaluated with 3D subtractive analysis technique.	Flexural strength: 812 ± 128 MPa. Cement space: 63.40 ± 6.54 µm in occlusal area, 135.08 ± 10.55 µm in axial area and 169.58 ± 18.13 µm in marginal area. Strength: adequate for fabricating dental crowns, but internal and marginal adaptation not ideal for clinical application.
Li 2021	N=30 crowns 47 vol% 3 monolitic zirconia	SLA	Milling: partially sintered zirconia blank (SHT, Aidite, China)	three-dimensional fabrication accuracy analysis: root mean square (RMS)	External design: 19.22 ± 0.91 µm, 26.20 ± 2.04 µm and 25.92 ± 3.62 µm; Intaglio design: 22.68 ± 4.03 µm, 17.04 ± 2.65 µm and 22.48 ± 6.00 µm. RMS value influenced by finish line design, with external (*p*= 0.027) and intaglio (*p*= 0.049), but not by fabrication method.
Revilla-León 2019	N = 20 crowns Zirconia stabilized with 3% Yttria, 3DMix ZrO_2 (3DCeram) Anatomically contoured (AM) and splinted (SAM) samples	SLA	Milling 5-axis CNC anatomically contoured CARES Zirconia-dioxide (Straymann)	Marginal and internal discrepancies with silicone replica method	Marginal discrepancy: higher with AM compared to CNC and SAM and higher with SAM compared to CNC (p<0.001). Internal discrepancy: higher with SAM and AM compared to CNC (p<0.001), lower with compared to AM (p=0.001).
Revilla-León 2020b	N= 10 bar specimens (25×4×1.2 mm) zirconia (3DMix ZrO2; 3DCeram) stabilized with 3% yttria	SLA	Milling: (IPS e.max ZirCAD; Ivoclar Vivadent AG)	Flexural strength (3-point bend tests) with artificial aging procedures	Flexural strength: 320.32 ± 40.55 MPa. Manufacturing, mastication simulating aging procedure and the interaction between them affected flexural strength (p<0.001). mastication simulation produced a reduction in flexural strength for AM group compared to

					milling ($p<0.001$).
Ucar 2019	N = 10 disc-shaped specimens (16 mm diameter, 1.2 mm thick) LCM alumina Lithography (Lithoz, Vienna, Austria)	SLA	Dry-pressing: In-Ceram alumina (Vita Zahnfabrik, Bad Sackingen,Germany and milling: ZirkonZahn CAD/CAM (Zirkonzahn, South Tyrol, Italy)	Biaxial flexural strength test ("piston on 3-ball" technique), fracture toughness determination, microhardness test (Vickers Hardness).	Flexural strength: 490 ± 44 MPa. LCM alumina had the highest mean hardness value. Significant difference considering the peak strength and hardness values for all pairwise comparisons ($p<=0.05$).
Wang 2018	N=10 crowns for maxillary second molar ZrO2 paste (3DMIXZrO2L; 3DCeram Co)	SLA (CERAMAKER 900; 3DCeramCo)	Milling (DWX-50; Roland DG Corp): ZrO2 block (Zenostar; Wieland Dental)	Trueness of different locations: External and Intaglio surface, Marginal area, Intaglio occlusal surface)	Trueness of AM crowns was no worse than the milled ones ($p<0.05$). External: 53 ±9 µm; Intaglio: 38 ±12 µm; Marginal: 34 ±5 µm; Occlusal: 27 ±17 µm.
Wang 2020	N=10 crowns for first molar Zirconia and Alumina multifunctional acrylate	2 SLA systems: CeraFab7500 (CF); Lithoz for alumina and CSL150 (CL) and PORIMY for zirconia	Milling: (X-MILL500 (XM) ; XTCERA) for Zirconia HDDAPET4A	Dimensional accuracy with Geomagic Qualify software and silicone replica method for clinical adaptation	Accuracy: 65 ± 6 µm. Marginal discrepancy: 109 ± 27 µm. Internal fit: 71 ± 15 µm (axial), 98 ± 29 µm (corner) and 149 ± 46 (occlusal). CF had better dimensional accuracy compared to others ($p<0.001$). Differences only apparent in the axial and occlusal areas between CF and CL ($p<0.05$).
Zandinejad 2019	N=10 crowns on zirconia implant abutments (CARES zirconium-dioxide abutment; Straumann, Arlington, TX) and chamfer finish line. Zirconia (3D Mix ZrO2 (3D Ceram) (AMZr)	SLA (CeraMaker 900; 3DCeram Co.)	Milling: lithium disilicate (IPS e.max CAD crown HT A1; IvoclarVivadent, Amherst, NY) (MLD) and zirconia (Lava Plus Zirconia W1, 3M Co., St. Paul, MN) (MZr)	Fracture resistance with vertical force application with universal testing machine (crosshead speed of 2 mm/min)	Fracture load: 1243 ± 265.5 N. No significant differences observed. All specimens fractured at the implant-abutment interface.
METALS					
Al Maaz 2019	N=90 crowns with chamfer (C), deep chamfer (DC), or shoulder (S) finish lines	SLM	None	Fitting evaluated with inverted bright field metallurgical microscope. Marginal and internal	Marginal gap: significant differences between B and N groups, and B and HN groups ($p<0.001$).

	Base alloy (Co-Cr) (B group), high noble (Au-Pd-Ag) (HN group) and noble alloy (Co-Pd) (N group)			gaps measured at 5 locations: buccal margin, midfacial, incisal, midlingual, and lingual margin.	Significant difference between the DC finish line and the C and S finish lines (p<0.001). Significant influence on marginal gap of alloy type and finish line and on internal gap of alloy type (p<0.001).
Arnold 2017	N=3 clasps Co-Cr-Si-Mn-N-Nb-Fe Remanium Star CL (Dentaurum GmbH & Co. KG) for SLM	SLM (CNC Construction mlab: M1 cusing, Concept Laser GmbH)	Lost-wax casting technique (LWT); indirect milling (wax milling with LWT), and direct milling: PEEK.	RPD fit accuracy	Vertical: 363 ± 133 μm and Horizontal: 365 ± 205 μm. The direct RP had significantly higher vertical values than the others (p<0.001). unsuitable for clinical use.
Bae 2016	N=20 inlay Co-Cr alloy (SP2, EOS, GmbH) for SLS and UV polymerizable polymer (VisiJet FTX Gree, 3D Systems Co) for SLA	SLS and SLA	Milling: wax block (D-max) and Zirconia block (D-max)	Accuracy evaluation with RMS formula.	SLA specimens had the smallest differences from reference data and significant differences compared with wax (p=0.021) and zirconia samples (p=0.048). SLS specimens deviation was different from wax (p<0.001), and zirconia samples (p=0.001).
Bae 2020	N = 20 bar specimens Co-Cr metal powder (SP2; EOS GmbH): group without porosities (PF group) and with porosities (PP group)	SLS	Casting (CP group): Co-Cr alloy (StarLoy C; Degudent GmbH).	Flexural strength: 3-point bending test with universal testing machine (cross head speed 2mm/min)	Mean values differences were statistically similar (p=0.058): PP (35.6 ±9.1 MPa), CP (43.5 ±7.8 MPa) and PF (47.7 ± 4.5 MPa). Clinical implications: high bond strength is essential for successful metal-ceramic restorations and SLS porous samples had statistically similar bond strength to other systems.
Barazanchi 2019	N=17 rectangular specimens (1.5 mm, 8 mm, 30 mm) CoCr powder (Cobalt Chrome MP1, EOS)	DMLS Eos int M270, (EOS GmBH, Munich, Germany)	Milling: pre sintered CoCr specimen	Hardness before /after porcelain firing. Fracture surface and micro-structural changes (before/after porcelain firing) with SEM.	Hardness: 4.4 ± 0.2 GPa; hardness increased post porcelain firing. Analysis of the fracture surfaces showed a predominantly adhesive mode of

					failure.
Braian 2018	N = 10, inlay-shaped and four-bridge specimens Ti and Co-Cr (only with EOS®)	EBM technology (Arcam®), laser sintering (SLM solutions ®), DMLM (Concept Laser ®), DMLS (EOS ®).	Milling (SM)(Mikron®)	Accuracy with linear measurements in 3 axes (X, Y, Z).	In inlay model, EBM: precision 0.078 in X and 0.117 mm in Y and accuracy 0.176 mm in X. DMLS: precision 0.282 mm and accuracy 1.026 mm in Z. EBM had lowest precision (>0.3°) and accuracy (>1.0◦). In bridge model, EBM: precision 0.079 in X and 0.250mm in Z and accuracy 0.161 in X and 0.243 in Y and −0.975 mm in Z. SLM: accuracy −0.005 mm. EBM had highest precision, DMLM had lowest precision (>0.09°) and SLM had highest accuracy and DMLM (> −0.07°) at 0.002◦ deviation.
Chen 2019	RPD frameworks designs: palatal plate-type connector with 2 clasps (Type I), anterior and posterior palatal strap-type connector with 4 clasps (Type II), complete palatal connector with no clasps (Type III), and anterior palatal plate-type connector with 4 clasps (Type IV) Co-Cr alloys (remanium star CL; DENTAURUM GmbH & Co KG)	SLM (Mlab cusing R; Concept Laser GmbH)	lost-wax casting technique: (Wironit, extra-hard; Bego GmbH & Co. KG)	Average and maximum gaps with silicone impression technique	Average gaps: influenced by production methods, design types, and interactions (p<0.001). design I and II with average gaps of SLM larger than the cast ones (p<0.001).
Fiore 2020	N=160 fixed partial denture frameworks and flat specimens (25×3×0.5 mm) Co-Cr alloy (EOS M270; EOS GmbH Electro Optical Systems), made of EOS Co-Cr SP2 powder	SLM	None	Marginal gap before/after ceramic firing	Significant marginal gap difference of the frameworks before ceramic firing (p=0.001).
Kim 2017	N = 30 crowns	SLM	Milling: Co– Cr alloy (StarLoy C; DeguDent, Hanau-Wolfgang,	Marginal and internal gap with silicone replica technique: 12 internal	Average marginal gap: 239 ± 126µm; Occlusal gap: 384 ±

	Co– Cr powder (StarbondCoS powder 55; S&S Scheftner GmbH, Mainz, Germany)		Germany) and soft block (SMB; SoftMetal; LHK, Chilgok, Korea) and conventional lost wax technique: Co–Cr alloy (StarLoy C; DeguDent, Hanau-Wolfgang, Germany) for µ-SLA (Micro-stereolithography) + Casting	spots (marginal, axial wall and occlusal) measured with digital microscope.	67,8µm. Significant differences (p<0 .05). Further improvements in SLM may be required prior to clinical implementation.
Munoz 2016	N= 30 crowns Gold	DLP (ProJet DP 3000)	Milling(LAVA CNC 500) and hand wax	Margin discrepancy evaluation with light microscopy and 10 measures for vertical discrepancy	Marginal discrepancy: 59.9 ± 16.81 µm. Significant differences between milled and hand-waxed overall mean (p<0.001). AM printed patterns produced a significantly higher number of crowns with unacceptable margin discrepancy (>120 mm).
Øilo 2018	N = 10 RPD frameworks Cara Co-Cr (Heraeus Kulzer, GmbH)	SLM	Milling: Cara Co-Cr (Heraeus Kulzer, GmbH)and traditional casting (Wirobond C, BEGO Implant Systems)	Vickers hardness and roughness with Ra and Rmax evaluation.	Hardness: 4570,062 ± 127 Mpa. Roughnes: Ra (µm) 1,65 ± 0,55 and Rmax 13,58 ± 3,38 µm. Significant differences in hardness, wall thickness, weight, and connector size (p<0.05)
Revilla León 2018	complete-arch frameworks Ti6Al4V ELI Metal powder; Arcamn for EBM and LaserFormTi Grade 23; 3D Systems for SLM	EBM and SLM	None	Discrepancy with 3 measurements at x- (mesio-distal), y- (bucco-lingual), and z- (occluso-gingival) axes	Mean accuracy: 3 ±3 mm. The most favorable results were obtained in the z-axis. The highest discrepancy was observed in the y-axis (37 to 56 mm), followed by the x- (16 to 44 mm) and z- (6 to 11 mm) axes (p<0.05).
Revilla-León 2020a	N=40 disks (5 mm x 1 mm) Co-Cr alloy: SP2 (EOS), Co-Cr 3DS (3D Systems Laverwise), Remanium star CL (Concept Laser 100W/200W)	SLM: EOS, 3D Systems Layerwise, Concept Laser 100W, Concept Laser 200W	Milling: (DMG 10 Ultrasonic; DMG) Co-Cr (Starbond CoS Disc basic; Scheftner)	Roughness	Roughness: 2.43 ± 0.34, 1.80 ± 0.43, 1.57 ± 0.15 and 2.84 ± 0.27 µm. Differences were obtained in Wt%, At%, and Ra values among Co-Cr alloys (p<0.05).
Soltanzadeh 2018	N=10 RPD maxillary frameworks for a Kennedy class III Modification I arch. Co-Cr alloy (ST2724G;	SLM (CAD printing and CAD printing from stone model)	Conventional method: Lost-wax technique from stone model and Lost-wax technique from printable resin	RPD accuracy and fitting	RPD accuracy: 0.005 ± 0.030 mm. AM frameworks had lower fit (*p* < 0.05) in the major connectors and guide plates. The biggest gap (0.33 mm

	Sint-Tech, Canelli, Italia)		model		± 0.20 mm) was in anterior strap of the major connector. Method of fabrication did not affect the adaptation of the rests or reciprocation plates.
Svanborg 2018	N=2 implant frameworks Renishaw AM250, Renishaw DG1 powder for Co-Cr implant and Ti TiAl6V4 extra low interstitial (ELI) powder (Renishaw) frameworks	AM technique no specified	CNC-milling: Co-Cr and Ti alloy	Fitting with measurements in 3 dimensions (x, y, and z axes) before/after ceramic veneering	AM Ti: the difference in fit in y (p=0.002) and the 3D distortion (p=0.008) were significant. AM Co-Cr: significant differences in z (p=0.011), in Y/Z and X/Z angles (p<0.0001) after ceramic veneering.
Takahashi 2020	n=15 clasps for RPD 38 to 45 µm CP Ti grade 2 powder (EOS GmbH Electro Optical Sys- tems, Krailling, Germany), 39 ± 3 µm Ti-6Al-4V powder (EOS GmbH Electro Optical Systems, Krailling, Germany), 50 µm Ti-6Al-7Nb powder (Matsuura)	SLS	Lost wax conventional technique with Ti alloys: Ti-6Al-4V (Ti64; 64 Ti billet, Toho Tec., Chigasaki), Ti-6Al-7Nb (Ti67; T- alloy Tough, GC Corp.), and CP Ti grade 2 (CPTi; T-alloy M, GC Corp.)	Roughness with 3D measuring surface profile device (NH-3N) and fitness accuracy with silicone impression technique (Fit Checker)	AM clasps surfaces were 5 to 10 times rougher ($p< 0.05$).
Tasaka 2019a	n=10 RPD frameworks Co–Cr alloy (Dan Cobalt Chuukou-shitsu; NIHON SHIKA KINZOKU Co., Ltd., Osaka, Japan)	SLS	3D printing casts (AM-cast)	Discrepancy measured at 5 random points on the inner surface.	Discrepancy: SLS-cast from 0.166 ± 0.009 to 0.123 ± 0.009 mm. Significant differences observed at the rests, proximal plates, connectors, and clasp arms.
Tasaka 2019 b	N = 5 clasps for RPD framework Co-Cr alloy: EOS Cobalt Chrome SP2 (EOS)	SLS	Milling: Co – Cr alloy, KM-Cobalt Chrome (Kyocera) and AM+ Lost-wax casting: Co-Cr alloy, Dan cobalt Chuukou-shitsu (Nihon Shika Kinzoku)	RPD accuracy: 7 sites analyzed on the inner surfaces (tip, center, and shoulders of both sides of the clasp arm, and rest).	Range of differences for AM, milling and SLS were –85.20 to 72.80 µm, 66.40 to 136.80 µm, and –3.20 to 52.40 µm, respectively. Significant differences observed at the tip and at the center of the clasp arm, and at the shoulder of both sides of the clasp arms and rest.
Tasaka 2021a	RPD frameworks Co-Cr alloy powder	SLS (EOSINT M270, EOS)	3D-printed pattern casting (AM-Cast) (Projet 3510DP, 3D Systems Corporation): resin	Accuracy under different conditions with a reinforcement bar.	Significant median value on occlusal rest and on right-side of joining area (p<0.05),

	(SP2, EOS, Kailling, Germany)		pattern (VisiJet M3 Dentcast, 3D Systems Corporation, Circle Rock Hill, SC, USA) shaped by AM Co-Cr alloy (Dan Cobalt Chuukou-shitsu, Nihon Shika Kinzoku, Osaka, Japan)		and on the center and left-side of joining area of the lingual bar ($p<0.01$) in SLS. 0 reinforcement samples more accurate on the rest compared with 1 bar samples and on right and left side of the joining area compared with 2 bar samples and 1 reinforcement samples more accurate on the center compared with 2 bar samples ($p<0.01$).
Wang 2019	N=30 rectangular specimens (hole-free, circular-hole, and rhombic-hole designs with (25×3×0.5 mm) Co-Cr alloy and Ceramic VITA VM13 fused layer (8 x 3×1.1 mm) to the center of the specimens	SLS (EOSINT M270; EOS GmbH, Munich, Germany)	None	3-points bending test and microscope evaluation.	Significant differences in bending energy observed between the rhombic-hole and the hole-free and circular-hole specimens ($p< 0.05$). Microscope evaluation: circular-hole and rhombic-hole specimens not printed perfectly.
Ye 2017	N=15 RPD framework Co-Cr alloy wirebond C+, BEGO	SLM (M270, EOS)	Casting technique	Fitness evaluation by visual inspection and measurements of the gap between occlusal rest and relevant rest seat	RPD fitting: 174 ± 117 µm. Average gap between occlusal rest and corresponding rest seat larger than casting frameworks ($p<0$ .05), but acceptable for clinical application.
			POLYMERS		
Alharbi 2016	n=18 crown (90, 120, 135, 150, 180, 210, 225, 240 and 270 building angles) hybrid composite resin material (Temporis DD-1000, DWS)	SLA (DW028D, DWS)	None	Dimensional accuracy (root mean square estimate RMSE)	120-degree build angle had a minimal deviation for thin (0.029mm) and thick printing support (0.031mm) with an accurate fit.
Alharbi 2017	N= 40 crowns: knife-edge (KE), chamfer (C), rounded-shoulder (RS), rounded-shoulder with bevel (RSB)	DLP	Milling: PMMA-based acrylate resin (Polycon ae; Straumann; shade A2)	Marginal fit using vertical (VG) and horizontal gap (HG), and absolute marginal discrepancy (AMD).	Internal fit: 110 ± 33 µm. Internal and marginal gaps influenced by fabrication method and finish-line design ($p=0.000$). AM

	Hybrid composite resin material (Temporis, shade A2, LOT: 040725; DWS)				samples had significant lower mean gap compared to milled samples at all points (p= 0.000).
Alsandi 2019	N=30 crown shape specimen (d=10mm inside, 15mm outside, h=10 mm) thermoplastic elastomers: Acrylonitrile-Butadiene-styrene (ABS), Poly lactic acid (PLA) and an acrylic block copolymer Kurarity (KUR) and a dental self-curing resin Unifast III A3 (PMMA)	FDM (Value 3D MagiX MF-1000)	None	Dimensional accuracy	No significant data reported.
Ashtiani 2018	N = 30 inlay and onlay Resin material WIC 300A envision (Envision TEC)	DLP CP group: conventional impression + 3D printing. IP group: digital impression + 3D printing.	Conventional: Resin material WIC 300A envision (Envision TEC)	Internal fit (silicone replica technique)	Marginal discrepancy: pulpal (p=0.025) and lingual (p=0.031) areas. Significantly lower in the lingual surface of IP group (p=0.031). Absolute discrepancy between groups CC and CP significantly different (p=0.020).
Bae 2016	N=20 inlay Co-Cr alloy (SP2, EOS, GmbH) for SLS and UV polymerizable polymer (VisiJet FTX Gree, 3D Systems Co) for SLA	SLS and SLA	Milling: wax block (D-max) and Zirconia block (D-max)	Accuracy evaluation (RMS formula).	SLA samples had the smallest difference from reference data and significant differences compared with wax (p=0.021) and zirconia (p=0.048). SLS samples deviation was significantly different from wax (p<0.001) and zirconia (p=0.001).
Choi 2019	N=30 specimen: 25 x 4 x 3 mm Dima Print Denture Base and Dima Print Denture Teeth (Kulzer, USA) Denture-based resins and commercial denture teeth	DLP (Cara Print 4.0, Kulzer, USA)	Milling and heat curing: denture-based resins and commercial denture teeth (Unfilled PMMA, double cross-linked PMMA, PMMA with nanofiller)	fracture toughness (K1C) and flexural strength, thermocycling for aging simulation (4-point bend test, using the chevron-notched beam method).	Flexural strength: decreased significantly with aging (p<0.01). Fracture toughness: Mean K1C had significant differences (p<0.01). Teeth bonded to 3D printed DBRs showed a mean fracture toughness significantly lower than that of teeth bonded to heat-cured and CAD/CAM.
Choi 2020	N=60 specimen: 25 x 4	DLP (Cara Print 4.0, Kulzer,	Heat-curing: PMMA (Vertex Rapid Simplified,	Fracture toughness K1C (MPa x m1/2) and	Flexural strength post ageing: 0.73 ± 0.23

	x 3 mm PMMA (Polymethyl Methacrylate) Kulzer 3D Dima, Kulzer denture resin materials and two commercially available denture characterizing composites (SR Nexco paste and Kulzer Creactive gingiva)	USA)	Vertex) and milling: PMMA (IvoCAD, Ivoclar Vivodent)	flexural strength (MPa) with 4-point bend test using the chevron-notched beam method, thermocycling for aging simulation.	and 0.1 ± 0.03 MPa; after 6 months ageing: 0.64 ± 0.2 and 0.17 ± 0.02 MPa; after 12 months ageing: 0.57 ± 0.18 and 0.44 ± 0.06 MPa. The mean K1C for K groups bonded to the 3 different denture bases were significantly lower compared to the SR group ($p<0.001$). Within K groups ageing showed significant mean K1C ($p=0.002$).
Deng 2018	n=5 maxillary complete denture polylactic acid (PLA)	FDM	3D printed wax patterns	Accuracy with silicone film thickness measurements, into 4 areas: primary stress-bearing, secondary stress-bearing, border seal, and relief areas (RMS formula)	PLA enlarged compared with the CAD data (0.016 ± 0.007 mm, RMS: 0.143±0.01 mm). Space between denture surface and plaster model for PLA: 0.277 ± 0.021mm. Values of secondary stress-bearing and relief areas were smaller than primary stress-bearing and the border seal areas. FDM is comparable to wax printer and satisfy accuracy requirements.
Herpel 2021	N= 40 removable complete denture VeroWhite Plus RGD 835 (Stratasys) for MJ; FREEPRINT denture (Detax), V-Print Try-In (VOCO) and DENTCA Denture Teeth (DENTCA) for DLP; UV-Sensitive Resin Basic (Anycubic 3D) for LCD-based SLA.	MJ, DLP, LCD-based SLA.	Milling	Trueness (RMS formula) and precision	Trueness: 154 ± 25, 142 ± 32, 145 ± 30, 82 ± 8 and 147 ± 32 µm. Trueness and precision (SD): AM less true (16–65 µm) and less precise (8–66 µm). Significant differences between the groups ($p<0.001$).
Hsu 2020	N=40 maxillary and mandibular denture base MiiCraft BV-005 printable resin (Young Optics Inc) and 20 from NextDent Base printable resin (NextDent BV)	DLP (MiiCraft 125; Young Optics Inc).	Milling (CCM), injection molded (IM), and compression molded (CM).	Denture base adaptation measuring thickness of silicone between denture base and model.	The 3DP had greater thickness than the IM and CM groups ($p<0.05$). In the mandible, 3DP recorded the lowest silicone thickness and trueness among all the groups.

Ishida 2016	Crowns PLA Blue M (X12052013-1PLA MLU) PLA (3D Systems (Rock Hill, USA)) for CX, B9-R-1-RED (021813) UV curing Acrylic resin (B9Creations (Rapid City, USA)) for B9, VisiJet DP200 (DP132502A) UV curing Acrylic resin (3D Systems (Rock Hill)) for PJ and RF080 (4120225), Wax resin (DWS s.r.l. (Vicenza, Italy)) for DW.	CX (CubeX Trio), DLP stereo-lithograph (B9Creator), laser stereo-lithograph (DW028D) and multi-jet modeling (Projet DP3000)	None	Dimensional accuracy and surface roughness	Significant differences for the type of printer, the enlargement ratio and the interaction between these factors for outer and inner diameter (p<0.01) and for expansion rate of depth and surface roughness (p<0.05)
Kalberer 2019	N=10 maxillary complete dentures monomer based on acrylic resin esters for fabricating denture bases (NextDent Denture 3+; Next- Dent B.V.)	Rapid prototyping	Milling: (AvaDent Digital Dental Solutions Europe, Global Dental Science Europe BV) from prepolymerized acrylic resin pucks.	Trueness: analyses were performed for the entire intaglio surface and specific regions: posterior crest, palatal vault, posterior palatal seal area, tuberosity, anterior ridge, vestibular flange, and mid-palatal raphae.	Trueness: 95.3 ±7.5 µm; after ageing: 76.6 ±7.2 and 83.0 ±7.9 µm. Milled prostheses had significantly better trueness than rapid prototyping for the entire intaglio surface (p<0.001) and anterior ridge (baseline: p<0.001; after immersion in saliva: p=0.001; after wet-dry cycle: p=0.011).
Kebler 2021	N = 360 specimen 2x2x25 mm^3 Nextdentc&b (Nextdent, Soesterberg, the Netherlands); 3Delta temp (Deltamed, Friedberg, Germany); Freeprint temp (Detax, Ettlingen, Germany)	DLP	None	Flexural strength: 3-point bending test (FS), (crosshead speed 0,5mm/min) with 3 testing modalities 'horizontal parallel', 'horizontal perpendicular', and 'vertical'. Before testing, two ageing procedures: a) 1-day storage in distilled water at 37°C; b) additionally followed by thermocycling between 5 (±2) and 55°C (±2) for 10,000 cycles, dwell time: 30 s; transfer	3Delta temp had the highest significant FS in aged and non-aged samples and significant lower values for FS in vertical compared to both horizontal directions (*p*<0.05). The parameter material had the highest influence on FS (*p*<0.001).

				time: 5 s.	
Kim 2016	N = 54 crowns UV polymerizing plastic cartridge resin (Visijet FTX Green; 3Dsystems):	μ-SLA	None	Marginal discrepancy: buccal, mesial marginal, lingual marginal and distal marginal: One array (OA) group Three arrays (TA) group Six arrays (SA) group	Marginal discrepancy: TA with best result (61.2 ± 37.3 μm), while SA with poorest result (92.5 ± 54.1 μm). All 3 groups showed significant differences by pairwise comparisons ($p<0.001$). The greatest discrepancy was in the buccal area for all groups.
Kim 2020a	Toronto all-on-4 Biocompatible photopolymer (Raydent C&B; Ray). the printed prosthesis were polymerized in 3 different ways: a) alone (P group), b) with support (PS group), c) on stone model (PM group)	SLA	None	Geometric accuracy and marginal and internal gap	PM group had the lowest mean discrepancy. The highest discrepancy was in occlusal area, especially in P group. PM group exhibited significantly smaller marginal gaps.
Kim 2020b	N= 21 crowns Photopolymer material (RAYDent C&B; Ray Co., Ltd., Hwaseong-si, Korea)	DLP	None	Accuracy (silicone replica method) and marginal and internal gaps	RMS values ranged from 41.00 to 126.60 μm, and the mean was 60.12 μm. Mean values of marginal, internal and total gaps: 132.96 ±139.23, 137.86 ± 103.09 and 135.68 ± 120.30 μm. Significant mean differences: marginal 132.96 μm and occlusal area 255.88 μm. Marginal gap of fabricated interim crowns based on CBCT STL data was within the acceptable clinical range.
Li 2020	Complete denture denture base material (FREEPRINT denture, Detax, Ettlingen, Germany).	DLP	None	Roughness evaluation (Sa) with profilometer, calculation of Sa parameter, SEM. groups: thermal cycling(5,000 thermal cycles at 5 °C - 55 °C, 70s per cycle) (aged) and without thermal cycling (non-aged). Subgroups: a) no surface treatment – control b) wetting with MMA + air-drying 120’’ c)grounding with P600 silicon carbide abrasive paper d)125 μm aluminum oxide abrasive distance 10mm pressure 0.2MPa 10’’	Roughness: for non-aged groups, Sa (4.13 ± 1.43 μm) was significantly higher ($p < 0.05$) as for aged group, samples displayed the roughest surfaces (7.15 ± 1.67 μm), with significantly higher mean Sa ($p < 0.05$).
Liu 2018	N =20 crowns	FDM and DLP	Milling and traditional	internal adaption(3D	FDM: Axial: 0.1299 ± 0.0311 mm and

	polylactic acid		handmade wax	analysis)	Occlusal: 0.764 ± 0366 mm. DLP: Axial: 0.0373 ± 0.0126 mm and Occlusal: 0.808 ± 0245 mm. Occlusal gap of DLP did not satisfy the assumption of normality (*p*=0 .02). Marginal and axial gaps did not satisfy the assumption of equality of variance (*p*<0 .05).
Mahmood 2019	n=30 crowns polymermaterial (Castable V2, Formlabs, Somerville, MA, USA).	SLA	Conventional method (manual layering technique) and milling: wax blank (CAD/CAM wax blanks, YETI Dentalpro- dukte, Engen, Germany)	Fit checking measurement (impression replica method) in 11 points.	AM samples had smaller mean cement gaps compared to conventional or subtractive (p ≤ 0.001) in the axial area, and to the milled ones (p=0.002) in the occlusal area. Among crowns with smaller gaps, AM copings had significantly smaller mean gaps compared to milled ones in the marginal and axial areas (p ≤ 0.001).
Mai 2017	N= 12 crowns biocompatible photopolymer (VeroGlaze MED620; Stratasys)	PJ	Molding method: autopolymerizing acrylic resin (Alike; GC Europe) Milling: PMMA and methacrylic acid ester-based cross-linked resin blocks (Ceramill TEMP; Amann Girrbach)	Fitting evaluated in proximal, marginal, internal axial and occlusal regions (silicone-replica techniques)	RMS: 99 ± 19 μm. Absolute marginal discrepancy was smallest in PJ group at 99 ±19 mm.
Molinero-Mourelle 2018	n= 15 crowns Polyalactid acid (PLA)	FDM	FDM: PMMA samples	Marginal fit evaluation with a profile projector (Toupview Serial No. C1604280431) at 6 points.	PLA marginal fit of provisional restorations was clinically acceptable and the results were comparable to those observed with PMMA samples.
Muta 2020	N = 10 crowns PVA models for indirect resin composite (Gradia, GC, Tokyo, Japan)	FDM	Conventional method with self-curing : acrylic resin (Curegrace, Tokuyama Dental, Tokyo, Japan)	Dimensional accuracy and RMS differences of intaglio surface (3D digital analysis), internal crowns adaption (silicone-fitting test) and surface roughness.	RMS: 310 ± 50μm. Marginal discrepancy: within 100 μm. Surface roughness: 5.6 ± 0.72 and 3.25 ± 0.68 μm.
Oguz 2021	N = 11 complete dentures	UV-light curing	Milling: prepolymerized PMMA blocks	Scanning with μ-CT and volumetric gap evaluation between	Interactions between fabrication method and location had

	3D printable resin (E-Denture; EnvisionTEC)		Compression molding: PMMA resin (Integra Heat Cure Acrylic; Birlesik Grup Dental, Ankara, Turkey) Injiection molding: PMMA resin (Ivobase Hybrid; Ivoclar Vivadent AG, Schaan, Liechtenstein)	denture base and cast using six region of interest for maxilla (anterior and posterior ridge crest, labial and buccal vestibule, palate, and posterior palatal seal) and 3 for mandible (intermolar, molar, and retromolar) in addition to overall gap measurements for edentulous arches.	significant effects on mean volumetric gap measurements for both edentulous arches (p=0.0001). Significant differences detected among fabrication methods for locations and for overall volumetric gap measurements (p = 0.0001). The highest gap measurements were at palate in the maxilla.
Osman 2017	Crowns (building angles: 90-120-135-150-180-210-225-240-270) NextDent C&B resin	DLP (RapidShape D30)	None	dimentional accuracy using digital subtraction technique	The build angle influenced dimensional accuracy. The lowest RMSE was recorded for the 135-degree and 210-degree build angles. The overall deviation pattern was more favorable with the 135- in contrast with the 210-degree build angle.
Park 2016	N = 40 crowns and bridges PMMA (E-Dent; Envision TEC)	DLP	Milling: 4-axial milling machine, Pekkton milling blank (Pekkton Ivory; Cendres&Metaux) Conventional system: autoplymerizing PMMA resin (Jet; Lang Dental Mfg Co Inc)	Marginal and internal discrepancies with silicone replica method and digital microscope for internal space between abutment and interim restoration	Mean marginal discrepancy: 56.85 ± 22.24 μm. Fabrication method had significant effect on discrepancy at each measurement point (p<0.001). DLP was superior to the other fabrication methods but all methods were suitable and produced a marginal fit within the clinically acceptable range.
Peng 2019	N=16 crowns 3D-printed methacrylic oligomers (NextDent C&B MFH; NextDent by 3d system)	DLP	Milling: PMMA resin (ZCAD Temp Fix 98; Harvest Dental) Manually direct fabrication technique: Autoplymerized PMMA resin (Jet; Lang Dental	Silicone replica technique (non-cementation method) to determine internal discrepancy, microcomputed tomographic (μCT) scan assessment with 3D images and 2D images, marginal discrepancy measured (polyvinyl siloxane impression technique and stereomicroscope).	μCT 2D: 0.17 ± 0.04 mm. No significant effects reported.
Peng 2020	N = 12 crowns 3D printed methacrylic oligomers (NextDent C&B MFH; NextDent by 3D system, Soesterberg,	DLP	Milling: PMMA resin (ZCAD Temp Fix; Harvest Dental, Brea, CA) Manually fabrication technique: Bis-acrylic composite fabricated (Protemp Plus; 3M ESPE)	Internal fit evaluation (silicone replica technique and X-ray microcomputed tomography (μCT) technique), marginal discrepancy (vinyl polysiloxane (VPS) (Aquasil Ultra XLV)	Silicone technique: 36.55 ± 4.22 mm^3; μCT 2D: 0.17 ± 0.04 mm; μCT 3D: 26.64 ± 3.07 mm^3. No significant effects

	Netherlands)			impression technique and optical coherence tomography (OCT) technique)	reported.
Prechtel 2019	N= 16/group indirect inlays on extracted molars Essentium PEEK (ESS) (Essentium Inc., Pflugerville, USA), KetaSpire® PEEK MS-NT1 (KET) (Solvay Specialty Polymers USA, L.L.C., Alpharetta GA, USA), VESTAKEEP® i4 G (VES) (exp. material) (Evonik Industries AG, Essen, Germany) and VICTREX® PEEK 450G (VIC) (Victrex plc., Thornton Cleveleys, UK)	FLM (HTRD1.2, KUMOVIS, Munich, Germany)	Unprepared and unrestored teeth (positive control) and milling: JUVORA Dental Disc 2 (JUV) and direct resin composite fillings out of Tetric EvoCeram (TET).	Fracture load evaluation. N = 8/group treated in a chewing simulator combined with thermal cycling (1.2 million × 50 N; 12,000 × 5 °C/55 °C).	ESS had the lowest fracture load with a minimum of 956 N. Chewing simulation combined with thermal cycling did not cause any fractures. With respect to fracture types, differences between the groups were observed ($p<0.001$). All indirect restorations, regardless of the fatigue process, showed a significantly higher tooth fracture rate (75–100%) than TET. All 3Dprinted inlays remained intact after the fracture load test.
Prechtel 2020	N = 120 samples printed on horizontal or vertical directions Essentium PEEK (ESS) (Essentium Inc., Pflugerville, USA), KetaSpire PEEK MPS-NT1(KET) (Solvay Specialty Polymers USA, L.L.C., Alpharetta GA, USA), VICTREX PEEK 450G (VIC) (Victrex plc., Thornton Cleveleys, UK), VESTAKEEP i4 G (VES) (Evonik Industries AG, Essen, Germany)	FLM (HTRD1.1, KUMOVIS GmbH, Munich, Germany)	Milling: PEEK blanks from breCAM.BioHPP, Dentokeep, JUVORA Dental Disc 2 and Ultaire AKP	Martens hardness (HM) determined at baseline and longitudinally after thermocycling (5−55◦C, 10,000x) and autoclaving (134◦C, 2 bar).	Hardness: 185 ± 3.51, 179 ± 14.5 , 171 ± 33.2, 150 ± 17.8, 168 ± 10.4, 153 ± 19.1, 176 ± 20.0 and 102 ± 13.8 MPa. Material had the highest impact on HM followed by printing direction ($p<0.001$) and aging process ($p=0.036$). ESS showed the highest and VIC the lowest values initially and after thermocycling and autoclaving ($p<0.001$). VIC showed initially a comparable HM value with VES ($p=0.290$) and KET ($p=0.104$). KET and VES showed comparable HM values ($p=0.403$).
Prpić 2020	N = 10 rectangular specimen	UV light curing (3DP)	Conventionally heat polymerized PMMA: ProBase Hot PBH	3-point flexural strength test (universal testing machine) and Brinell	Flexural strength: 71.70 ± 7.38 MPa. 3D-printed samples

	NextDent Base NDB = Monomer based on acrylic esters (Nextdent B.V.)		(IvoclarVivadent AG), Paladon 65 PAL (Kulzer GmbH), Interacryl Hot IAH (Interdent d.o.o.) Injection molding: Polyamide Vertex ThersmoSens VTS = Polyamide (Vertex-Dental B.V.) Milling: IvoBase CAD IBC (IvoclarVivadent AG), Interdent CC disc PMMA IDP(Interdentd.o.), Polident CAD/CAM disc basic PDD (Polident d.o.o.)	hardness	had the lowest flexural strength. Hardness: 116.29 ± 6.28 MPa. The maximal and minimal surface hardness values were 123.19 and 106.0 MPa.
Reymus **2020**	N= 60 fixed dental prosthesis (FDP) Experimental resin (EXP), NextDent C&B (CB), Freeprint temp (FT), and 3Delta temp (DT)	DLP (Rapidshape, GMBH)	Milling: PMMA, (TC) (TelioCAD, Ivoclar-Vivadent, Schaan, Liechtenstein) and conventional: interim material Luxatemp (LT).	Impact of 3D print material, build direction, post-curing, and artificial aging on fracture load	The highest values was for CB, DT and EXP showed the lowest values followed by FT (p<0.001). After artificial ageing there was a decrease in fracture load for EXP and DT (p<0.001). The highest impact on mechanical stability was exerted by material and post-curing unit (ηP2 =0.233), followed by material (ηP2 = 0.219) and curing device (ηP2 = 0.108) (p <0.001).
Schönhoff 2021	N = 368 cubic (10x10x4 mm) and bar (2x3x15mm) specimens poluphenylene sulfone: Fil-A-Gehr PPSU Radel (Gehr) and Ultrason P 3010 NAT (BASF)	FFF	Extrusion technique: Radel R-5000 NT (Solvay) and PEEK Juvora (Juvora)	Flexural strength, baseline and after 5.000 and 10.000 TC (5°-55°C, 20s) with 3-point flexural strength in universal testing machine (crosshead speed of 1 mm/min) and martens hardness (HM) by pressing a Vickers diamond indenter (α=136°) with a max load of 9.807 N for 20’’ vertically. All specimens were tested longitudinally after aging by TC (5°-55°C, 20s) after 5000 TC, 10.000 TC, 10.000 TC + 36 days dry storage, and 20.000 TC.	Flexural strength: after 5000 TC the lowest values were for PPSU2-3D (p<0.001). In PPSU1-3D values at 10,000 TC were higher than initial flexural strength results (p =0.009). Hardness: lowest for PPSU1-3D (p < 0.001).

Scotti 2020	3D-printed resin (PR) (NextDent C&B MFH; 3D Systems), autopolymerizing interim material (BA) (Protemp 4; 3M ESPE), and composite resin (Z350) (Filtek Z350XT; 3M ESPE)	SLA	None	Flexural strength (s) with 3-point bend test; Knoop hardness (H) and surface roughness (Ra) with a profilometer.	Z350 showed the highest values for s and H, followed by PR. BA showed the lowest results for both tests ($p<0.05$). Roughness: Z350 showed similar values to BA but lower than PR; PR showed similar roughness of BA.
Shim 2019	Bar specimen (80x10x4 mm) with 3 printing orientations (0, 45, and 90 degrees). PMMA NextDent Base; Vertex Dental)	SLA	None	Flexural strength and roughness	90° samples had the lowest error rates for length and 45° had higher error rates for thickness than other groups ($p<0.001$). Flexural strength increased in order 90°<45°<0° ($p<0.05$). The 45° samples had higher roughness ($p<0.001$).
Sim 2018	N = 8 crowns, bridges and inlay photoreactive liquid resin	DLP	None	Trueness	Trueness: 55.16 ± 2.70. Precision: 54.93 ± 8.44. 3D samples had the poorest accuracy with significant intergroup differences ($p<0.001$). Significant differences in trueness among model groups and types of preparation ($p<0.001$).
Tahayeri 2017	Samples bars (25 × 2 × 2 mm) commercial printable resin (NextDent C&B Vertex Dental) for provisional crowns and bridges.	SLA (FormLabs1+ printer)	Conventionally cured provisional materials (Integrity®, Dentsply; and Jet®, LangDental Inc.).	Accuracy (comparing width, length and thickness of samples for different printing orientation) and 3-point bending test.	Accuracy in relation to orientation: higher in thickness of 90° compared to 0° ($p<0.0001$) and 45° compared to 0° ($p < 0.001$) with 100 μm layer thickness.
Tasaka 2018	Denture base UV-curable acrylic resin (Vero Clear RGD835, Stratasys)	UV light curing	Heat cured molding: heat-curing resin (Acron No.5, GC, Tokyo, Japan)	Accuracy	The experimental denture base fabricated using AM was more accurate than the denture base fabricated with heat curing.
Tasaka 2021b	Maxillary and mandibular denture Ultravioletcured acrylic	PJ (Objet260 Connex; Stratasys).	Heat curing	Accuracy	Significant displacement of artificial tooth between experimental maxillary denture

	resin (UV)-cured acrylic resin (Vero Clear RGD835; Stratasys, Eden Prairie, MN, USA)				AM compared to heat curing samples ($p<0.05$).
Wang 2021	N = 170 bar shape (18 x 6 x 2mm) samples PEEK (VESTAKEEP® i4G, Evonik Industries AG, Essen, Germany)	FFF	None	3-point bending test	Flexural strengths: maximal value obtained with 0.4 mm nozzle; 0.6 mm were the stiffest, with the least deformation, while samples with a 0.2 mm nozzle were flexible compared to others. The differences between the 3 groups were significant ($p<0.05$).
Wemken 2020	n=16 complete denture base Photopolymerizable resin (Denture Base LP, Formlabs)	SLA (Form 2, Formlabs)	injection moldin (IM) and milling (MIL) samples (Zenotec Select, Wieland Dental).	3D surface deviation of the total intaglio surface, the palate, the alveolar ridge, and the border seal region evaluated (RMSE) after 5000 hydrothermal cycles in water baths (5°-55°C, dwell time 30s each), and microwave sterilization in distilled water (6 cycles at 640 W for 6 min + 24h dry).	Trueness: SLA had the highest total RMSE of 96 ± 17 µm (+53/-84 µm) ($p\leq 0.001$), with increased negative deviations in the same region. Trueness after hydrothermal cycling: no differences between MIL and IM but measured for SLA (*p* =0 .001). Trueness after microwave sterilization: total RMSE and all regions of SLA were lower compared with MIL and IM ($p =0.001$). Solely SLA printed denture bases were dimensionally stable after microwave sterilization
Wemken 2021	N = 24 specimen 30 x10x1.5 mm Photopolymerizable resin containing aliphatic urethane dimethacrylate (V-print dentbase, VOCO, Cuxhaven, Germany)	DLP (SolFlex 170, VOCO, Cuxhaven, Germany)	Conventional (CB) and milling (SB)	4-point bending test, and fracture analysis performed after either pre-treatment by water storage (50h, 37°C), hydrothermal cycling (5000 cycles, 5°C and 55°C, 30s each), or microwave irradiation (6 cycles, 640W, 2min, wet)	Flexural strength post ageing: 94.0 ± 11.5, 78.8 ± 14.5 and 73.8 ± 15.0 MPa. Flexural strength: AB showed a resistance of 94.0 ± 11.5 MPa after water storage (comparable to CB). Strength of AB was reduced after hydrothermal cycling and microwave irradiation. AM leads to reduced flexural strength compared to pouring.
Wu 2021	N=16 crowns Dima print denture teeth (Kulzer North	SLA	Milling (LuxaCrown, DMG, Hamburg, Germany) and manually manufactured (Lava Ultimate, 3M ESPE, St.	internal fit (silicone-checked method to measure internal gap) and marginal discrepancy (polyvinylsiloxane	Internal fit: 28.3 ± 9.3 axial, 101.9 ± 20.4 occlusal 108.7 ± 9.7 central

	America South Bend, IN, Usa)		Paul, MN, USA)	(PVS) replica method), optical coherence tomographic (OCT) scanning technique	pit. 3DP was significantly higher in gap distance at the occlusion than MAN and CAM ($p<0.05$). Marginal discrepancy: 120.8 ± 70.9 and 143.1 ± 39.9 µm. Considering absolute and horizontal marginal discrepancy, 3DP group had higher values than CAM and MAN ($p < 0.05$).
You 2020	N= 20 dentures (50µm and 100µm thickness) Resinliquid (ZMD-1000B; Dentis)	SLA	None	Trueness and accuracy evaluated with RMS formula.	Significant differences in trueness for intaglio and cameo surfaces ($p<0.05$). The cameo surface show a significant difference in precision ($p<0.001$). It is clinically more appropriate to set the layer thickness to 100 µm rather than 50 µm.

FIGURES

Figure 1: PRISMA flow-diagram reporting the study selection.

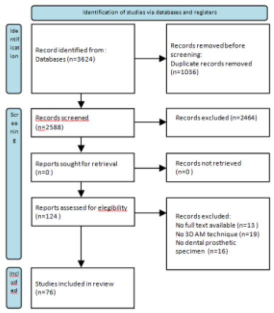

Figure 2: Flexural strength forest plot.

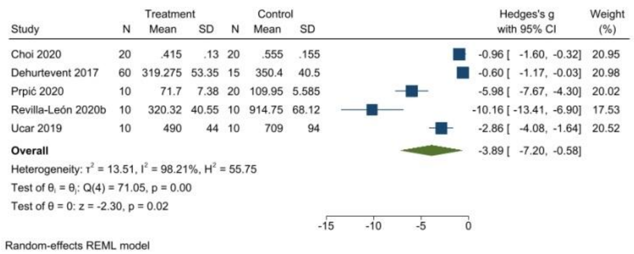

Figure 3: Flexural strength post-ageing forest plot.

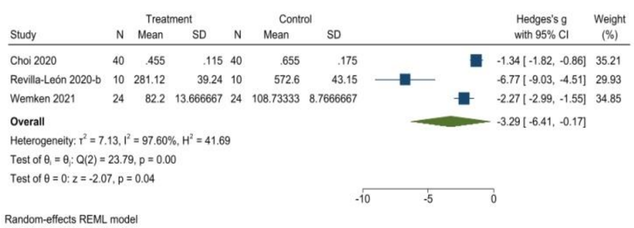

Figure 4: Fracture load forest plot.

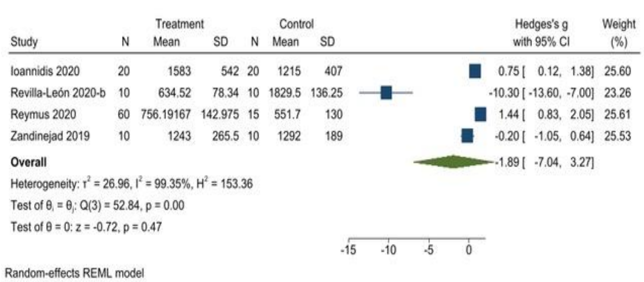

Figure 5: Hardness forest plot.

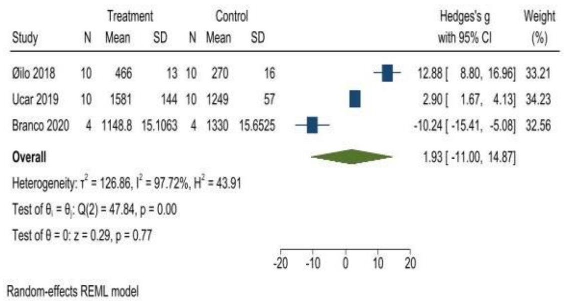

Figure 6: Roughness forest plot.

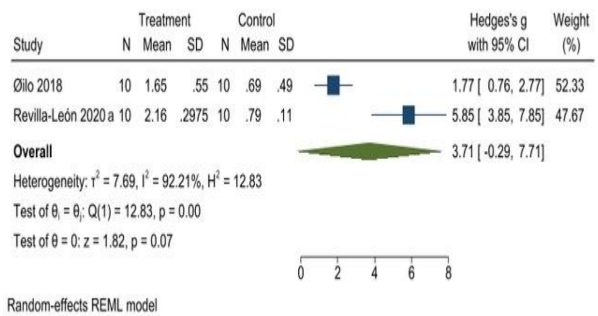

Figure 7: Trueness forest plot.

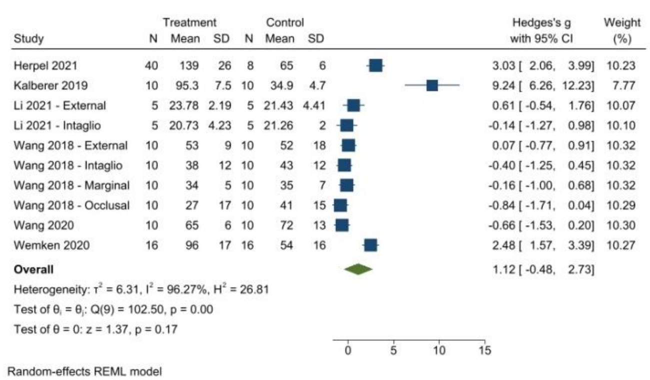

Figure 8: Trueness post-ageing forest plot.

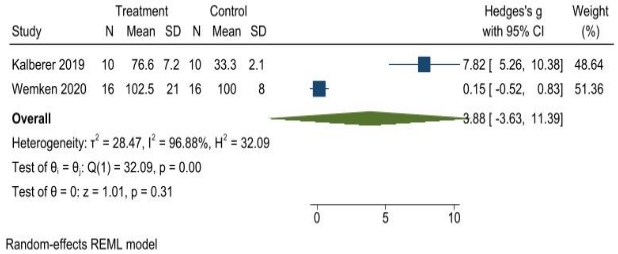

Figure 9: Marginal discrepancy forest plot.

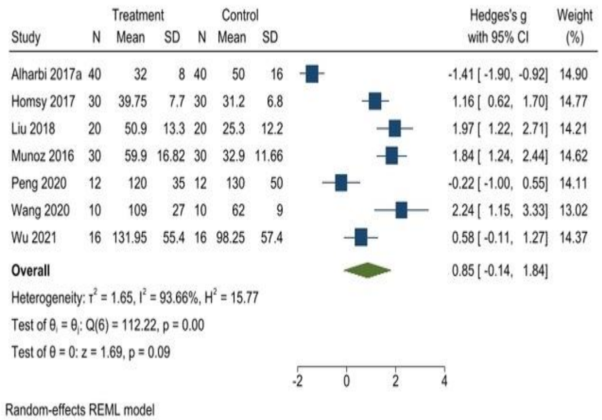

Figure 10: Internal fit forest plot.

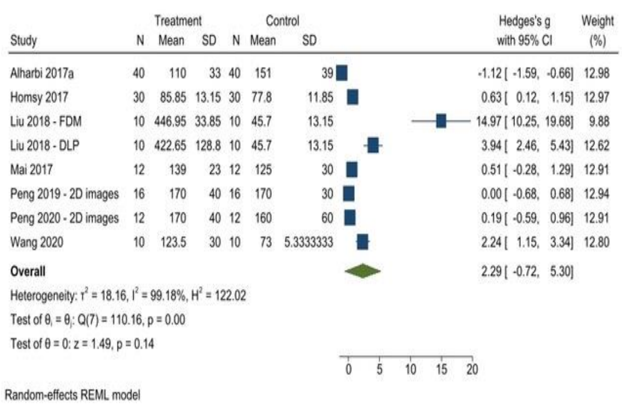

Supplementary Figure 1: PRISMA checklist.

PRISMA 2020 Checklist

Section and Topic	Item #	Checklist item	Location where item is reported
TITLE			
Title	1	Identify the report as a systematic review.	page 1
ABSTRACT			
Abstract	2	See the PRISMA 2020 for Abstracts checklist.	pages 2-3
INTRODUCTION			
Rationale	3	Describe the rationale for the review in the context of existing knowledge.	pages 3-5
Objectives	4	Provide an explicit statement of the objective(s) or question(s) the review addresses.	page 5
METHODS			
Eligibility criteria	5	Specify the inclusion and exclusion criteria for the review and how studies were grouped for the syntheses.	page 6, Table 1
Information sources	6	Specify all databases, registers, websites, organisations, reference lists and other sources searched or consulted to identify studies. Specify the date when each source was last searched or consulted.	page 6
Search strategy	7	Present the full search strategies for all databases, registers and websites, including any filters and limits used.	page 6, Supplementary Table 1
Selection process	8	Specify the methods used to decide whether a study met the inclusion criteria of the review, including how many reviewers screened each record and each report retrieved, whether they worked independently, and if applicable, details of automation tools used in the process.	pages 6-7
Data collection process	9	Specify the methods used to collect data from reports, including how many reviewers collected data from each report, whether they worked independently, any processes for obtaining or confirming data from study investigators, and if applicable, details of automation tools used in the process.	page 7
Data items	10a	List and define all outcomes for which data were sought. Specify whether all results that were compatible with each outcome domain in each study were sought (e.g. for all measures, time points, analyses), and if not, the methods used to decide which results to collect.	page 7
	10b	List and define all other variables for which data were sought (e.g. participant and intervention characteristics, funding sources). Describe any assumptions made about any missing or unclear information.	page 7
Study risk of bias assessment	11	Specify the methods used to assess risk of bias in the included studies, including details of the tool(s) used, how many reviewers assessed each study and whether they worked independently, and if applicable, details of automation tools used in the process.	page 8
Effect measures	12	Specify for each outcome the effect measure(s) (e.g. risk ratio, mean difference) used in the synthesis or presentation of results.	page 7
Synthesis methods	13a	Describe the processes used to decide which studies were eligible for each synthesis (e.g. tabulating the study intervention characteristics and comparing against the planned groups for each synthesis (item #5)).	page 7
	13b	Describe any methods required to prepare the data for presentation or synthesis, such as handling of missing summary statistics, or data conversions.	page 7
	13c	Describe any methods used to tabulate or visually display results of individual studies and syntheses.	page 7
	13d	Describe any methods used to synthesize results and provide a rationale for the choice(s). If meta-analysis was performed, describe the model(s), method(s) to identify the presence and extent of statistical heterogeneity, and software package(s) used.	pages 7-8
	13e	Describe any methods used to explore possible causes of heterogeneity among study results (e.g. subgroup analysis, meta-regression).	pages 7-8
	13f	Describe any sensitivity analyses conducted to assess robustness of the synthesized results.	pages 7-8
Reporting bias	14	Describe any methods used to assess risk of bias due to missing results in a synthesis (arising from reporting biases).	page 8

PRISMA 2020 Checklist

Section and Topic	Item #	Checklist item	Location where item is reported
assessment			
Certainty assessment	15	Describe any methods used to assess certainty (or confidence) in the body of evidence for an outcome.	page 8
RESULTS			
Study selection	16a	Describe the results of the search and selection process, from the number of records identified in the search to the number of studies included in the review, ideally using a flow diagram.	pages 8-9, Figure 1
	16b	Cite studies that might appear to meet the inclusion criteria, but which were excluded, and explain why they were excluded.	pages 8-9, Figure 1
Study characteristics	17	Cite each included study and present its characteristics.	pages 9-12, Table 2 and 3
Risk of bias in studies	18	Present assessments of risk of bias for each included study.	page 9, Table 3
Results of individual studies	19	For all outcomes, present, for each study: (a) summary statistics for each group (where appropriate) and (b) an effect estimate and its precision (e.g. confidence/credible interval), ideally using structured tables or plots.	pages 9-12, Table 2 and 3
Results of syntheses	20a	For each synthesis, briefly summarise the characteristics and risk of bias among contributing studies.	pages 9-12
	20b	Present results of all statistical syntheses conducted. If meta-analysis was done, present for each the summary estimate and its precision (e.g. confidence/credible interval) and measures of statistical heterogeneity. If comparing groups, describe the direction of the effect.	Figures 2-10, Supplementary Figures 2-10
	20c	Present results of all investigations of possible causes of heterogeneity among study results.	pages 10-12
	20d	Present results of all sensitivity analyses conducted to assess the robustness of the synthesized results.	pages 10-12
Reporting biases	21	Present assessments of risk of bias due to missing results (arising from reporting biases) for each synthesis assessed.	Pages 9-12
Certainty of evidence	22	Present assessments of certainty (or confidence) in the body of evidence for each outcome assessed.	pages 9-12
DISCUSSION			
Discussion	23a	Provide a general interpretation of the results in the context of other evidence.	pages 12-15
	23b	Discuss any limitations of the evidence included in the review.	page 15
	23c	Discuss any limitations of the review processes used.	page 15
	23d	Discuss implications of the results for practice, policy, and future research.	pages 15-16
OTHER INFORMATION			
Registration and protocol	24a	Provide registration information for the review, including register name and registration number, or state that the review was not registered.	pages 5-6
	24b	Indicate where the review protocol can be accessed, or state that a protocol was not prepared.	pages 5-6
	24c	Describe and explain any amendments to information provided at registration or in the protocol.	pages 5-6
Support	25	Describe sources of financial or non-financial support for the review, and the role of the funders or sponsors in the review.	page 26
Competing interests	26	Declare any competing interests of review authors.	page 26
Availability of	27	Report which of the following are publicly available and where they can be found: template data collection forms; data extracted from included	N/A

PRISMA 2020 Checklist

Section and Topic	Item #	Checklist item	Location where item is reported
data, code and other materials		studies; data used for all analyses; analytic code; any other materials used in the review.	

From: Page MJ, McKenzie JE, Bossuyt PM, Boutron I, Hoffmann TC, Mulrow CD, et al. The PRISMA 2020 statement: an updated guideline for reporting systematic reviews. BMJ 2021;372:n71.doi: 10.1136/bmj.n71

For more information, visit:http://www.prisma-statement.org/

Supplementary Figure 2: Flexural strength funnel.

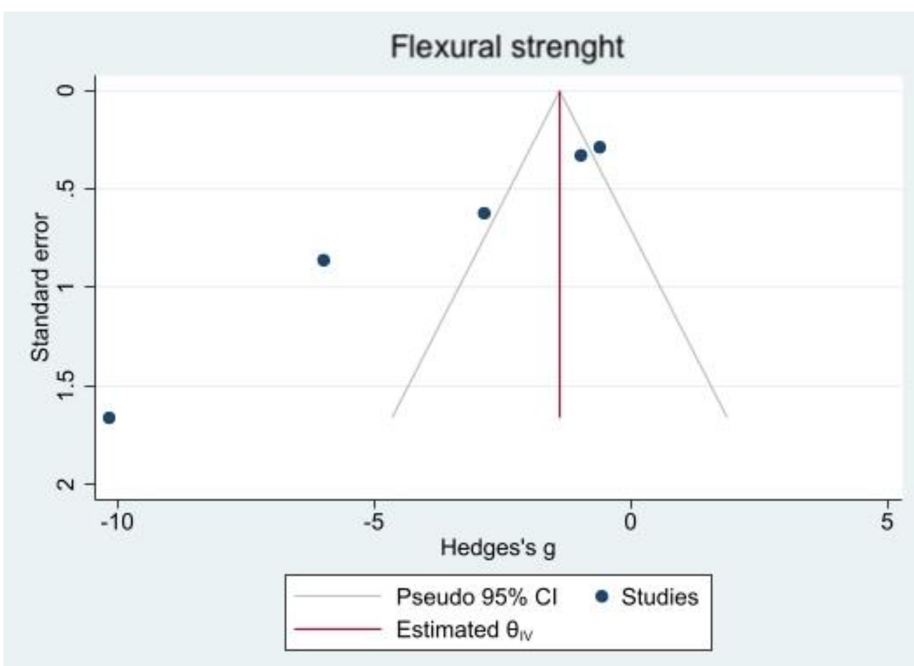

Supplementary Figure 3: Flexural strength post-ageing funnel.

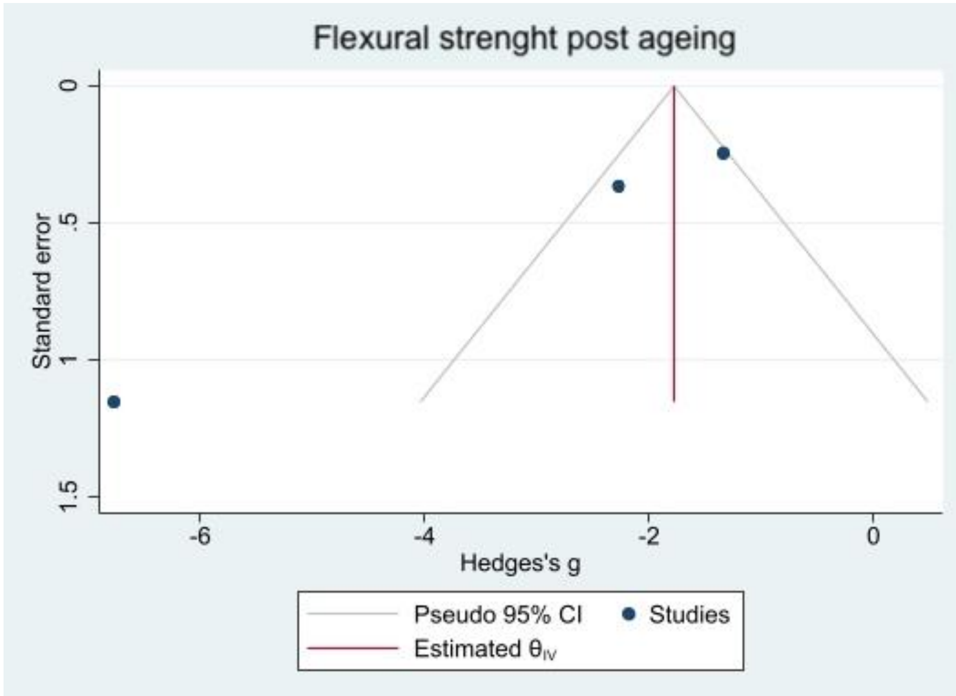

Supplementary Figure 4: Fracture load funnel.

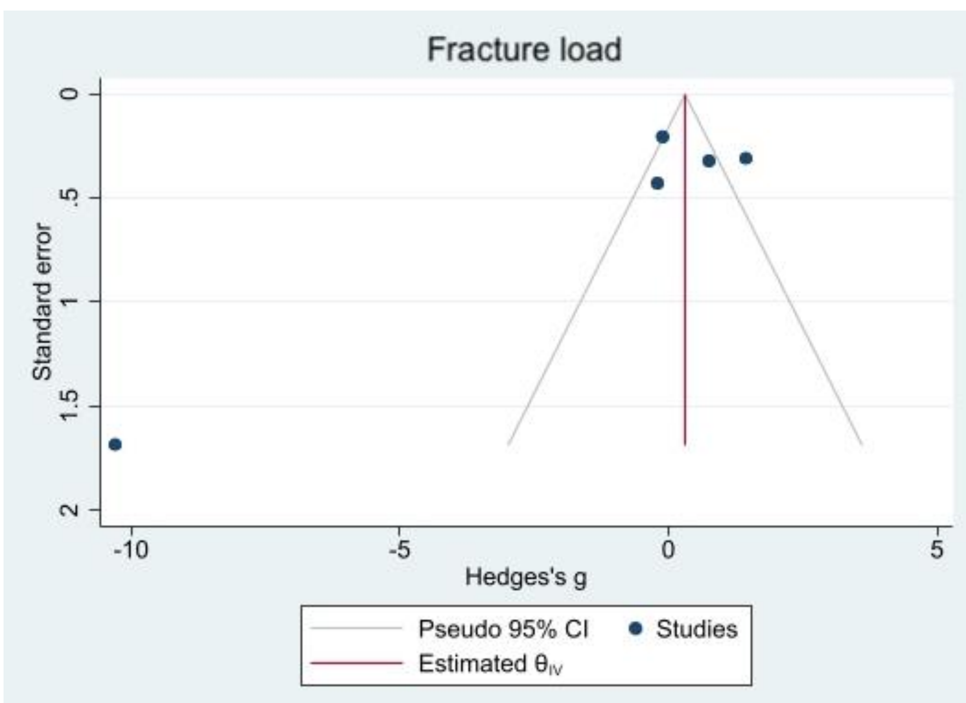

Supplementary Figure 5: Hardness funnel.

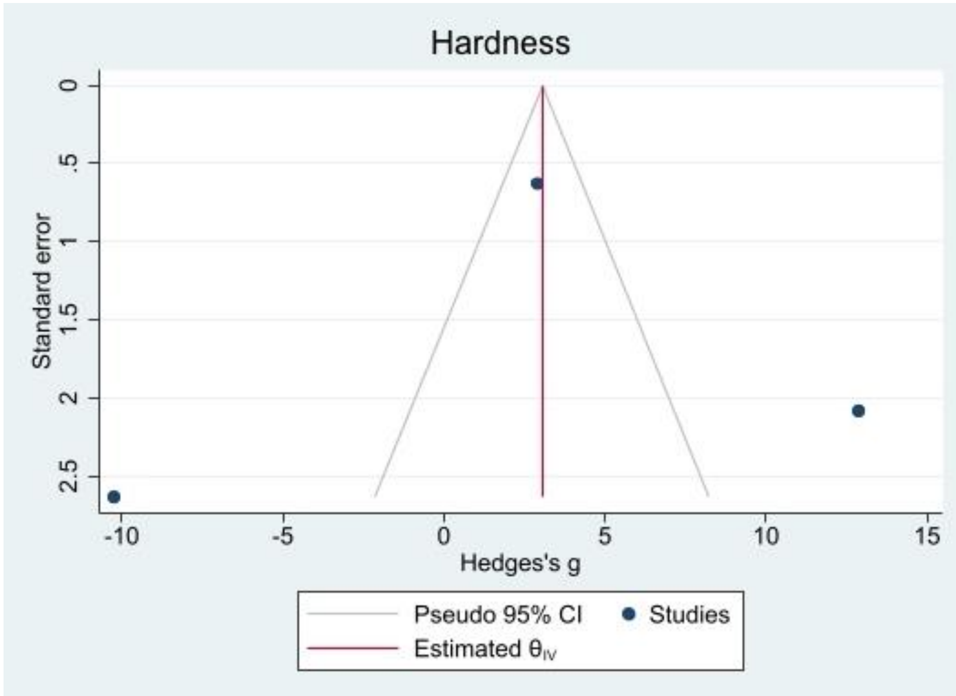

Supplementary Figure 6: Roughness funnel.

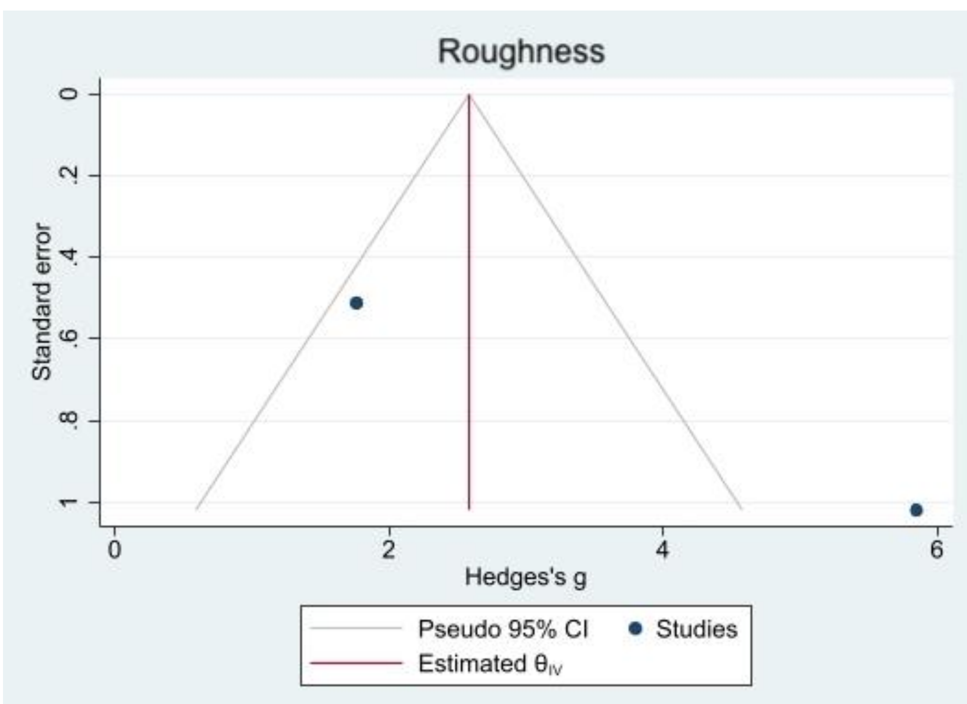

Supplementary Figure 7: Trueness funnel.

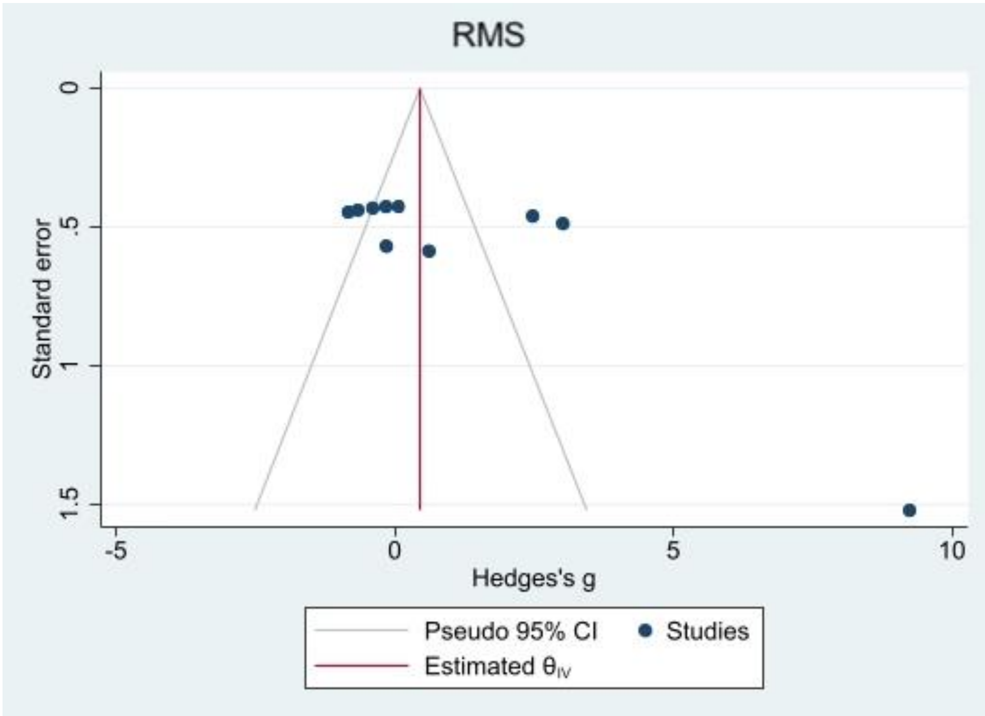

Supplementary Figure 8: Trueness post-ageing funnel.

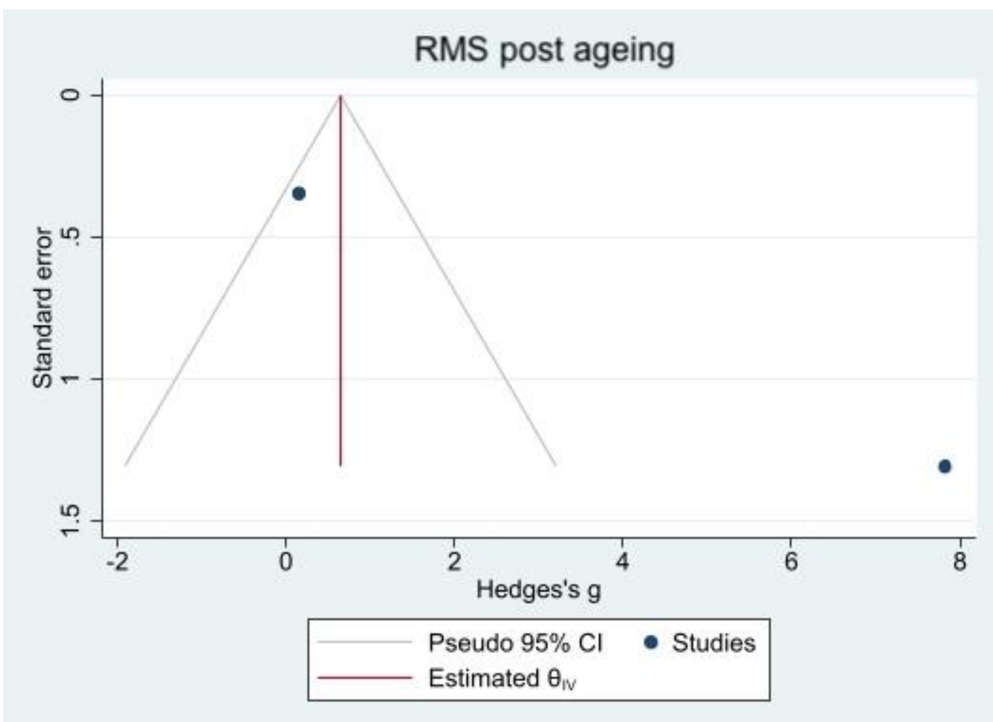

Supplementary Figure 9: Marginal discrepancy funnel.

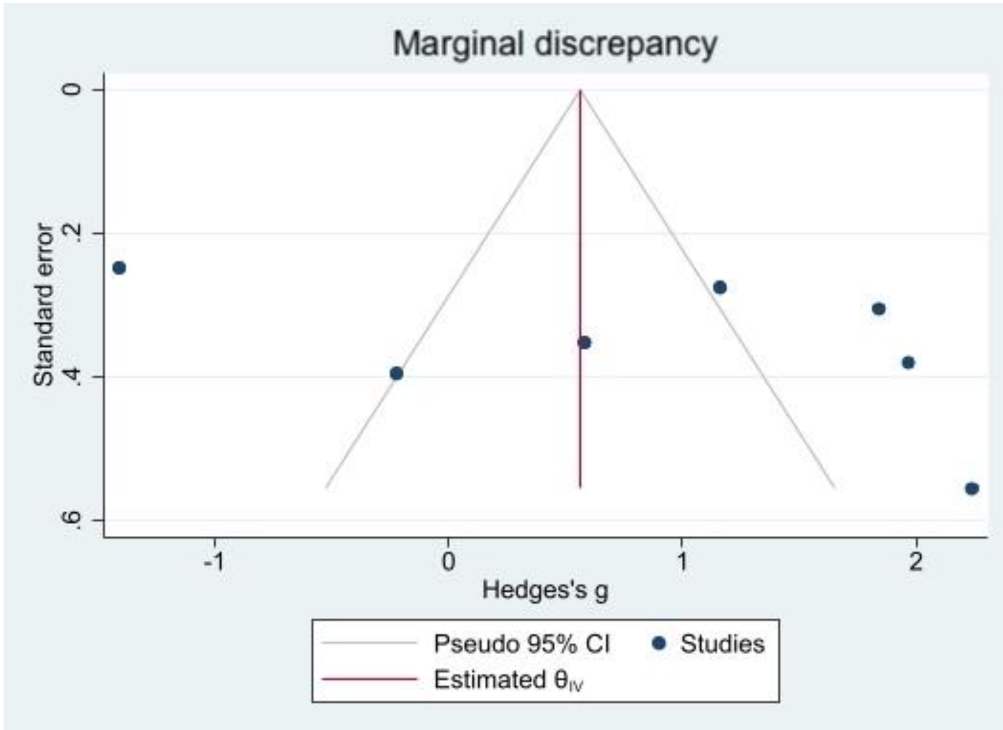

Supplementary Figure 10: Internal fit funnel.

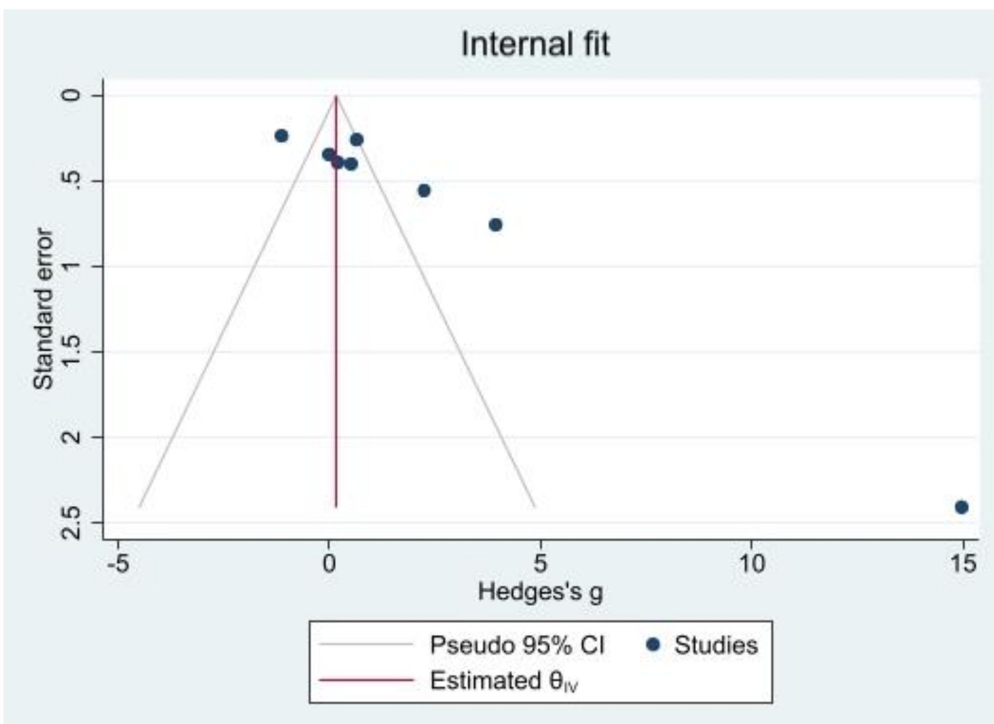

Supplementary Table 1

	Pubmed (12/05/2021)
Search	Query
#1	("additive manufacturing"[All Fields] OR "3D printing dentistry "[All Fields] OR "3D printing"[All Fields] OR (3D print* [title/abstract]) OR (additive manufact* [title/abstract]) OR “RP Technologies” [title/abstract] OR “Rapid Prototyping” [title/abstract] OR “three-dimensional printing” [title/abstract] OR “stereolithographic” [title/abstract] OR ("Printing, Three-Dimensional"[MeSH Terms]) OR ("Stereolithography"[MeSH Terms]) AND (("2011/05/05"[Date - Publication] : "2021/05/05"[Date - Publication]))) NOT (Systematic Review [Publication Type] OR Review [Publication Type] OR Meta-Analysis [Publication Type] OR Comment [Publication Type] OR Congress [Publication Type] OR Editorial [Publication Type] OR Case Reports [Publication Type] OR Clinical Conference [Publication Type] OR Comment [Publication Type] OR Consensus Development Conference [Publication Type])
#2	("Dental Prosthesis"[MeSH Terms] OR "Prosthodontics"[MeSH Terms] OR "Dentistry, Operative"[Mesh] OR "dental prosthesis"[All Fields] OR "crowns"[All Fields] OR "denture"[All Fields] OR "Prosthetic Dentistry"[All Fields] OR "Dental Materials"[Mesh] OR "Biomedical and Dental Materials"[Mesh] OR "Dental Materials"[All Fields] OR Dental Material* AND (("2011/05/05"[Date - Publication] : "2021/05/05"[Date - Publication]))) NOT (Systematic Review [Publication Type] OR Review [Publication Type] OR Meta-Analysis [Publication Type] OR Comment [Publication Type] OR Congress [Publication Type] OR Editorial [Publication Type] OR Case Reports [Publication Type] OR Clinical Conference [Publication Type] OR Comment [Publication Type] OR Consensus Development Conference [Publication Type])
#3	#1 AND #2 Filters: English, Italian

Fig. 1

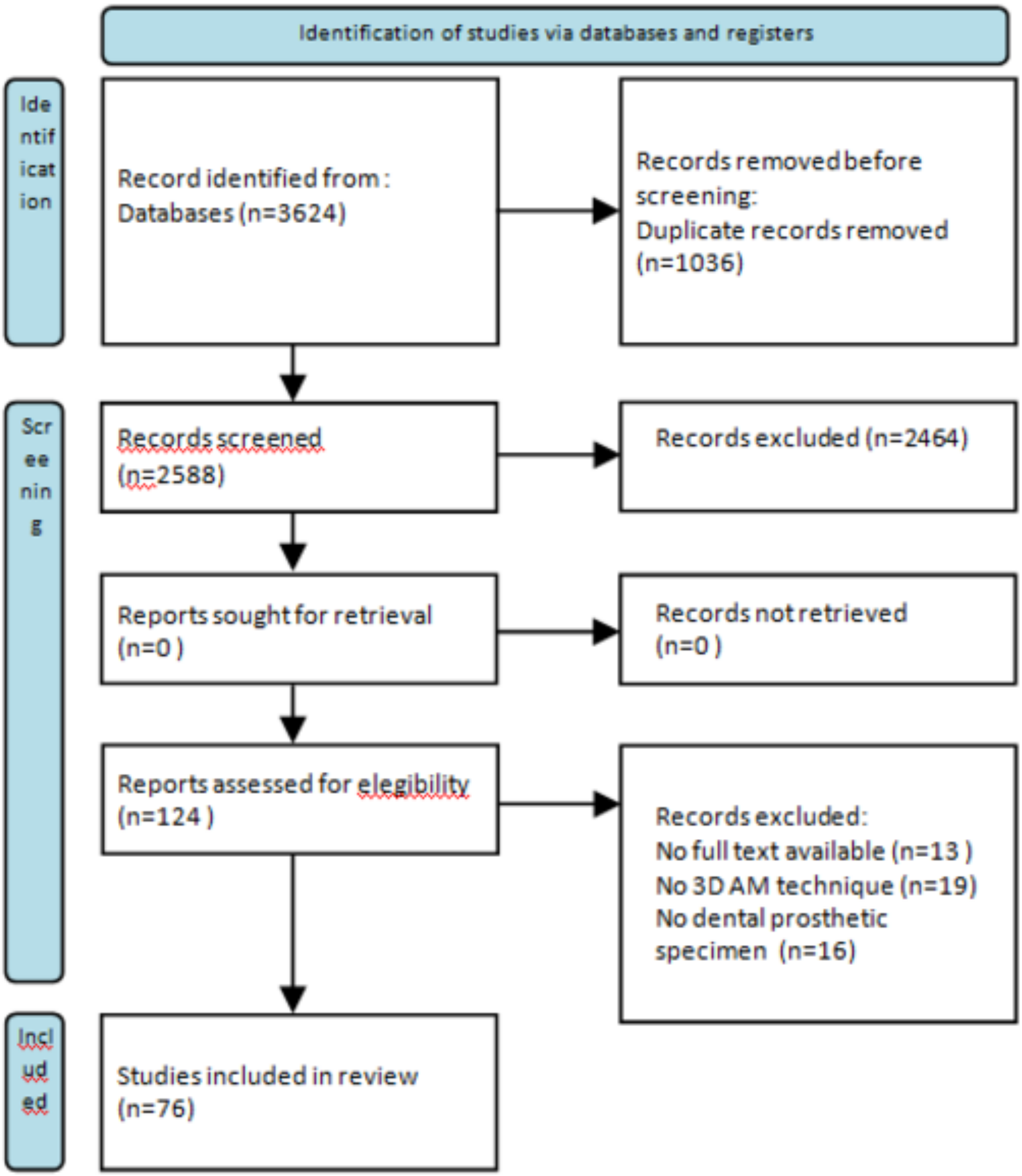
Identification of studies via databases and registers
Ide ntif icat ion
Record identified from : Databases (n=3624)
Records removed before screening: Duplicate records removed (n=1036)
Scr ee nin g
Records screened (n=2588)
Records excluded (n=2464)
Reports sought for retrieval (n=0)
Records not retrieved (n=0)
Reports assessed for elegibility (n=124)
Records excluded: No full text available (n=13) No 3D AM technique (n=19) No dental prosthetic specimen (n=16)
Incl ud ed
Studies included in review (n=76)

Fig. 2

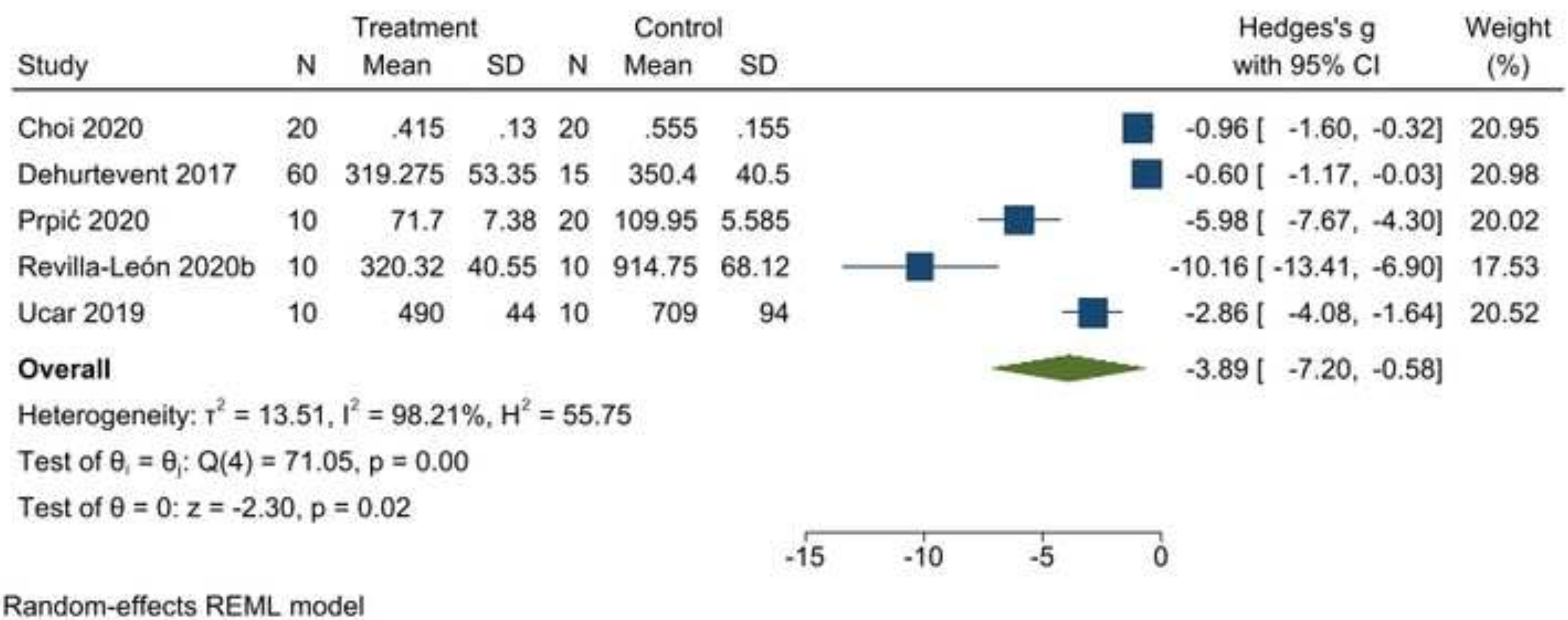
Treatment
Control
Hedges's g with 95% CI
Weight (%)
Study N Mean SD N Mean SD
Choi 2020 20 .415 .13 20 .555 .155 -0.96 [-1.60, -0.32] 20.95
Dehurtevent 2017 60 319.275 53.35 15 350.4 40.5 -0.60 [-1.17, -0.03] 20.98
Prpić 2020 10 71.7 7.38 20 109.95 5.585 -5.98 [-7.67, -4.30] 20.02
Revilla-León 2020b 10 320.32 40.55 10 914.75 68.12 -10.16 [-13.41, -6.90] 17.53
Ucar 2019 10 490 44 10 709 94 -2.86 [-4.08, -1.64] 20.52
Overall -3.89 [-7.20, -0.58]
Heterogeneity: τ² = 13.51, I² = 98.21%, H² = 55.75
Test of θᵢ = θⱼ: Q(4) = 71.05, p = 0.00
Test of θ = 0: z = -2.30, p = 0.02
-15
-10
-5
0
Random-effects REML model

Fig.3

Click here to access/download;Figure;Fig. 3 jpeg.jpg

Study	Treatment N	Treatment Mean	Treatment SD	Control N	Control Mean	Control SD	Hedges's g with 95% CI	Weight (%)
Choi 2020	40	.455	.115	40	.655	.175	-1.34 [-1.82, -0.86]	35.21
Revilla-León 2020-b	10	281.12	39.24	10	572.6	43.15	-6.77 [-9.03, -4.51]	29.93
Wemken 2021	24	82.2	13.666667	24	108.73333	8.7666667	-2.27 [-2.99, -1.55]	34.85
Overall							-3.29 [-6.41, -0.17]	

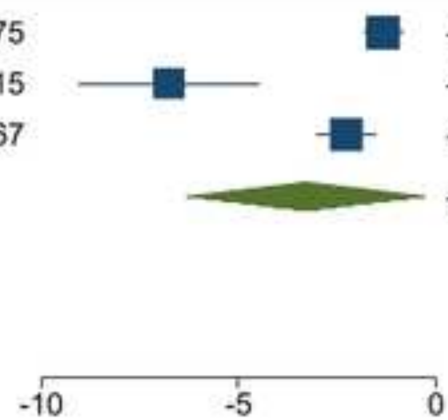

Heterogeneity: $\tau^2 = 7.13$, $I^2 = 97.60\%$, $H^2 = 41.69$

Test of $\theta_i = \theta_j$: $Q(2) = 23.79$, $p = 0.00$

Test of $\theta = 0$: $z = -2.07$, $p = 0.04$

Random-effects REML model

Fig. 4

Study	Treatment N	Treatment Mean	Treatment SD	Control N	Control Mean	Control SD	Hedges's g with 95% CI	Weight (%)
Ioannidis 2020	20	1583	542	20	1215	407	0.75 [0.12, 1.38]	25.60
Revilla-León 2020-b	10	634.52	78.34	10	1829.5	136.25	-10.30 [-13.60, -7.00]	23.26
Reymus 2020	60	756.19167	142.975	15	551.7	130	1.44 [0.83, 2.05]	25.61
Zandinejad 2019	10	1243	265.5	10	1292	189	-0.20 [-1.05, 0.64]	25.53
Overall							-1.89 [-7.04, 3.27]	

Heterogeneity: $\tau^2 = 26.96$, $I^2 = 99.35\%$, $H^2 = 153.36$

Test of $\theta_i = \theta_j$: Q(3) = 52.84, p = 0.00

Test of $\theta = 0$: z = -0.72, p = 0.47

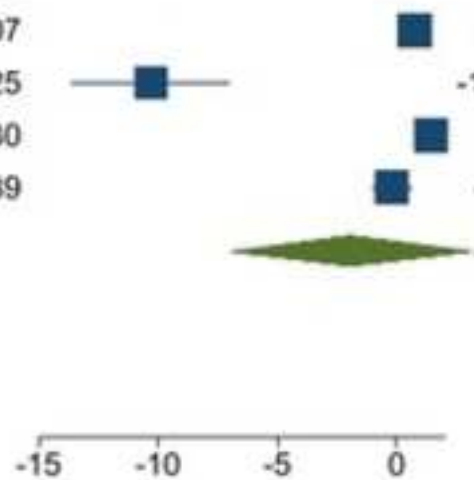

Random-effects REML model

Fig. 5

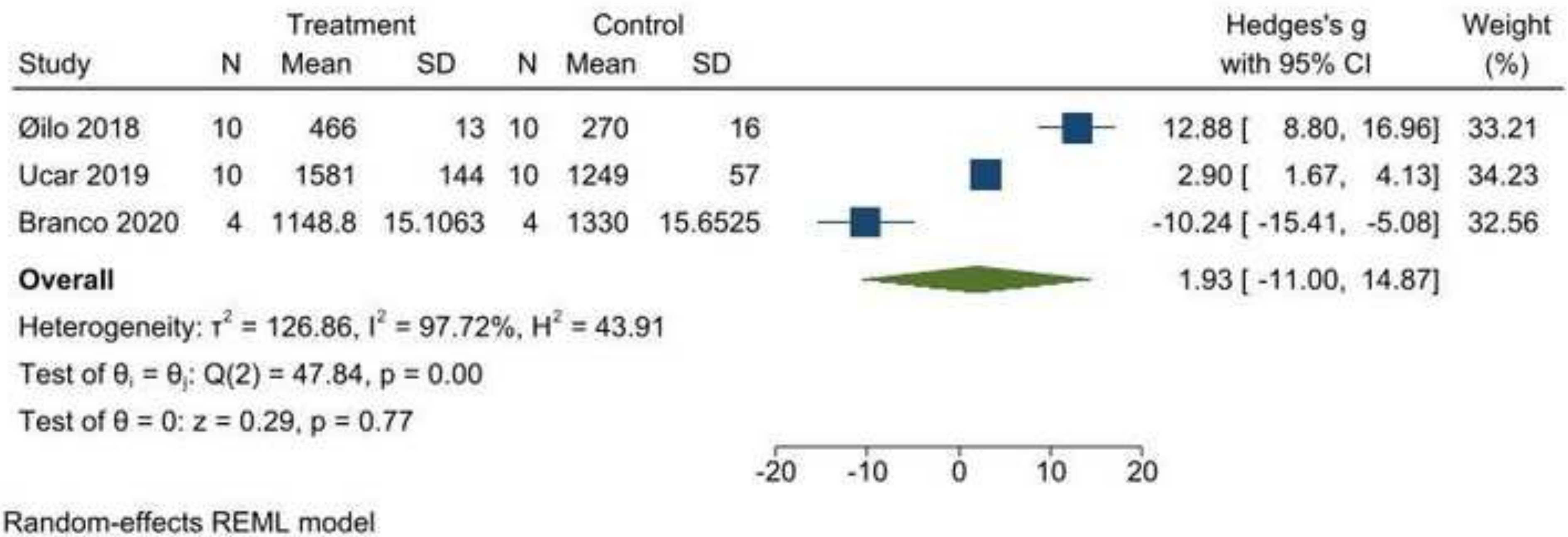

Treatment
Control
Study N Mean SD N Mean SD
Hedges's g with 95% CI
Weight (%)
Øilo 2018 10 466 13 10 270 16 12.88 [8.80, 16.96] 33.21
Ucar 2019 10 1581 144 10 1249 57 2.90 [1.67, 4.13] 34.23
Branco 2020 4 1148.8 15.1063 4 1330 15.6525 -10.24 [-15.41, -5.08] 32.56
Overall 1.93 [-11.00, 14.87]
Heterogeneity: τ² = 126.86, I² = 97.72%, H² = 43.91
Test of θi = θj: Q(2) = 47.84, p = 0.00
Test of θ = 0: z = 0.29, p = 0.77
-20 -10 0 10 20
Random-effects REML model

Fig. 6

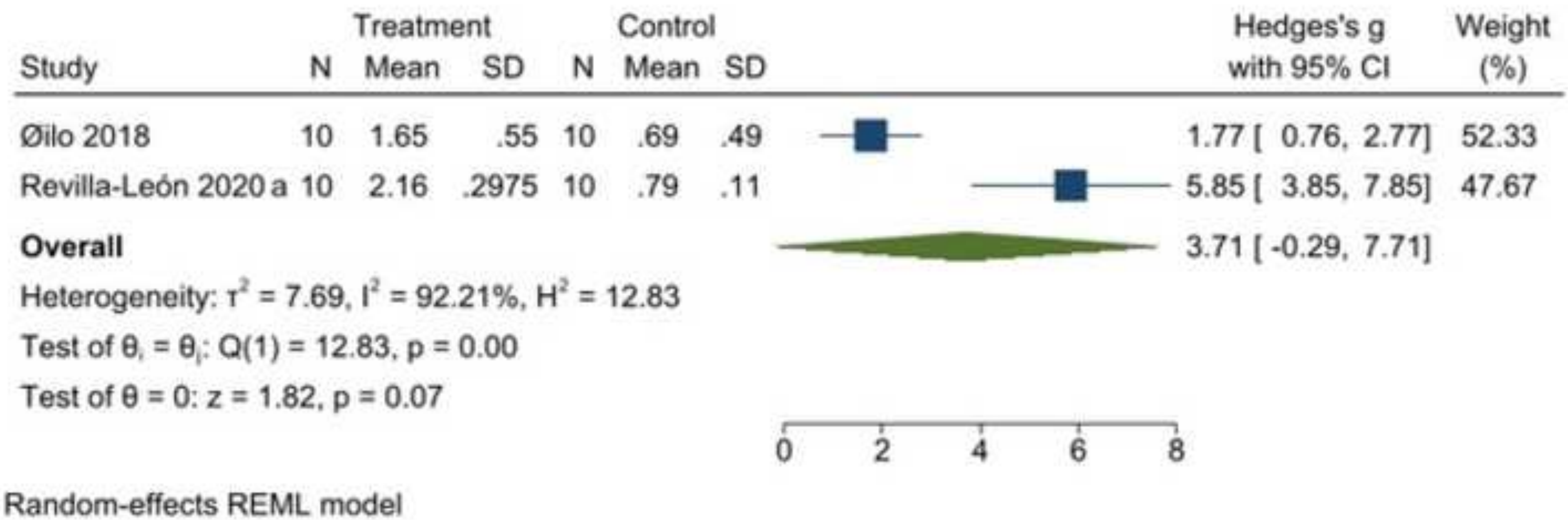
Treatment
Control
Hedges's g with 95% CI
Weight (%)
Study
N
Mean
SD
N
Mean
SD
Øilo 2018 10 1.65 .55 10 .69 .49
1.77 [0.76, 2.77] 52.33
Revilla-León 2020 a 10 2.16 .2975 10 .79 .11
5.85 [3.85, 7.85] 47.67
Overall
3.71 [-0.29, 7.71]
Heterogeneity: τ² = 7.69, I² = 92.21%, H² = 12.83
Test of θi = θj: Q(1) = 12.83, p = 0.00
Test of θ = 0: z = 1.82, p = 0.07
0
2
4
6
8
Random-effects REML model

Fig. 7

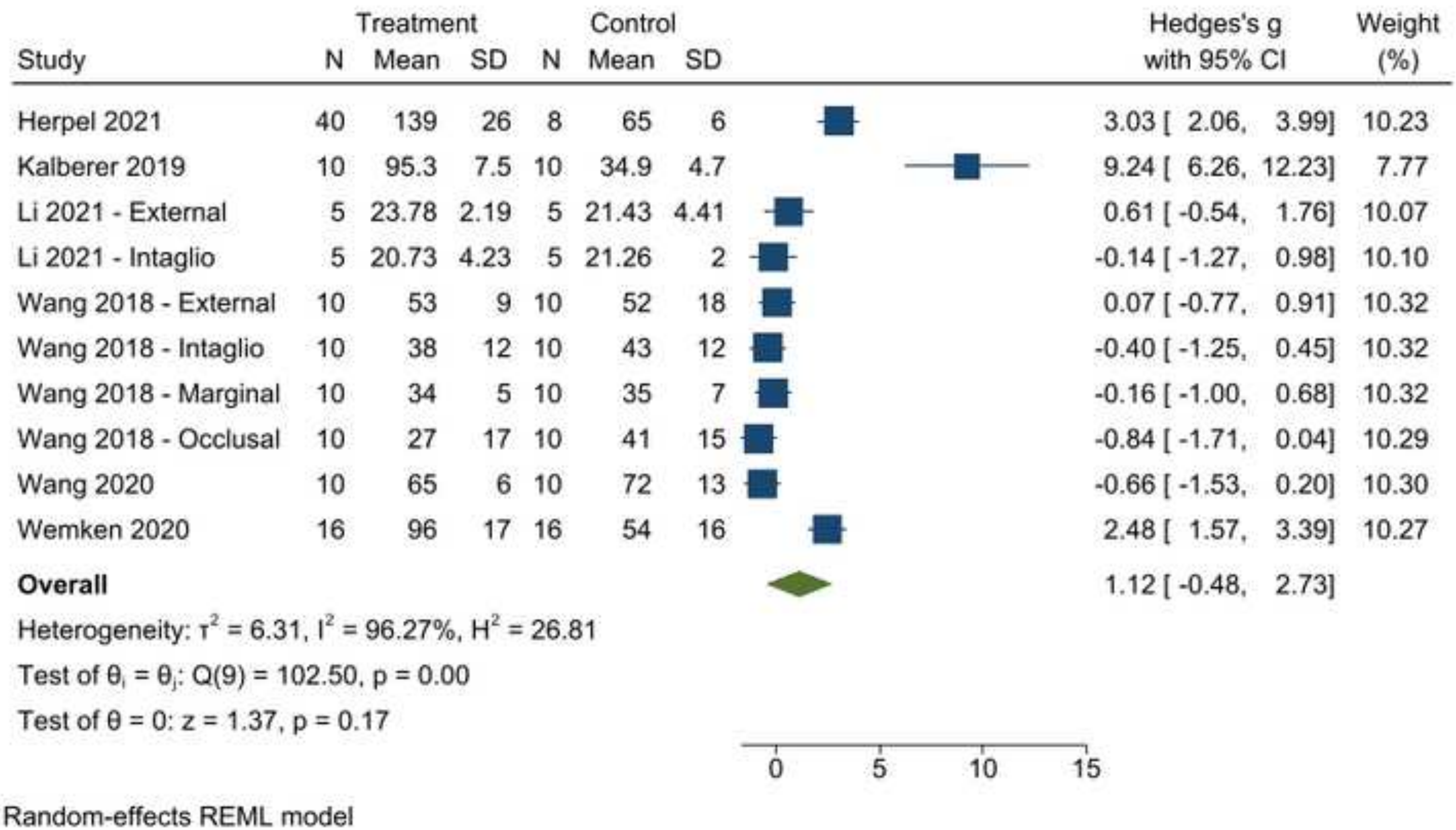
Treatment
Control
Study
N Mean SD N Mean SD
Hedges's g with 95% CI
Weight (%)
Herpel 2021 40 139 26 8 65 6 3.03 [2.06, 3.99] 10.23
Kalberer 2019 10 95.3 7.5 10 34.9 4.7 9.24 [6.26, 12.23] 7.77
Li 2021 - External 5 23.78 2.19 5 21.43 4.41 0.61 [-0.54, 1.76] 10.07
Li 2021 - Intaglio 5 20.73 4.23 5 21.26 2 -0.14 [-1.27, 0.98] 10.10
Wang 2018 - External 10 53 9 10 52 18 0.07 [-0.77, 0.91] 10.32
Wang 2018 - Intaglio 10 38 12 10 43 12 -0.40 [-1.25, 0.45] 10.32
Wang 2018 - Marginal 10 34 5 10 35 7 -0.16 [-1.00, 0.68] 10.32
Wang 2018 - Occlusal 10 27 17 10 41 15 -0.84 [-1.71, 0.04] 10.29
Wang 2020 10 65 6 10 72 13 -0.66 [-1.53, 0.20] 10.30
Wemken 2020 16 96 17 16 54 16 2.48 [1.57, 3.39] 10.27
Overall 1.12 [-0.48, 2.73]
Heterogeneity: τ² = 6.31, I² = 96.27%, H² = 26.81
Test of θi = θj: Q(9) = 102.50, p = 0.00
Test of θ = 0: z = 1.37, p = 0.17
0
5
10
15
Random-effects REML model

Fig. 8

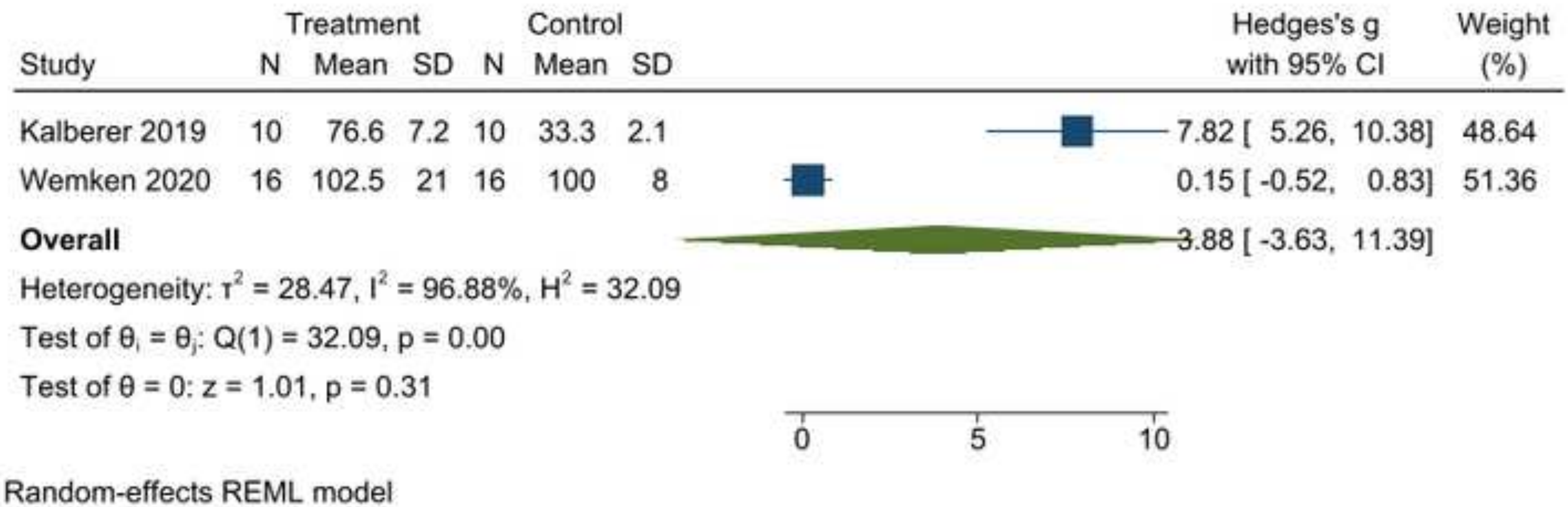
Treatment
Control
Hedges's g with 95% CI
Weight (%)
Study
N
Mean
SD
N
Mean
SD
Kalberer 2019 10 76.6 7.2 10 33.3 2.1
7.82 [5.26, 10.38] 48.64
Wemken 2020 16 102.5 21 16 100 8
0.15 [-0.52, 0.83] 51.36
Overall
3.88 [-3.63, 11.39]
Heterogeneity: τ² = 28.47, I² = 96.88%, H² = 32.09
Test of θi = θj: Q(1) = 32.09, p = 0.00
Test of θ = 0: z = 1.01, p = 0.31
0
5
10
Random-effects REML model

Fig. 9

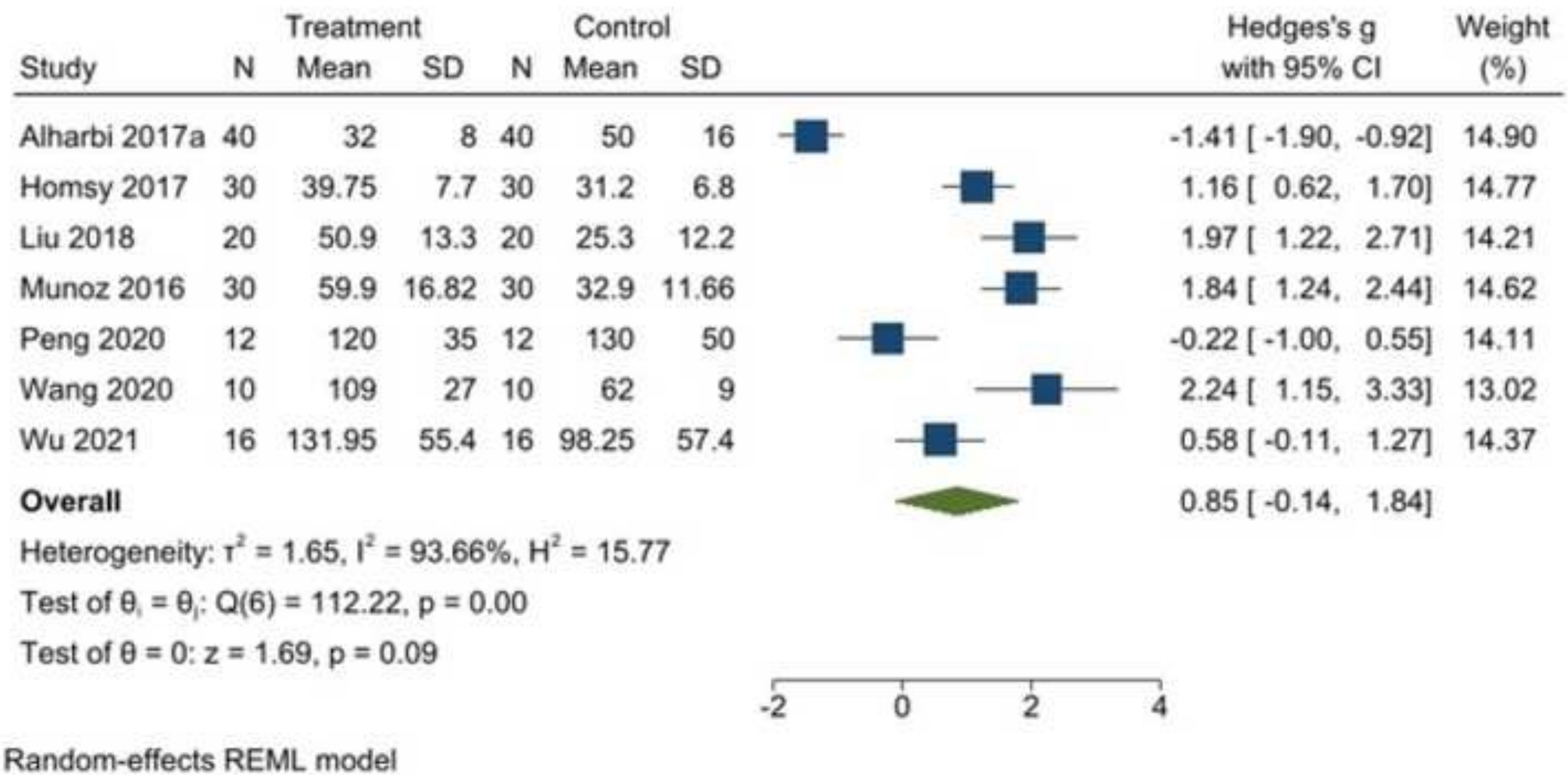
Treatment
Control
Study N Mean SD N Mean SD
Hedges's g with 95% CI
Weight (%)
Alharbi 2017a 40 32 8 40 50 16 -1.41 [-1.90, -0.92] 14.90
Homsy 2017 30 39.75 7.7 30 31.2 6.8 1.16 [0.62, 1.70] 14.77
Liu 2018 20 50.9 13.3 20 25.3 12.2 1.97 [1.22, 2.71] 14.21
Munoz 2016 30 59.9 16.82 30 32.9 11.66 1.84 [1.24, 2.44] 14.62
Peng 2020 12 120 35 12 130 50 -0.22 [-1.00, 0.55] 14.11
Wang 2020 10 109 27 10 62 9 2.24 [1.15, 3.33] 13.02
Wu 2021 16 131.95 55.4 16 98.25 57.4 0.58 [-0.11, 1.27] 14.37
Overall 0.85 [-0.14, 1.84]
Heterogeneity: τ² = 1.65, I² = 93.66%, H² = 15.77
Test of θi = θj: Q(6) = 112.22, p = 0.00
Test of θ = 0: z = 1.69, p = 0.09
-2
0
2
4
Random-effects REML model

Fig. 10

Click here to access/download;Figure;Fig. 10 jpeg.jpeg

Study	Treatment N	Treatment Mean	Treatment SD	Control N	Control Mean	Control SD	Hedges's g with 95% CI	Weight (%)
Alharbi 2017a	40	110	33	40	151	39	-1.12 [-1.59, -0.66]	12.98
Homsy 2017	30	85.85	13.15	30	77.8	11.85	0.63 [0.12, 1.15]	12.97
Liu 2018 - FDM	10	446.95	33.85	10	45.7	13.15	14.97 [10.25, 19.68]	9.88
Liu 2018 - DLP	10	422.65	128.8	10	45.7	13.15	3.94 [2.46, 5.43]	12.62
Mai 2017	12	139	23	12	125	30	0.51 [-0.28, 1.29]	12.91
Peng 2019 - 2D images	16	170	40	16	170	30	0.00 [-0.68, 0.68]	12.94
Peng 2020 - 2D images	12	170	40	12	160	60	0.19 [-0.59, 0.96]	12.91
Wang 2020	10	123.5	30	10	73	5.3333333	2.24 [1.15, 3.34]	12.80
Overall							2.29 [-0.72, 5.30]	

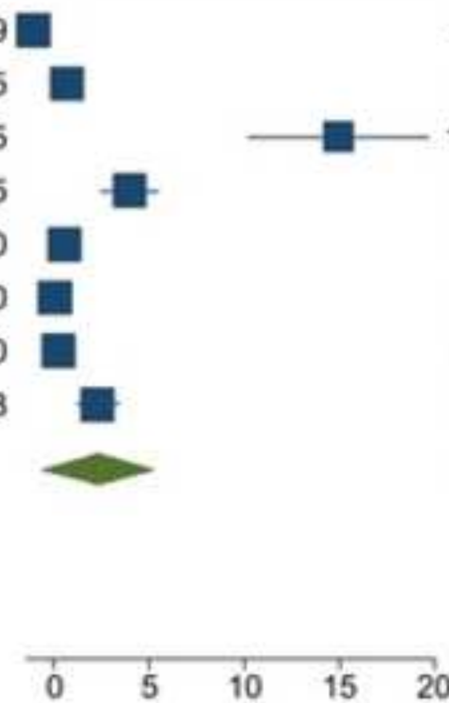

Heterogeneity: $\tau^2 = 18.16$, $I^2 = 99.18\%$, $H^2 = 122.02$

Test of $\theta_i = \theta_j$: $Q(7) = 110.16$, $p = 0.00$

Test of $\theta = 0$: $z = 1.49$, $p = 0.14$

Random-effects REML model

PRISMA 2020 Checklist

Section and Topic	Item #	Checklist item	Location where item is reported
TITLE			
Title	1	Identify the report as a systematic review.	page 1
ABSTRACT			
Abstract	2	See the PRISMA 2020 for Abstracts checklist.	pages 2-3
INTRODUCTION			
Rationale	3	Describe the rationale for the review in the context of existing knowledge.	pages 3-5
Objectives	4	Provide an explicit statement of the objective(s) or question(s) the review addresses.	page 5
METHODS			
Eligibility criteria	5	Specify the inclusion and exclusion criteria for the review and how studies were grouped for the syntheses.	page 6, Table 1
Information sources	6	Specify all databases, registers, websites, organisations, reference lists and other sources searched or consulted to identify studies. Specify the date when each source was last searched or consulted.	page 6
Search strategy	7	Present the full search strategies for all databases, registers and websites, including any filters and limits used.	page 6, Supplementary Table 1
Selection process	8	Specify the methods used to decide whether a study met the inclusion criteria of the review, including how many reviewers screened each record and each report retrieved, whether they worked independently, and if applicable, details of automation tools used in the process.	pages 6-7
Data collection process	9	Specify the methods used to collect data from reports, including how many reviewers collected data from each report, whether they worked independently, any processes for obtaining or confirming data from study investigators, and if applicable, details of automation tools used in the process.	page 7
Data items	10a	List and define all outcomes for which data were sought. Specify whether all results that were compatible with each outcome domain in each study were sought (e.g. for all measures, time points, analyses), and if not, the methods used to decide which results to collect.	page 7
	10b	List and define all other variables for which data were sought (e.g. participant and intervention characteristics, funding sources). Describe any assumptions made about any missing or unclear information.	page 7
Study risk of bias assessment	11	Specify the methods used to assess risk of bias in the included studies, including details of the tool(s) used, how many reviewers assessed each study and whether they worked independently, and if applicable, details of automation tools used in the process.	page 8
Effect measures	12	Specify for each outcome the effect measure(s) (e.g. risk ratio, mean difference) used in the synthesis or presentation of results.	page 7
Synthesis methods	13a	Describe the processes used to decide which studies were eligible for each synthesis (e.g. tabulating the study intervention characteristics and comparing against the planned groups for each synthesis (item #5)).	page 7
	13b	Describe any methods required to prepare the data for presentation or synthesis, such as handling of missing summary statistics, or data conversions.	page 7
	13c	Describe any methods used to tabulate or visually display results of individual studies and syntheses.	page 7
	13d	Describe any methods used to synthesize results and provide a rationale for the choice(s). If meta-analysis was performed, describe the model(s), method(s) to identify the presence and extent of statistical heterogeneity, and software package(s) used.	pages 7-8
	13e	Describe any methods used to explore possible causes of heterogeneity among study results (e.g. subgroup analysis, meta-regression).	pages 7-8
	13f	Describe any sensitivity analyses conducted to assess robustness of the synthesized results.	pages 7-8
Reporting bias	14	Describe any methods used to assess risk of bias due to missing results in a synthesis (arising from reporting biases).	page 8

PRISMA 2020 Checklist

Section and Topic	Item #	Checklist item	Location where item is reported
assessment			
Certainty assessment	15	Describe any methods used to assess certainty (or confidence) in the body of evidence for an outcome.	page 8
RESULTS			
Study selection	16a	Describe the results of the search and selection process, from the number of records identified in the search to the number of studies included in the review, ideally using a flow diagram.	pages 8-9, Figure 1
	16b	Cite studies that might appear to meet the inclusion criteria, but which were excluded, and explain why they were excluded.	pages 8-9, Figure 1
Study characteristics	17	Cite each included study and present its characteristics.	pages 9-12, Table 2 and 3
Risk of bias in studies	18	Present assessments of risk of bias for each included study.	page 9, Table 3
Results of individual studies	19	For all outcomes, present, for each study: (a) summary statistics for each group (where appropriate) and (b) an effect estimate and its precision (e.g. confidence/credible interval), ideally using structured tables or plots.	pages 9-12, Table 2 and 3
Results of syntheses	20a	For each synthesis, briefly summarise the characteristics and risk of bias among contributing studies.	pages 9-12
	20b	Present results of all statistical syntheses conducted. If meta-analysis was done, present for each the summary estimate and its precision (e.g. confidence/credible interval) and measures of statistical heterogeneity. If comparing groups, describe the direction of the effect.	Figures 2-10, Supplementary Figures 2-10
	20c	Present results of all investigations of possible causes of heterogeneity among study results.	pages 10-12
	20d	Present results of all sensitivity analyses conducted to assess the robustness of the synthesized results.	pages 10-12
Reporting biases	21	Present assessments of risk of bias due to missing results (arising from reporting biases) for each synthesis assessed.	Pages 9-12
Certainty of evidence	22	Present assessments of certainty (or confidence) in the body of evidence for each outcome assessed.	pages 9-12
DISCUSSION			
Discussion	23a	Provide a general interpretation of the results in the context of other evidence.	pages 12-15
	23b	Discuss any limitations of the evidence included in the review.	page 15
	23c	Discuss any limitations of the review processes used.	page 15
	23d	Discuss implications of the results for practice, policy, and future research.	pages 15-16
OTHER INFORMATION			
Registration and protocol	24a	Provide registration information for the review, including register name and registration number, or state that the review was not registered.	pages 5-6
	24b	Indicate where the review protocol can be accessed, or state that a protocol was not prepared.	pages 5-6
	24c	Describe and explain any amendments to information provided at registration or in the protocol.	pages 5-6
Support	25	Describe sources of financial or non-financial support for the review, and the role of the funders or sponsors in the review.	page 26
Competing interests	26	Declare any competing interests of review authors.	page 26
Availability of	27	Report which of the following are publicly available and where they can be found: template data collection forms; data extracted from included	N/A

PRISMA 2020 Checklist

Section and Topic	Item #	Checklist item	Location where item is reported
data, code and other materials		studies; data used for all analyses; analytic code; any other materials used in the review.	

From: Page MJ, McKenzie JE, Bossuyt PM, Boutron I, Hoffmann TC, Mulrow CD, et al. The PRISMA 2020 statement: an updated guideline for reporting systematic reviews. BMJ 2021;372:n71. doi: 10.1136/bmj.n71

For more information, visit: http://www.prisma-statement.org/

Supplementary Fig. 2

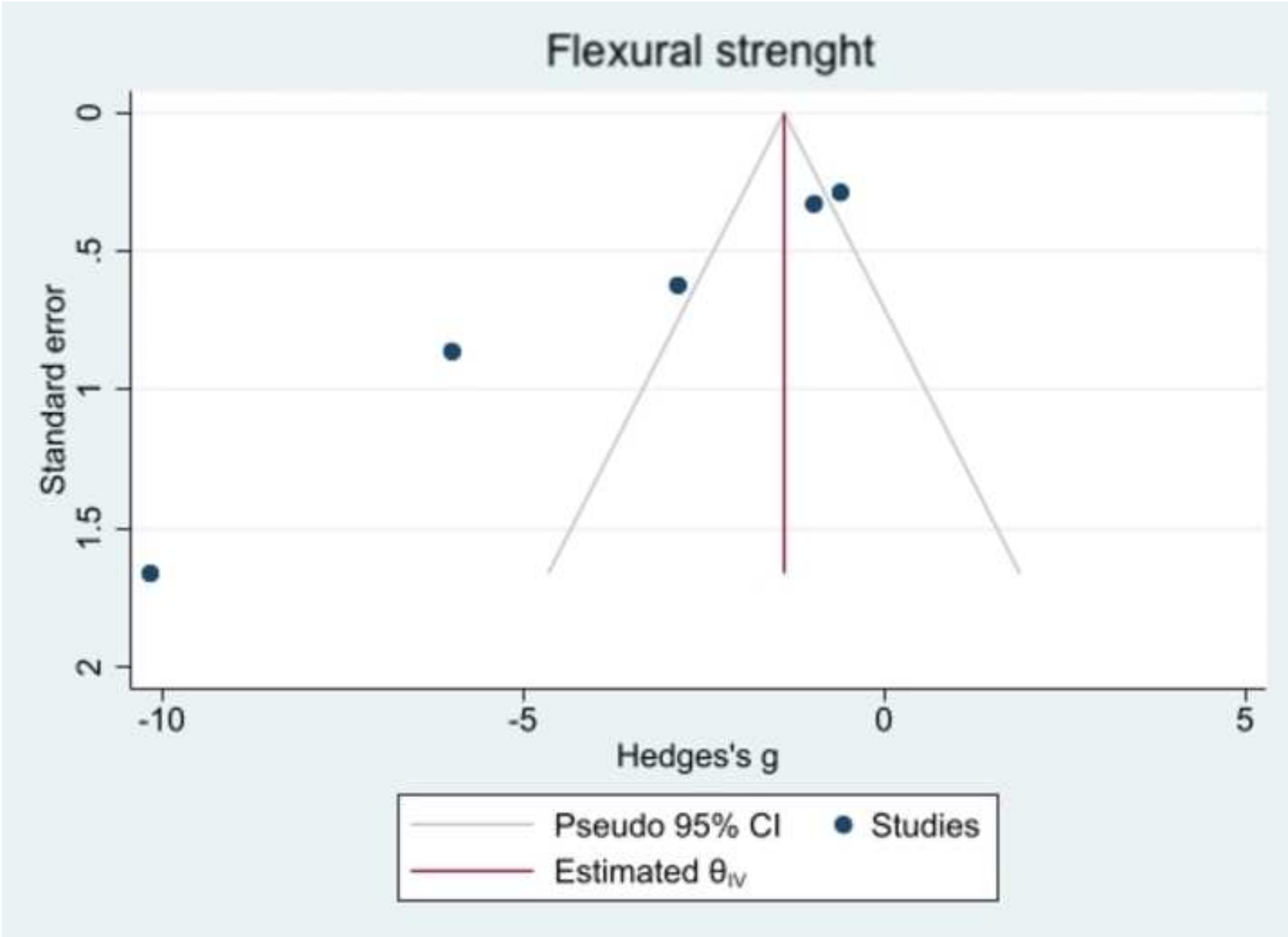

Supplementary Fig. 3

Click here to access/download;Figure;Figure 3.jpg

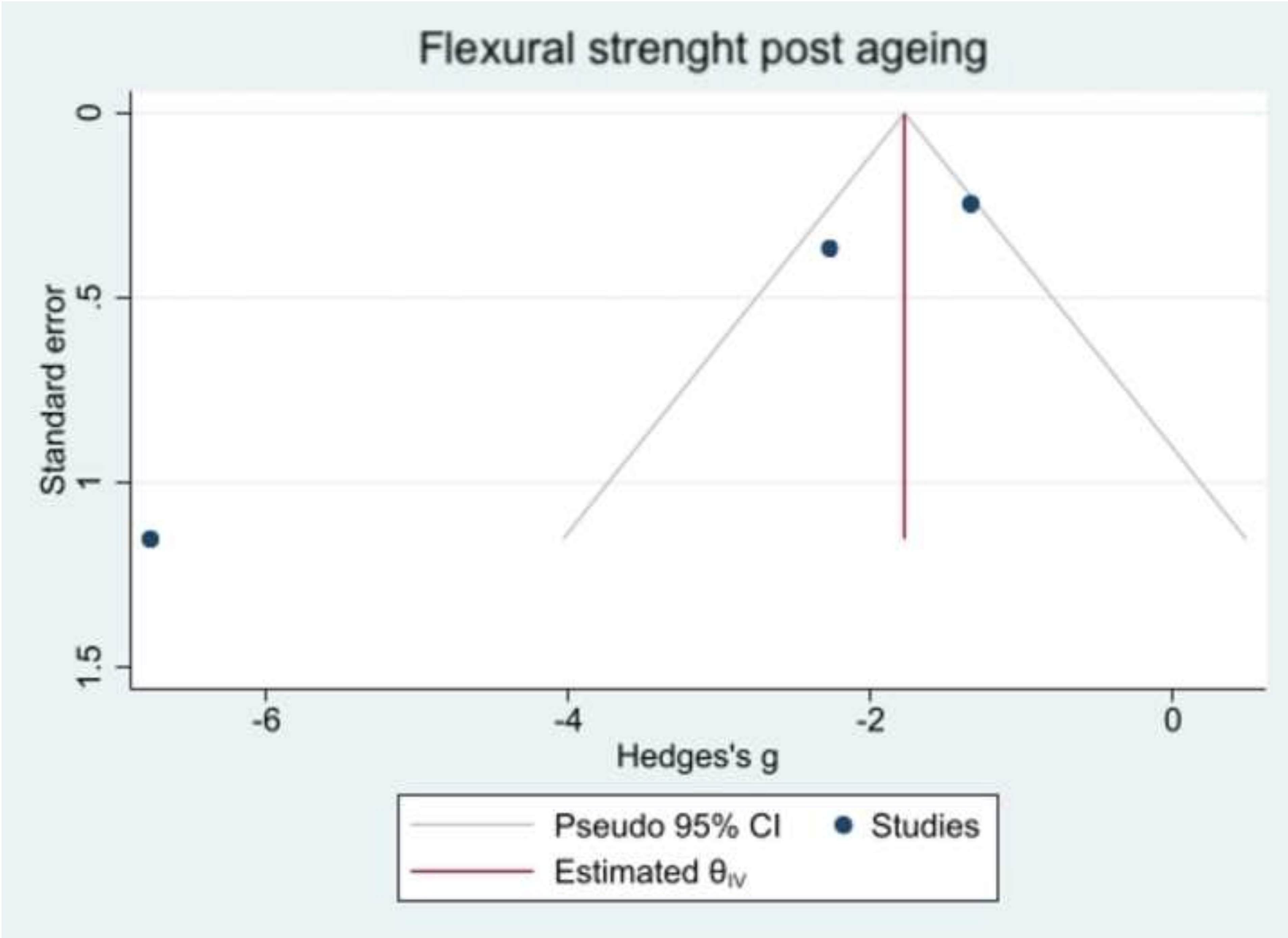

Supplementary Fig. 4

Click here to access/download;Figure;Figure 4.jpg

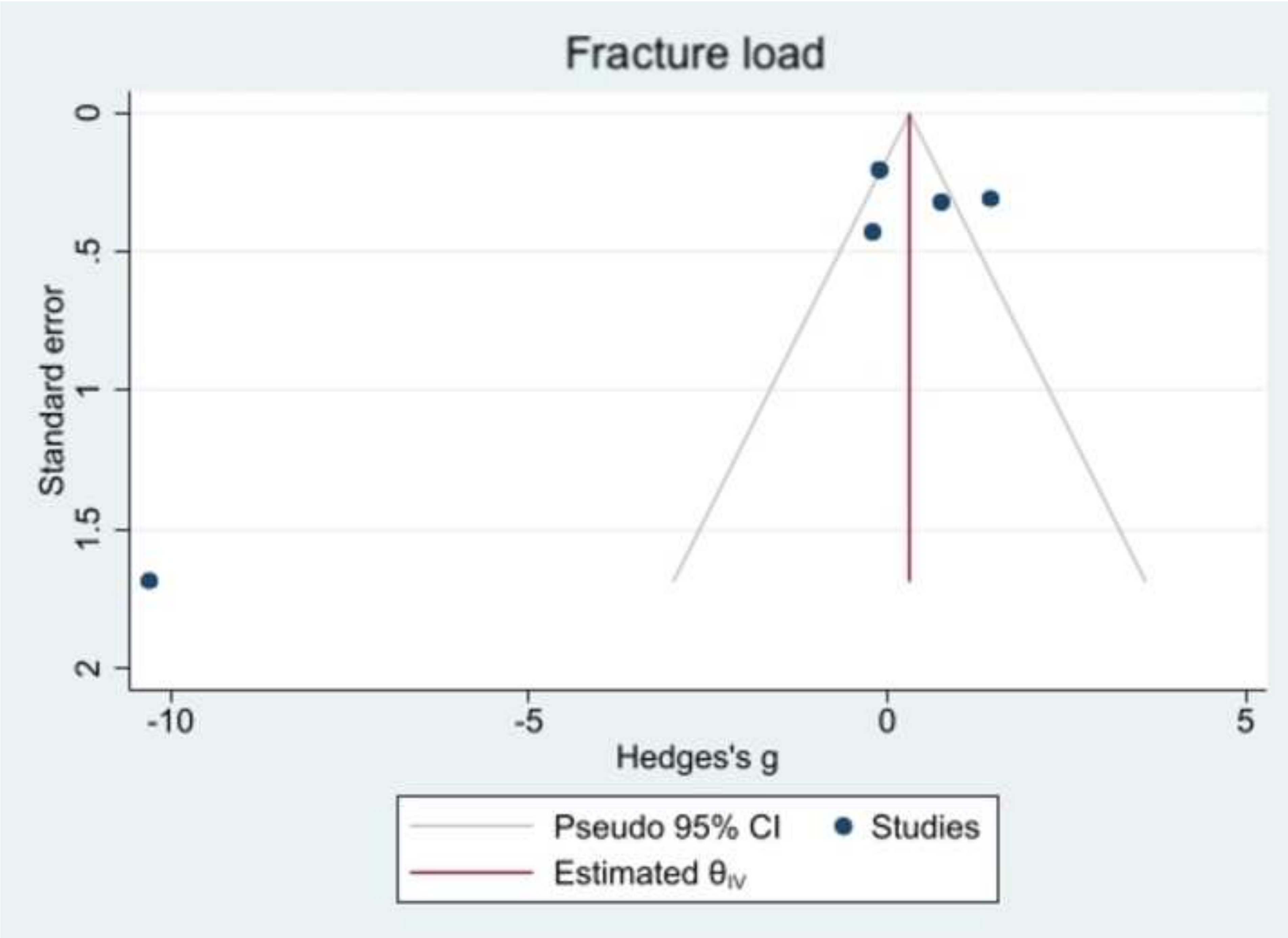

Supplementary Fig. 5 Click here to access/download;Figure;Figure 5.jpg

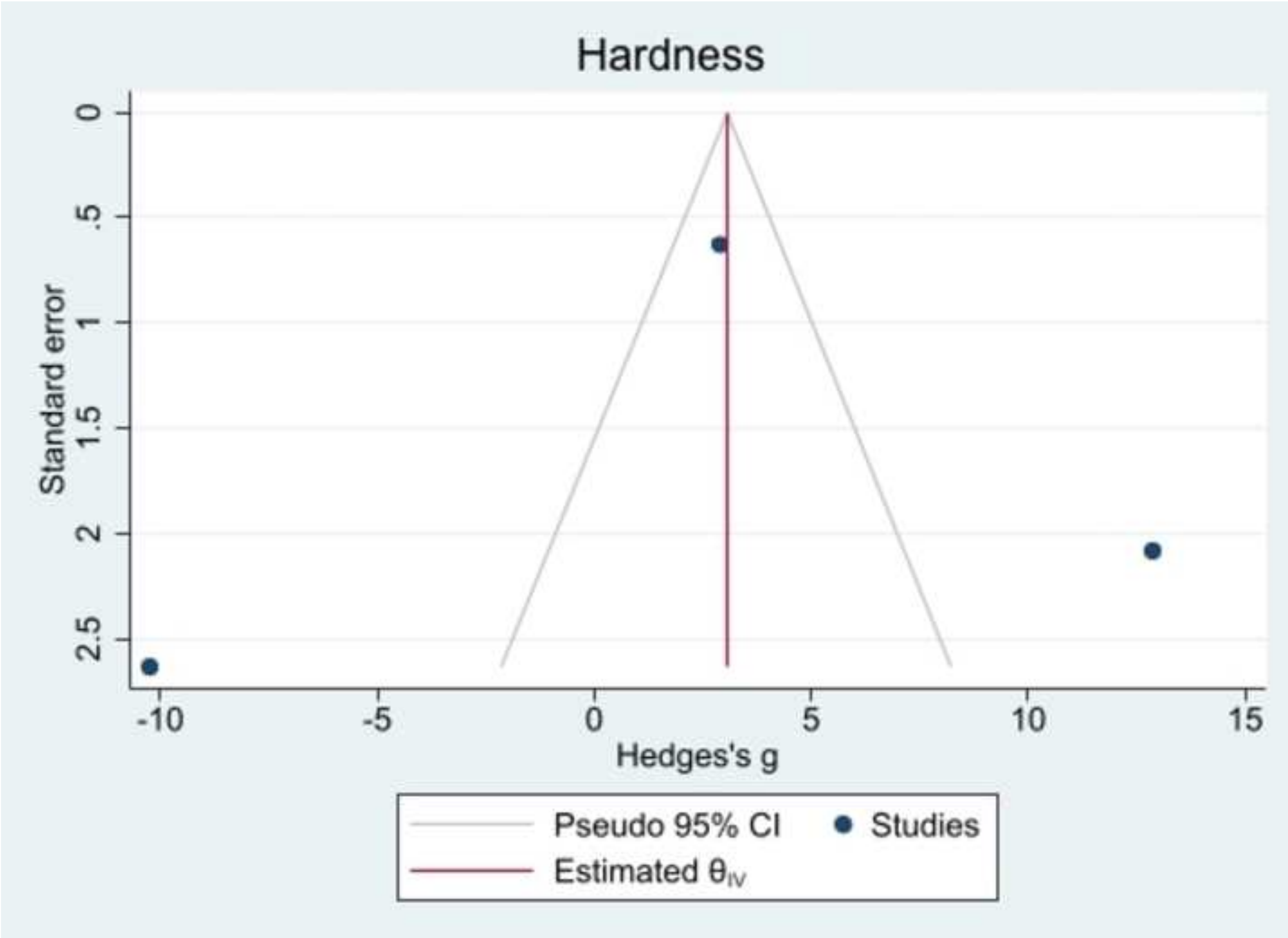

Supplementary Fig. 6

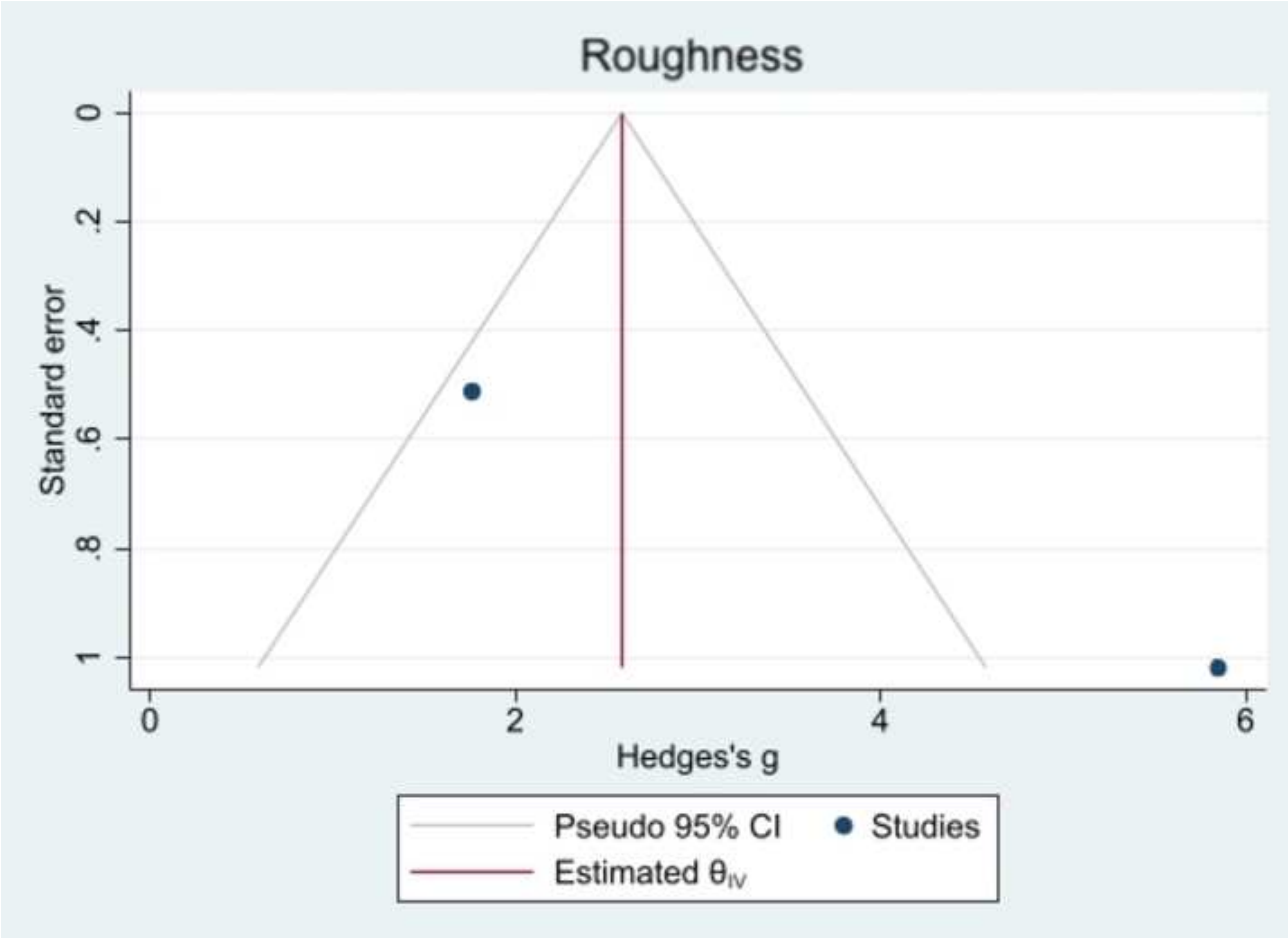

Supplementary Fig. 7

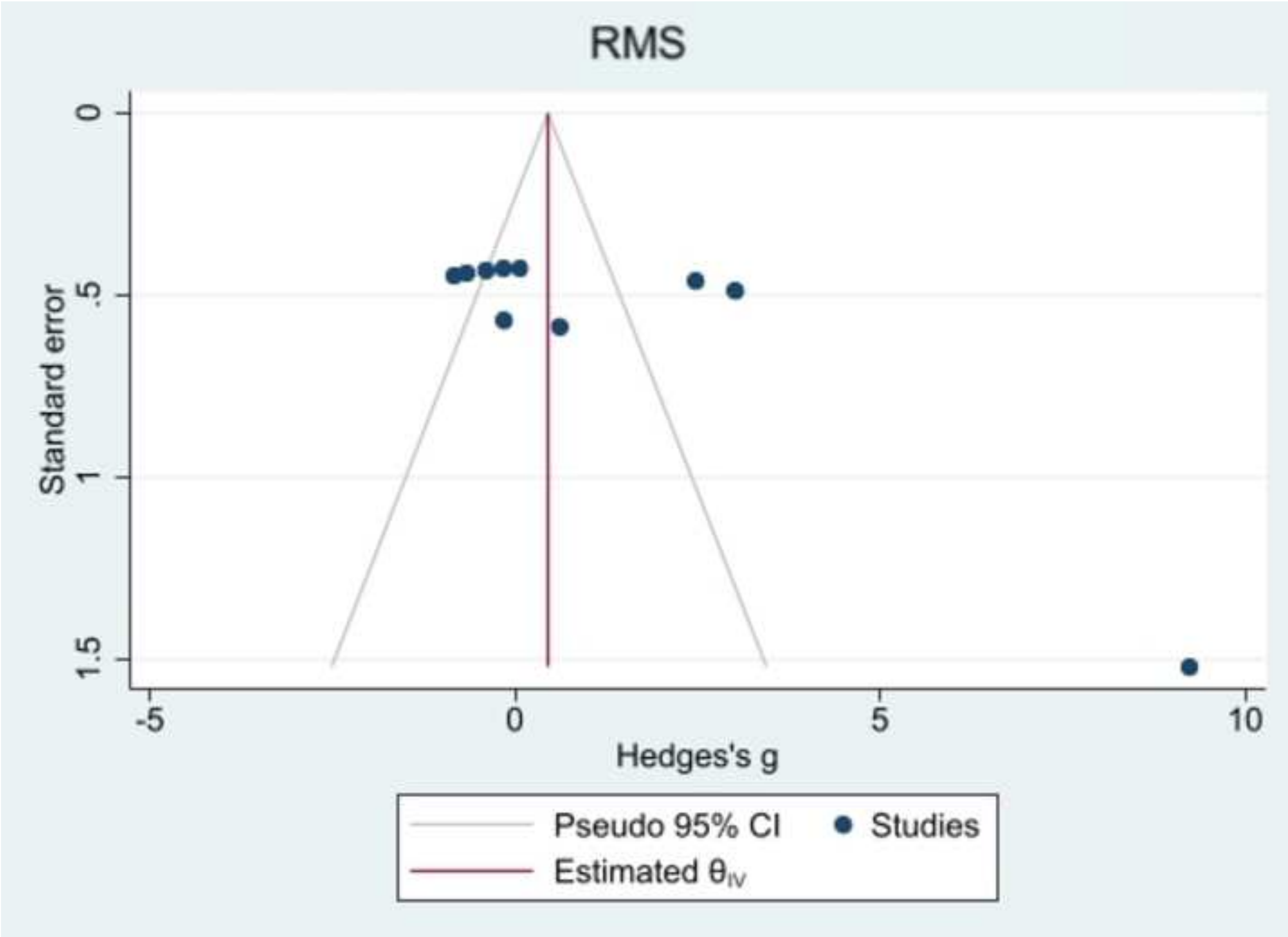

Supplementary Fig. 8

Click here to access/download;Figure;Figure 8.jpg

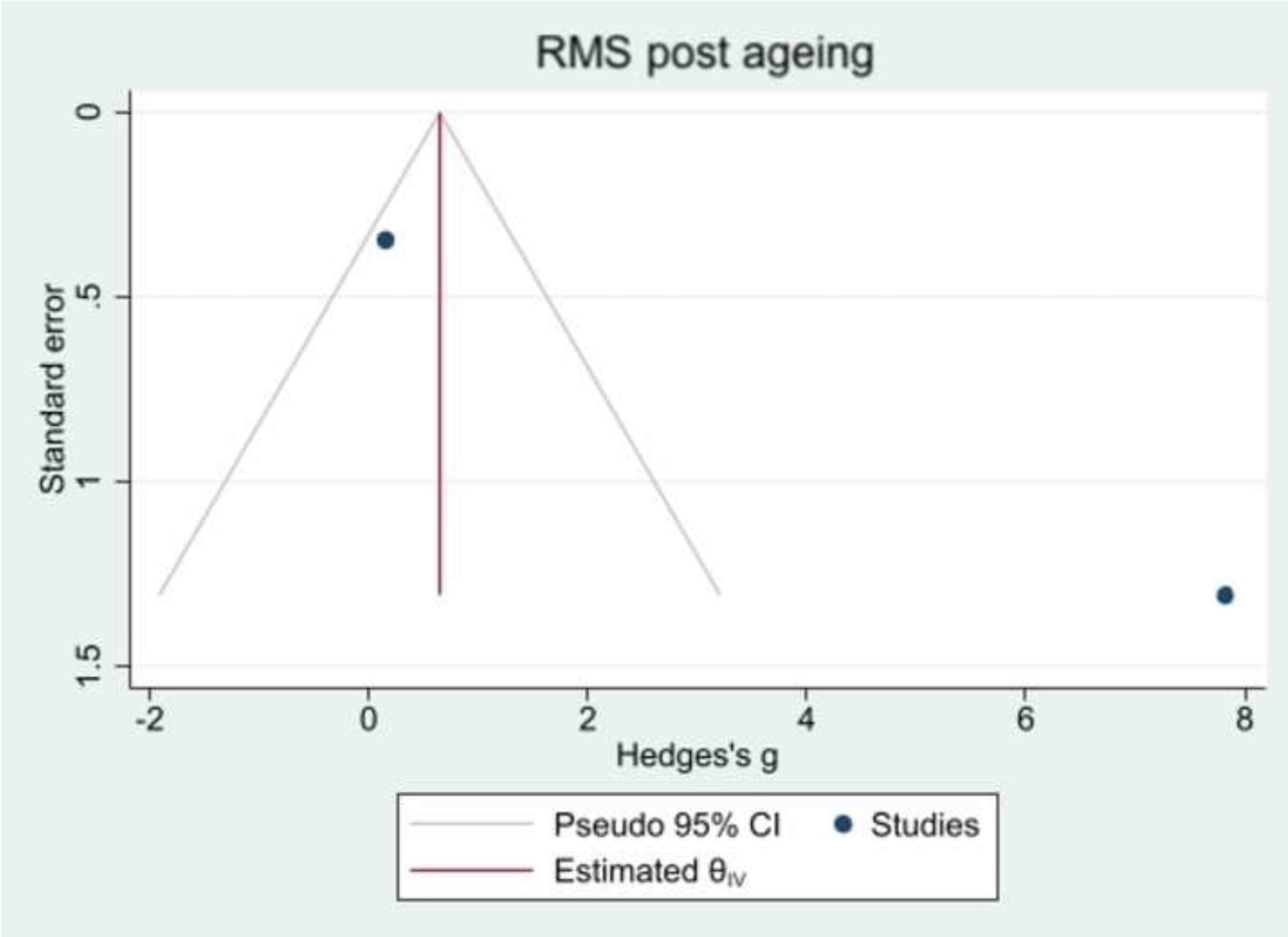

Supplementary Fig. 9

Click here to access/download;Figure;Figure 9.jpg

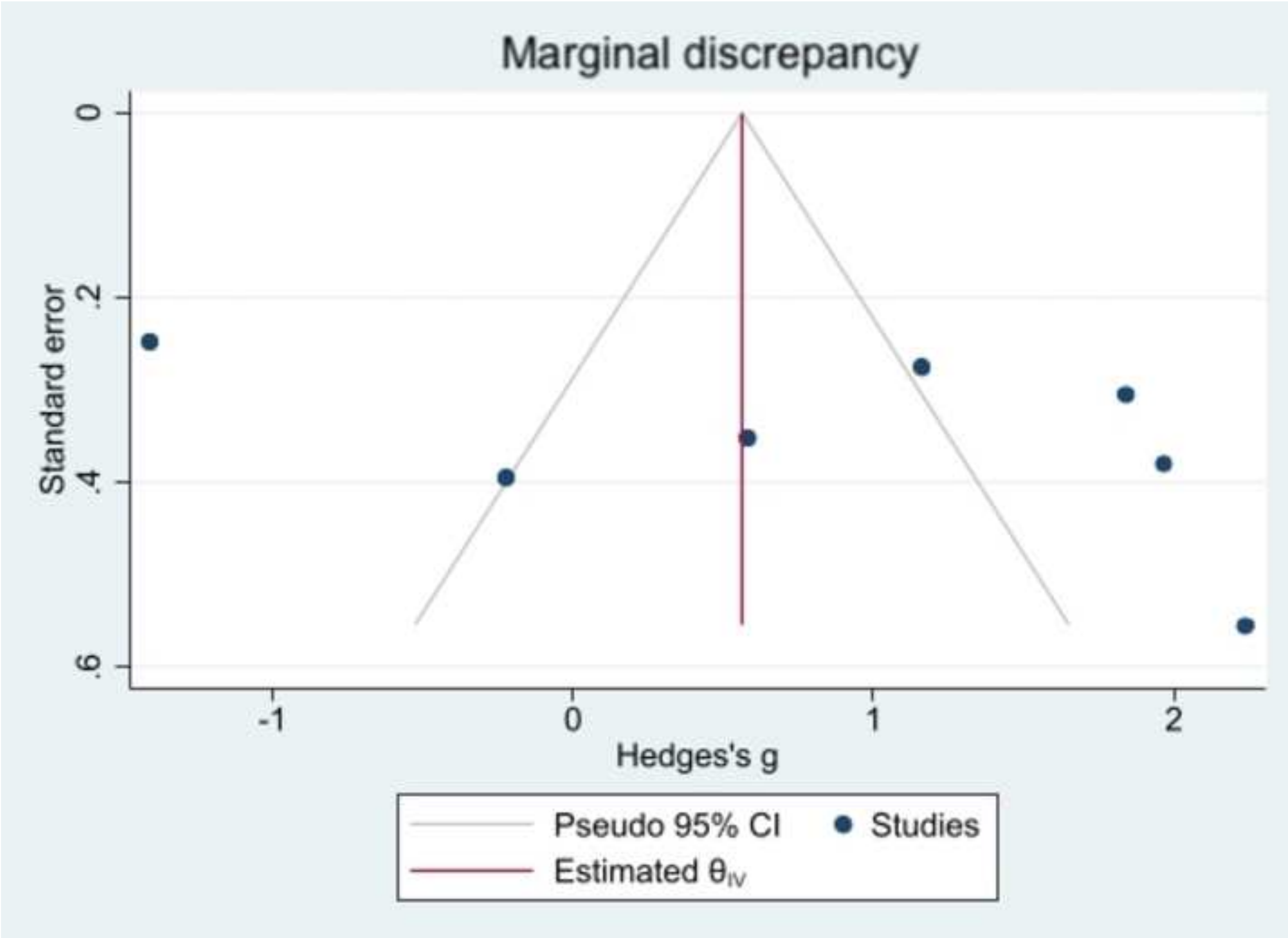

Supplementary Fig. 10

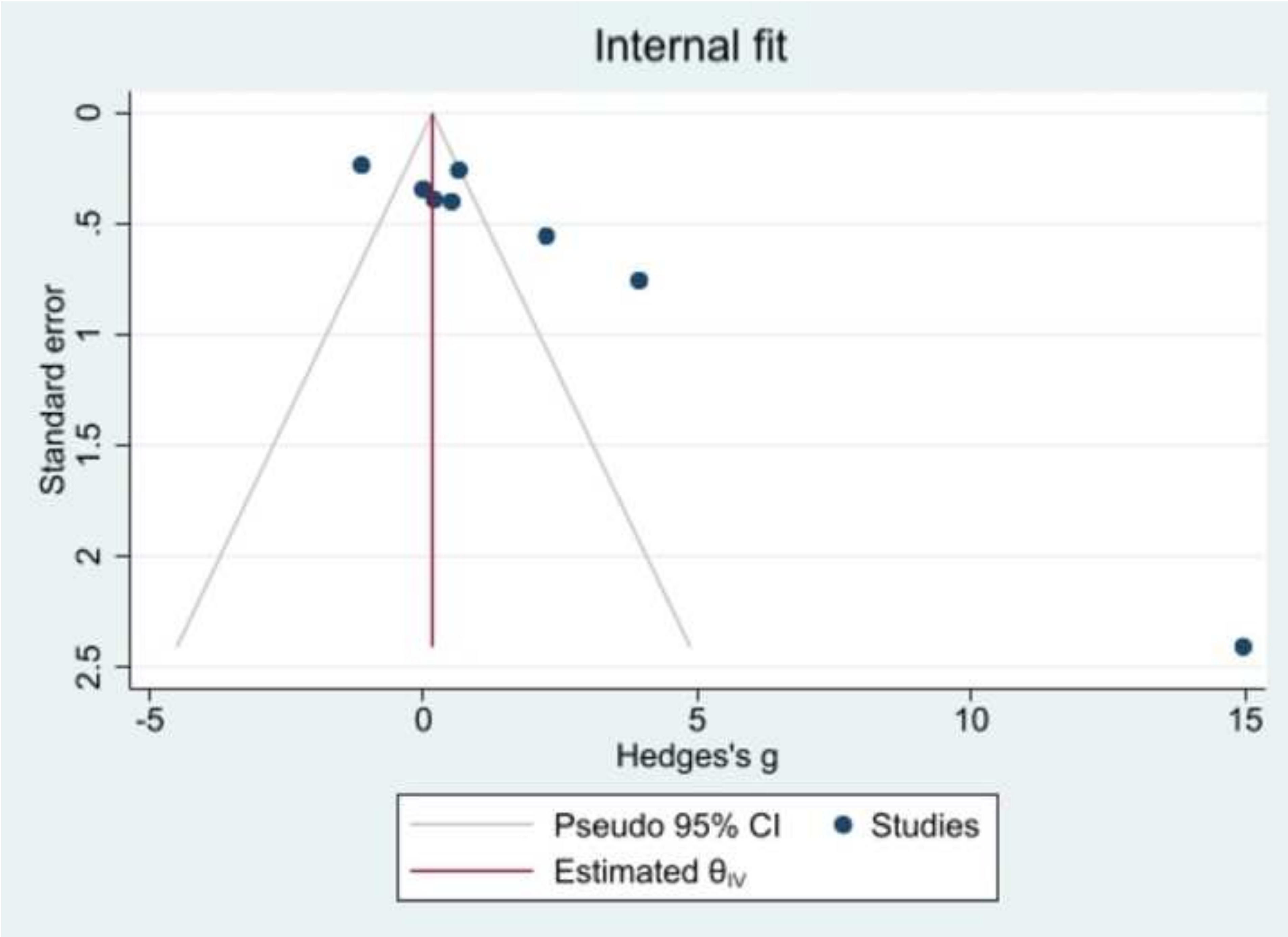

Table 2

Click here to access/download;Table;Table 2.docx

Author/s And Year	Flexural Strength	Fracture Load	Hardness	Roughness	RPD Fit Accuracy	RMS/ Trueness	Marginal Discrepancy	Internal Fit	Quality Assessment Score	Fundings
Al Maaz 2019							x	x	36/42	American Academy Of Fixed Prosthodontics
Alharbi 2016						x			31/42	Grant From King Saud University, Riyadh, Kingdom Of Saudi Arabia
Alharbi 2017							x	x	35/42	Supported By A Scholarship Grant Number 2/302626 From King Saud University, Riyadh, Kingdom Of Saudi Arabia.
Alsandi 2019						x			38/42	Grant From The Japan Society For The Promotion Of Science (No. 16H05515).
Arnold 2017					x				33/42	None
Ashtiani 2018								x	37/42	School Of Dentistry, Shahid Beheshti University Of Medical Science, Tehran, Iran.
Bae 2016						x			34/42	None
Bae 2020	x								49/42	Supported By The Basic Science Research Program Through The National Research Foundation (NRF) Of Korea, Funded By The Ministry Of Education (Grant No. 2017R1D1A1B03035688), The Technology Development Program (C0511440) Funded By The Ministry Of Smes And Startups (MSS, Korea), And The National Research Foundation Of Korea (NRF) Grant Funded By The Korea Government (MSIT) (No. 2018R1A5A7023490).
Barazanchi 2019		x							38/42	None
Braian 2018						x			36/42	None
Branco 2020			x	x					40/42	FundaçAo Para A Ciencia E A Tecnologia (FCT), Portugal, For Funding Through Projects 3D-Dentalprint (02/SAICT/2016/023940)
Chen 2019					x				38/42	National Natural Science Foundation Of China, Grant #51705006.
Choi 2019	x	x							38/42	None
Choi 2020	x	x							39/42	None
Dehurtevent 2017	x								30/42	None
Dehurtevent 2020	x	x	x						37/42	None
Deng 2018						x			39/42	Supported By The National Natural Science Foundation Of China (Grant No. 81271181) To YS And The Capital Health Research And Development Of Special (Grant No. 2016-1-4101) To YSZ.
Fiore 2020							x		38/42	None
Herpel 2021						x			41/42	None
Homsy 2017						x	x	x	37/42	Supported In Part By The National Council For Scientific Research, Beirut, Lebanon.
Hsu 2020						x			39/42	Supported By Grant From The National Taiwan University Hospital, Taipei, Taiwan, Republic Of China (NTUH.106-S3542).
Ioannidis 2020		x							40/42	None

Ishida 2016				x	x			38/42	None
Kalberer 2019					x			37/42	None
Kebler 2021	x							40/42	None
Kim 2016						x		36/42	None
Kim 2017						x	x	33/42	Supported By A Korean University Grant, The Mnistry Of Trade, Industry And Energy (20133110002881), And By SM (Smile Maker) Dental Laboratory.
Kim 2020a					x	x	x	41/42	None
Kim 2020b					x	x	x	41/42	Funded By The Ministry Of Trade,Industry And Energy (MOTIE, Korea).
Li 2019	x					x	x	38/42	Supported By The National Key R&D Program Of China [Grant Number 2018YFB1106900], The National Natural Science Foundation Of China [Grant Number 51475004], And The Capital's Funds For Health Improvement And Research [Grant Number 2018-2- 4103].
Li 2020				x				36/42	None
Li 2021					x			37/42	None
Liu 2018						x	x	35/42	National Natural Science Foundation Of China [Grant No. 51475004], Capital's Funds For Health Improvement And Research [Grant No. CHF 2016-1-4101], Project For Culturing Leading Talents In Scientific And Technological Innovation Of Beijing [Grant No. Z171100001117169].
Mahmood 2019							x	40/42	Odontologiskforskningi Region SkåNe, OFRS [Grant Number 509641].
Mai 2017						x	x	37/42	Basic Science Research Program Through The National Research Foundation Of Korea Funded By The Ministry Of Science, Information And Communication Technologies And Future Planning, Grant NRF-2014R1A1A1006073.
Molinero-Mourelle 2018						x		38/42	None
Munoz 2016						x		36/42	None
Muta 2020				x	x		x	40/42	None
Oguz 2021					x			38/42	Supported By Ankara University Scientific Research Projects Coordination Unit, Project Number: 18B0234003.
Øilo 2018			x	x				38/42	None
Osman 2017					x			36/42	Scholarship Grant Number 2/302626 From King Saud University, Riyadh, Kingdom Of Saudi Arabia.
Park 2016						x	x	33/42	None
Peng 2019					x	x		37/42	None
Peng 2020						x	x	37/42	Funding In Part By ACP Education Foundation Research Fellowships Program And Department Of Restorative Dentistry, University Of Washington, Grant #63–2073.
Prechtel 2019		x						38/42	None
Prechtel 2020			x					38/42	None
Prpić 2020	x		x					37/42	Supported By The University Of Zagreb Scientific Support "Diagnostic And Therapy Of Craniomandibular

										Dysfunctions.
Revilla León 2018							x		35/42	Supported By A Research Grant From The Spanish Association For Prosthodontics And Aesthetics.
Revilla-León,2019							x	x	34/42	None
Revilla-León 2020a				x					36/42	None
Revilla-León 2020b	x	x							37/42	None
Reymus 2020		x							32/42	None
Schönhoff 2021	x		x						38/42	Supported By Research Program ZF4052006AW8 (Aifprojekt Gmbh, Berlin, Germany, ZIM-Kooperationsprojekte, Projekttr¨Ager Des Bmwi).
Scotti 2020	x		x	x					39/42	None
Shim 2019	x			x					35/42	None
Sim 2018						x			33/42	None
Soltanzadeh 2018					x				36/42	None
Svanborg 2018								x	30/42	Supported By Grants From The Adlerbertska Research Foundation, The Sylvan Foundation, The Hjalmar Svenssons Foundation, Wilhelm And Martina Lundgren Foundation, And Dentsply Sirona Implants, IIS Grant I-IS-15-057.
Tahayeri 2017	x					x			32/42	National Institute Of Dental And Craniofacial Research (NIDCR) And The National Institutes Of Health (NIH) (R01DE026170 To LEB), And The Medical Research Foundation Of Oregon (MRF To LEB) And Apprenticeships In Science & Engineering Program At Saturday Academy.
Takahashi 2020				x		x		x	38/42	Supported By JSPS KAKENHI Grant Number 16H05526.
Tasaka 2018						x			33/42	None
Tasaka 2019a						x			33/42	None
Tasaka 2019b					x				35/42	None
Tasaka 2021a						x			36/42	None
Tasaka 2021b						x			36/42	None
Ucar 2019	x	x	x						31/42	None
Wang 2018						x			34/42	None
Wang 2019	x								36/42	Supported By The Technology Development Program Of Ministry Of Smes And Startups (MSS) [C0511440], The Technology Innovation Program Funded By The Ministry Of Trade, Industry & Energy (MOTIE, Korea) [10073062] And The National Research Foundation Of Korea (NRF) Grant Funded By The Korea Government (MSIT) [2018R1A5A7023490].
Wang 2020						x	x		38/42	None

Wang 2021	x						32/42	Scholarship From The China Scholarship Countil (Grant Number 201706240007)
Wemken 2020				x				None
Wemken 2021	x						34/42	Material And Financial Support From VOCO, Cuxhaven, Germany (ID 127105).
Wu 2021					x	x	37/42	Supported In Part By The Department Of Restorative Dentistry, University Of Washington [Grant #65-4909 Task 824].
Ye 2017			x				33/42	Supported By The Project For Culturing Leading Talents In Scientific And Technological Innovation Of Beijing (Z171100001117169), The PKU School Of Stomatology For Talented Young Investigators (PKUSS20120210), And The Construction Program For National Key Clinical Speciality From National Health And Familiy Planning Commission Of China (2011).
You 2020				x			36/42	Supported By Korea University Grant (No. K1711261).
Zandinejad 2019		x					34/42	Supported By The International Team For Implantology (ITI) Grant No. 929 2013.

Table 3

AUTHOR/s AND YEAR	MATERIALS AND SIZE	AM TYPES	CONTROL	MECHANICAL TESTS	DATA AND FINDINGS
			CERAMICS		
Branco 2020	N = 4 crowns Ceramic paste 3 mol % Yttria stabilized with zirconia powder (TZ-3Y-E, Tosoh)	Robocasting	Milling: zirconia powder containing a 3% of an organic binder (TZ-3YB-E, Tosoh)	surface roughness (Ra) with a surface roughness tester (SRT9 of 1,25 mm), Hardness (Vickers test)	Hardness: 1148.8 ± 15.1063; lower than control ($p < 0.001$). Roughness: almost four times higher than control samples ($p = 0.002$).
Dehurtevent 2020	Crowns Alumina powder (CT1200SG; Almatis) into a photosensitive acrylic resin (C1-alumina; CryoBerylSoftare)	SLA specimens oriented in 3 different planes (ZX, ZY and XY orientation)	None	3-point flexural strength (n= max force: 1kN), Vickers indentation hardness test, fracture toughness with 3-point bend test	Flexural strength: ZY-oriented specimens (409.7 ± 29.6 MPa) significantly higher (p<0.05). Fracture toughness (4.6 ±0.2 MPa.m$^{1/2}$) was higher than ZX-oriented ones (p<0.05).
Dehurtevent 2017	N = 60 rectangular specimens (1.3 × 4 × 22 mm) experimental groups: S80, S75, S70, L80, L75, L70 (C1 - Alumina, CT1200SG, Almatis, PA, USA)	SLA	Milling (In-Ceram AL, Vita Zahnfabrik.)	3-point flexural strengths (100N cell, maximum force of 1kN, constant speed of 0.5 mm/min)	L70 (273.8 ± 41.9 MPa) and S70 (271.7 ± 44.5 MPa) samples flexural strengths were lower than L80 (367.9 ± 52.4 MPa), L75 (363.7 ± 74.6 MPa), and control samples (350.4 ± 49.5 MPa) (p<0.05).
Homsy 2017	N=30 mesio-occlusal inlays lithium disilicate glass-ceramic: e.max Press inlays from 3D printed wax patterns (group CI3DW) and wax plasticized patterns (VisiJet FTX Green; 3D Systems) from scanning of the master and 3D printed wax patterns (group DI3DW).	MICRO-SLA (ProJet 1200; 3D Systems)	conventional impression and manual wax pattern (group CICW) or laboratory scanning; CAD-CAM milling wax blanks (group CIDW) and scanning of the master preparation and CAD-CAM milling (group DIDW)	marginal and internal fit accuracy with replica technique and stereomicroscopy.	Internal fit: 82.9 ± 11.8 µm and 88.8 ± 14.5 µm. Marginal discrepancy: no significant differences among groups CI3DW and DI3DW . The internal discrepancy was larger than the marginal discrepancy within all groups (p<0.001).
Ioannidis 2020	N=20 occlusal veneers (0.5 mm) zirconia (Lithoz, Vienna, Austria)	LCM	Milling: zirconia (Ceramill Zolid FX, Amann Girrbach, Pforzheim,Germany); and heat-pressed lithium disilicate (IPS e.max Press, Ivoclar Vivadent, Schaan,Liechtenstein).	Fracture load necessary to decrease the maximum load by 20% and initiate a crack (F initial) and the load needed to fracture the specimen (F max). Chewing simulation with cyclic fatigue and temperature variations.	Fracture load: 1583 ± 542 N. Significant median Finitial values differences between all groups (p <0.0001). The median Fmax values differences were significant between AM and milling (p = 0.0238).
Li 2019	Crowns Zirconia	SLA	None	Flexural strength (universal testing machine), internal and marginal adaptation evaluated with 3D subtractive analysis technique.	Flexural strength: 812 ± 128 MPa. Cement space: 63.40 ± 6.54 µm in occlusal area, 135.08 ± 10.55 µm in axial area and 169.58 ± 18.13 µm in marginal area. Strength: adequate for fabricating dental crowns, but internal and marginal adaptation not ideal for clinical application.
Li 2021	N=30 crowns 47 vol% 3 monolitic zirconia	SLA	Milling: partially sintered zirconia blank (SHT, Aidite, China)	three-dimensional fabrication accuracy analysis: root mean square (RMS)	External design: 19.22 ± 0.91 µm, 26.20 ± 2.04 µm and 25.92 ± 3.62 µm; Intaglio design: 22.68 ± 4.03 µm, 17.04 ± 2.65 µm and 22.48 ± 6.00 µm. RMS value influenced by finish line design, with external (p= 0.027) and intaglio (p= 0.049), but not by fabrication

					method.
Revilla-León 2019	N = 20 crowns Zirconia stabilized with 3% Yttria, 3DMix ZrO_2 (3DCeram) Anatomically contoured (AM) and splinted (SAM) samples	SLA	Milling 5-axis CNC anatomically contoured CARES Zirconia-dioxide (Straymann)	Marginal and internal discrepancies with silicone replica method	Marginal discrepancy: higher with AM compared to CNC and SAM and higher with SAM compared to CNC ($p<0.001$). Internal discrepancy: higher with SAM and AM compared to CNC ($p<0.001$), lower with compared to AM ($p=0.001$).
Revilla-León 2020b	N= 10 bar specimens (25×4×1.2 mm) zirconia (3DMix ZrO2; 3DCeram) stabilized with 3% yttria	SLA	Milling: (IPS e.max ZirCAD; Ivoclar Vivadent AG)	Flexural strength (3-point bend tests) with artificial aging procedures	Flexural strength: 320.32 ± 40.55 MPa. Manufacturing, mastication simulating aging procedure and the interaction between them affected flexural strength ($p<0.001$). mastication simulation produced a reduction in flexural strength for AM group compared to milling ($p<0.001$).
Ucar 2019	N = 10 disc-shaped specimens (16 mm diameter, 1.2 mm thick) LCM alumina Lithography (Lithoz, Vienna, Austria)	SLA	Dry-pressing: In-Ceram alumina (Vita Zahnfabrik, Bad Sackingen,Germany and milling: ZirkonZahn CAD/CAM (Zirkonzahn, South Tyrol, Italy)	Biaxial flexural strength test ("piston on 3-ball" technique), fracture toughness determination, microhardness test (Vickers Hardness).	Flexural strength: 490 ± 44 MPa. LCM alumina had the highest mean hardness value. Significant difference considering the peak strength and hardness values for all pairwise comparisons ($p<= 0.05$).
Wang 2018	N=10 crowns for maxillary second molar ZrO2 paste (3DMIXZrO2L; 3DCeram Co)	SLA (CERAMAKER 900; 3DCeramCo)	Milling (DWX-50; Roland DG Corp): ZrO2 block (Zenostar; Wieland Dental)	Trueness of different locations: External and Intaglio surface, Marginal area, Intaglio occlusal surface)	Trueness of AM crowns was no worse than the milled ones ($p<0.05$). External: 53 ±9 µm; Intaglio: 38 ±12 µm; Marginal: 34 ±5 µm; Occlusal: 27 ±17 µm.
Wang 2020	N=10 crowns for first molar Zirconia and Alumina multifunctional acrylate	2 SLA systems: CeraFab7500 (CF); Lithoz for alumina and CSL150 (CL) and PORIMY for zirconia	Milling: (X-MILL500 (XM) ; XTCERA) for Zirconia HDDAPET4A	Dimensional accuracy with Geomagic Qualify software and silicone replica method for clinical adaptation	Accuracy: 65 ± 6 µm. Marginal discrepancy: 109 ± 27 µm. Internal fit: 71 ± 15 µm (axial), 98 ± 29 µm (corner) and 149 ± 46 (occlusal). CF had better dimensional accuracy compared to others ($p<0.001$). Differences only apparent in the axial and occlusal areas between CF and CL ($p<0.05$).
Zandinejad 2019	N=10 crowns on zirconia implant abutments (CARES zirconium-dioxide abutment; Straumann, Arlington, TX) and chamfer finish line. Zirconia (3D Mix ZrO2 (3D Ceram) (AMZr)	SLA (CeraMaker 900; 3DCeram Co.)	Milling: lithium disilicate (IPS e.max CAD crown HT A1; IvoclarVivadent, Amherst, NY) (MLD) and zirconia (Lava Plus Zirconia W1, 3M Co., St. Paul, MN) (MZr)	Fracture resistance with vertical force application with universal testing machine (crosshead speed of 2 mm/min)	Fracture load: 1243 ± 265.5 N. No significant differences observed. All specimens fractured at the implant-abutment interface.
			METALS		
Al Maaz 2019	N=90 crowns with chamfer (C), deep chamfer (DC), or shoulder (S) finish lines Base alloy (Co-Cr) (B group), high noble (Au-Pd-Ag) (HN group)	SLM	None	Fitting evaluated with inverted bright field metallurgical microscope. Marginal and internal gaps measured at 5 locations: buccal margin, midfacial, incisal, midlingual, and lingual margin.	Marginal gap: significant differences between B and N groups, and B and HN groups ($p<0.001$). Significant difference between the DC finish line and the C and S finish lines ($p<0.001$). Significant influence on marginal gap of

	and noble alloy (Co-Pd) (N group)				alloy type and finish line and on internal gap of alloy type (p<0.001).
Arnold 2017	N=3 clasps Co-Cr-Si-Mn-N-Nb-Fe Remanium Star CL (Dentaurum GmbH & Co. KG) for SLM	SLM (CNC Construction mlab: M1 cusing, Concept Laser GmbH)	Lost-wax casting technique (LWT); indirect milling (wax milling with LWT), and direct milling: PEEK.	RPD fit accuracy	Vertical: 363 ± 133 µm and Horizontal: 365 ± 205 µm. The direct RP had significantly higher vertical values than the others (p<0.001). unsuitable for clinical use.
Bae 2016	N=20 inlay Co-Cr alloy (SP2, EOS, GmbH) for SLS and UV polymerizable polymer (VisiJet FTX Gree, 3D Systems Co) for SLA	SLS and SLA	Milling: wax block (D-max) and Zirconia block (D-max)	Accuracy evaluation with RMS formula.	SLA specimens had the smallest differences from reference data and significant differences compared with wax (p=0.021) and zirconia samples (p=0.048). SLS specimens deviation was different from wax (p<0.001), and zirconia samples (p=0.001).
Bae 2020	N = 20 bar specimens Co-Cr metal powder (SP2; EOS GmbH): group without porosities (PF group) and with porosities (PP group)	SLS	Casting (CP group): Co-Cr alloy (StarLoy C; Degudent GmbH).	Flexural strength: 3- point bending test with universal testing machine (cross head speed 2mm/min)	Mean values differences were statistically similar (p=0.058): PP (35.6 ±9.1 MPa), CP (43.5 ±7.8 MPa) and PF (47.7 ± 4.5 MPa). Clinical implications: high bond strength is essential for successful metal-ceramic restorations and SLS porous samples had statistically similar bond strength to other systems.
Barazanchi 2019	N=17 rectangular specimens (1.5 mm, 8 mm, 30 mm) CoCr powder (Cobalt Chrome MP1, EOS)	DMLS Eos int M270, (EOS GmBH, Munich, Germany)	Milling: pre sintered CoCr specimen	Hardness before /after porcelain firing. Fracture surface and micro-structural changes (before/after porcelain firing) with SEM.	Hardness: 4.4 ± 0.2 GPa; hardness increased post porcelain firing. Analysis of the fracture surfaces showed a predominantly adhesive mode of failure.
Braian 2018	N = 10, inlay-shaped and four-bridge specimens Ti and Co-Cr (only with EOS®)	EBM technology (Arcam®), laser sintering (SLM solutions ®), DMLM (Concept Laser ®), DMLS (EOS ®).	Milling (SM)(Mikron®)	Accuracy with linear measurements in 3 axes (X, Y, Z).	In inlay model, EBM: precision 0.078 in X and 0.117 mm in Y and accuracy 0.176 mm in X. DMLS: precision 0.282 mm and accuracy 1.026 mm in Z. EBM had lowest precision (>0.3°) and accuracy (>1.0◦). In bridge model, EBM: precision 0.079 in X and 0.250mm in Z and accuracy 0.161 in X and 0.243 in Y and −0.975 mm in Z. SLM: accuracy −0.005 mm. EBM had highest precision, DMLM had lowest precision (>0.09°) and SLM had highest accuracy and DMLM (> −0.07°) at 0.002◦ deviation.
Chen 2019	RPD frameworks designs: palatal plate-type connector with 2 clasps (Type I), anterior and posterior palatal strap-type connector with 4 clasps (Type II), complete palatal connector with no clasps (Type III), and anterior palatal plate-type connector with 4 clasps (Type IV) Co-Cr alloys (remanium star CL;	SLM (Mlab cusing R; Concept Laser GmbH)	lost-wax casting technique: (Wironit, extra-hard; Bego GmbH & Co. KG)	Average and maximum gaps with silicone impression technique	Average gaps: influenced by production methods, design types, and interactions (p<0.001). design I and II with average gaps of SLM larger than the cast ones (p<0.001).

	DENTAURUM GmbH & Co KG)				
Fiore 2020	N=160 fixed partial denture frameworks and flat specimens (25×3×0.5 mm) Co-Cr alloy (EOS M270; EOS GmbH Electro Optical Systems), made of EOS Co-Cr SP2 powder	SLM	None	Marginal gap before/after ceramic firing	Significant marginal gap difference of the frameworks before ceramic firing (p=0.001).
Kim 2017	N = 30 crowns Co– Cr powder (StarbondCoS powder 55; S&S Scheftner GmbH, Mainz, Germany)	SLM	Milling: Co– Cr alloy (StarLoy C; DeguDent, Hanau-Wolfgang, Germany) and soft block (SMB; SoftMetal; LHK, Chilgok, Korea) and conventional lost wax technique: Co– Cr alloy (StarLoy C; DeguDent, Hanau-Wolfgang, Germany) for μ-SLA (Micro-stereolithography) + Casting	Marginal and internal gap with silicone replica technique: 12 internal spots (marginal, axial wall and occlusal) measured with digital microscope.	Average marginal gap: 239 ± 126μm; Occlusal gap: 384 ± 67,8μm. Significant differences (p<0 .05). Further improvements in SLM may be required prior to clinical implementation.
Munoz 2016	N= 30 crowns Gold	DLP (ProJet DP 3000)	Milling(LAVA CNC 500) and hand wax	Margin discrepancy evaluation with light microscopy and 10 measures for vertical discrepancy	Marginal discrepancy: 59.9 ± 16.81 µm. Significant differences between milled and hand- waxed overall mean (p<0.001). AM printed patterns produced a significantly higher number of crowns with unacceptable margin discrepancy (>120 mm).
Øilo 2018	N = 10 RPD frameworks Cara Co-Cr (Heraeus Kulzer, GmbH)	SLM	Milling: Cara Co-Cr (Heraeus Kulzer, GmbH)and traditional casting (Wirobond C, BEGO Implant Systems)	Vickers hardness and roughness with Ra and Rmax evaluation.	Hardness: 4570,062 ± 127 Mpa. Roughnes: Ra (μm) 1,65 ± 0,55 and Rmax 13,58 ± 3,38 μm. Significant differences in hardness, wall thickness, weight, and connector size (p<0.05)
Revilla León 2018	complete-arch frameworks Ti6Al4V ELI Metal powder; Arcamn for EBM and LaserFormTi Grade 23; 3D Systems for SLM	EBM and SLM	None	Discrepancy with 3 measurements at x- (mesio-distal), y- (bucco-lingual), and z- (occluso-gingival) axes	Mean accuracy: 3 ±3 mm. The most favorable results were obtained in the z-axis. The highest discrepancy was observed in the y-axis (37 to 56 mm), followed by the x- (16 to 44 mm) and z- (6 to 11 mm) axes (p<0.05).
Revilla-León 2020a	N=40 disks (5 mm x 1 mm) Co-Cr alloy: SP2 (EOS), Co-Cr 3DS (3D Systems Laverwise), Remanium star CL (Concept Laser 100W/200W)	SLM: EOS, 3D Systems Layerwise, Concept Laser 100W, Concept Laser 200W	Milling: (DMG 10 Ultrasonic; DMG) Co-Cr (Starbond CoS Disc basic; Scheftner)	Roughness	Roughness: 2.43 ± 0.34, 1.80 ± 0.43, 1.57 ± 0.15 and 2.84 ± 0.27 µm. Differences were obtained in Wt%, At%, and Ra values among Co-Cr alloys (p<0.05).
Soltanzadeh 2018	N=10 RPD maxillary frameworks for a Kennedy class III Modification I arch. Co-Cr alloy (ST2724G; Sint-Tech, Canelli, Italia)	SLM (CAD printing and CAD printing from stone model)	Conventional method: Lost-wax technique from stone model and Lost-wax technique from printable resin model	RPD accuracy and fitting	RPD accuracy: 0.005 ± 0.030 mm. AM frameworks had lower fit (p < 0.05) in the major connectors and guide plates. The biggest gap (0.33 mm ± 0.20 mm) was in anterior strap of the major connector. Method of fabrication did not affect the adaptation of the rests or reciprocation plates.
Svanborg 2018	N=2 implant frameworks Renishaw AM250, Renishaw DG1	AM technique no specified	CNC-milling: Co-Cr and Ti alloy	Fitting with measurements in 3 dimensions (x, y, and z axes) before/after ceramic veneering	AM Ti: the difference in fit in y (p=0.002) and the 3D distortion (p=0.008) were significant.

	powder for Co-Cr implant and Ti TiAl6V4 extra low interstitial (ELI) powder (Renishaw) frameworks				AM Co-Cr: significant differences in z ($p=0.011$), in Y/Z and X/Z angles ($p<0.0001$) after ceramic veneering.
Takahashi 2020	n=15 clasps for RPD 38 to 45 µm CP Ti grade 2 powder (EOS GmbH Electro Optical Sys-tems, Krailling, Germany), 39 ± 3 µm Ti-6Al-4V powder (EOS GmbH Electro Optical Systems, Krailling, Germany), 50 µm Ti-6Al-7Nb powder (Matsuura)	SLS	Lost wax conventional technique with Ti alloys: Ti-6Al-4V (Ti64; 64 Ti billet, Toho Tec., Chigasaki), Ti-6Al-7Nb (Ti67; T- alloy Tough, GC Corp.), and CP Ti grade 2 (CPTi; T-alloy M, GC Corp.)	Roughness with 3D measuring surface profile device (NH-3N) and fitness accuracy with silicone impression technique (Fit Checker)	AM clasps surfaces were 5 to 10 times rougher ($p< 0.05$).
Tasaka 2019a	n=10 RPD frameworks Co–Cr alloy (Dan Cobalt Chuukou-shitsu; NIHON SHIKA KINZOKU Co., Ltd., Osaka, Japan)	SLS	3D printing casts (AM-cast)	Discrepancy measured at 5 random points on the inner surface.	Discrepancy: SLS-cast from 0.166 ± 0.009 to 0.123 ± 0.009 mm. Significant differences observed at the rests, proximal plates, connectors, and clasp arms.
Tasaka 2019 b	N = 5 clasps for RPD framework Co-Cr alloy: EOS Cobalt Chrome SP2 (EOS)	SLS	Milling: Co – Cr alloy, KM-Cobalt Chrome (Kyocera) and AM+ Lost-wax casting: Co-Cr alloy, Dan cobalt Chuukou-shitsu (Nihon Shika Kinzoku)	RPD accuracy: 7 sites analyzed on the inner surfaces (tip, center, and shoulders of both sides of the clasp arm, and rest).	Range of differences for AM, milling and SLS were –85.20 to 72.80 µm, 66.40 to 136.80 µm, and –3.20 to 52.40 µm, respectively. Significant differences observed at the tip and at the center of the clasp arm, and at the shoulder of both sides of the clasp arms and rest.
Tasaka 2021a	RPD frameworks Co-Cr alloy powder (SP2, EOS, Kailling, Germany)	SLS (EOSINT M270, EOS)	3D-printed pattern casting (AM-Cast) (Projet 3510DP, 3D Systems Corporation): resin pattern (VisiJet M3 Dentcast, 3D Systems Corporation, Circle Rock Hill, SC, USA) shaped by AM Co-Cr alloy (Dan Cobalt Chuukou-shitsu, Nihon Shika Kinzoku, Osaka, Japan)	Accuracy under different conditions with a reinforcement bar.	Significant median value on occlusal rest and on right-side of joining area ($p<0.05$), and on the center and left-side of joining area of the lingual bar ($p<0.01$) in SLS. 0 reinforcement samples more accurate on the rest compared with 1 bar samples and on right and left side of the joining area compared with 2 bar samples and 1 reinforcement samples more accurate on the center compared with 2 bar samples ($p<0.01$).
Wang 2019	N=30 rectangular specimens (hole-free, circular-hole, and rhombic-hole designs with (25×3×0.5 mm) Co-Cr alloy and Ceramic VITA VM13 fused layer (8 x 3×1.1 mm) to the center of the specimens	SLS (EOSINT M270; EOS GmbH, Munich, Germany)	None	3-points bending test and microscope evaluation.	Significant differences in bending energy observed between the rhombic-hole and the hole-free and circular-hole specimens ($p< 0.05$). Microscope evaluation: circular-hole and rhombic-hole specimens not printed perfectly.
Ye 2017	N=15 RPD framework Co-Cr alloy wirebond C+, BEGO	SLM (M270, EOS)	Casting technique	Fitness evaluation by visual inspection and measurements of the gap between occlusal rest and relevant rest seat	RPD fitting: 174 ± 117 µm. Average gap between occlusal rest and corresponding rest seat larger than casting frameworks ($p<0 .05$), but acceptable for clinical application.
			POLYMERS		
Alharbi 2016	n=18 crown (90, 120, 135, 150, 180, 210, 225, 240 and 270 building	SLA (DW028D, DWS)	None	Dimensional accuracy (root mean square estimate RMSE)	120-degree build angle had a minimal deviation for thin (0.029mm) and thick

	angles) hybrid composite resin material (Temporis DD-1000, DWS)				printing support (0.031mm) with an accurate fit.
Alharbi 2017	N= 40 crowns: knife-edge (KE), chamfer (C), rounded-shoulder (RS), rounded-shoulder with bevel (RSB) Hybrid composite resin material (Temporis, shade A2, LOT: 040725; DWS)	DLP	Milling: PMMA-based acrylate resin (Polycon ae; Straumann; shade A2)	Marginal fit using vertical (VG) and horizontal gap (HG), and absolute marginal discrepancy (AMD).	Internal fit: 110 ± 33 µm. Internal and marginal gaps influenced by fabrication method and finish-line design (p=0.000). AM samples had significant lower mean gap compared to milled samples at all points (p= 0.000).
Alsandi 2019	N=30 crown shape specimen (d=10mm inside, 15mm outside, h=10 mm) thermoplastic elastomers: Acrylonitrile-Butadiene-styrene (ABS), Poly lactic acid (PLA) and an acrylic block copolymer Kurarity (KUR) and a dental self-curing resin Unifast III A3 (PMMA)	FDM (Value 3D MagiX MF-1000)	None	Dimensional accuracy	No significant data reported.
Ashtiani 2018	N = 30 inlay and onlay Resin material WIC 300A envision (Envision TEC)	DLP CP group: conventional impression + 3D printing. IP group: digital impression + 3D printing.	Conventional: Resin material WIC 300A envision (Envision TEC)	Internal fit (silicone replica technique)	Marginal discrepancy: pulpal (p=0.025) and lingual (p=0.031) areas. Significantly lower in the lingual surface of IP group (p=0.031). Absolute discrepancy between groups CC and CP significantly different (p=0.020).
Bae 2016	N=20 inlay Co-Cr alloy (SP2, EOS, GmbH) for SLS and UV polymerizable polymer (VisiJet FTX Gree, 3D Systems Co) for SLA	SLS and SLA	Milling: wax block (D-max) and Zirconia block (D-max)	Accuracy evaluation (RMS formula).	SLA samples had the smallest difference from reference data and significant differences compared with wax (p=0.021) and zirconia (p=0.048). SLS samples deviation was significantly different from wax (p<0.001) and zirconia (p=0.001).
Choi 2019	N=30 specimen: 25 x 4 x 3 mm Dima Print Denture Base and Dima Print Denture Teeth (Kulzer, USA) Denture-based resins and commercial denture teeth	DLP (Cara Print 4.0, Kulzer, USA)	Milling and heat curing: denture-based resins and commercial denture teeth (Unfilled PMMA, double cross-linked PMMA, PMMA with nanofiller)	fracture toughness (K1C) and flexural strength, thermocycling for aging simulation (4-point bend test, using the chevron-notched beam method).	Flexural strength: decreased significantly with aging (p<0.01). Fracture toughness: Mean K1C had significant differences (p<0.01). Teeth bonded to 3D printed DBRs showed a mean fracture toughness significantly lower than that of teeth bonded to heat-cured and CAD/CAM.
Choi 2020	N=60 specimen: 25 x 4 x 3 mm PMMA (Polymethyl Methacrylate) Kulzer 3D Dima, Kulzer denture resin materials and two commercially available denture characterizing composites (SR Nexco paste and Kulzer Creactive gingiva)	DLP (Cara Print 4.0, Kulzer, USA)	Heat-curing: PMMA (Vertex Rapid Simplified, Vertex) and milling: PMMA (IvoCAD, Ivoclar Vivodent)	Fracture toughness K1C (MPa x m1/2) and flexural strength (MPa) with 4-point bend test using the chevron-notched beam method, thermocycling for aging simulation.	Flexural strength post ageing: 0.73 ± 0.23 and 0.1 ± 0.03 MPa; after 6 months ageing: 0.64 ± 0.2 and 0.17 ± 0.02 MPa; after 12 months ageing: 0.57 ± 0.18 and 0.44 ± 0.06 MPa. The mean K1C for K groups bonded to the 3 different denture bases were significantly lower compared to the SR group (p<0.001). Within K groups ageing

					showed significant mean K1C (p=0.002).
Deng 2018	n=5 maxillary complete denture polylactic acid (PLA)	FDM	3D printed wax patterns	Accuracy with silicone film thickness measurements, into 4 areas: primary stress-bearing, secondary stress-bearing, border seal, and relief areas (RMS formula)	PLA enlarged compared with the CAD data (0.016 ± 0.007 mm, RMS: 0.143±0.01 mm). Space between denture surface and plaster model for PLA: 0.277 ± 0.021mm. Values of secondary stress-bearing and relief areas were smaller than primary stress-bearing and the border seal areas. FDM is comparable to wax printer and satisfy accuracy requirements.
Herpel 2021	N= 40 removable complete denture VeroWhite Plus RGD 835 (Stratasys) for MJ; FREEPRINT denture (Detax), V-Print Try-In (VOCO) and DENTCA Denture Teeth (DENTCA) for DLP; UV-Sensitive Resin Basic (Anycubic 3D) for LCD-based SLA.	MJ, DLP, LCD-based SLA.	Milling	Trueness (RMS formula) and precision	Trueness: 154 ± 25, 142 ± 32, 145 ± 30, 82 ± 8 and 147 ± 32 µm. Trueness and precision (SD): AM less true (16–65 µm) and less precise (8–66 µm). Significant differences between the groups (p<0.001).
Hsu 2020	N=40 maxillary and mandibular denture base MiiCraft BV-005 printable resin (Young Optics Inc) and 20 from NextDent Base printable resin (NextDent BV)	DLP (MiiCraft 125; Young Optics Inc).	Milling (CCM), injection molded (IM), and compression molded (CM).	Denture base adaptation measuring thickness of silicone between denture base and model.	The 3DP had greater thickness than the IM and CM groups (p<0.05). In the mandible, 3DP recorded the lowest silicone thickness and trueness among all the groups.
Ishida 2016	Crowns PLA Blue M (X12052013-1PLA MLU) PLA (3D Systems (Rock Hill, USA)) for CX, B9-R-1-RED (021813) UV curing Acrylic resin (B9Creations (Rapid City, USA)) for B9, VisiJet DP200 (DP132502A) UV curing Acrylic resin (3D Systems (Rock Hill)) for PJ and RF080 (4120225), Wax resin (DWS s.r.l. (Vicenza, Italy)) for DW.	CX (CubeX Trio), DLP stereo-lithograph (B9Creator), laser stereo-lithograph (DW028D) and multi-jet modeling (Projet DP3000)	None	Dimensional accuracy and surface roughness	Significant differences for the type of printer, the enlargement ratio and the interaction between these factors for outer and inner diameter (p<0.01) and for expansion rate of depth and surface roughness (p<0.05)
Kalberer 2019	N=10 maxillary complete dentures monomer based on acrylic resin esters for fabricating denture bases (NextDent Denture 3+; Next- Dent B.V.)	Rapid prototyping	Milling: (AvaDent Digital Dental Solutions Europe, Global Dental Science Europe BV) from prepolymerized acrylic resin pucks.	Trueness: analyses were performed for the entire intaglio surface and specific regions: posterior crest, palatal vault, posterior palatal seal area, tuberosity, anterior ridge, vestibular flange, and mid-palatal raphae.	Trueness: 95.3 ±7.5 µm; after ageing: 76.6 ±7.2 and 83.0 ±7.9 µm. Milled prostheses had significantly better trueness than rapid prototyping for the entire intaglio surface (p<0.001) and anterior ridge (baseline: p<0.001; after immersion in saliva: p=0.001; after wet-dry cycle: p=0.011).
Kebler 2021	N = 360 specimen 2x2x25 mm^3 Nextdentc&b (Nextdent, Soesterberg, the Netherlands); 3Delta temp (Deltamed, Friedberg, Germany);	DLP	None	Flexural strength: 3-point bending test (FS), (crosshead speed 0,5mm/min) with 3 testing modalities ‘horizontal parallel’, ‘horizontal perpendicular’, and ‘vertical’. Before testing, two ageing procedures:	3Delta temp had the highest significant FS in aged and non-aged samples and significant lower values for FS in vertical compared to both horizontal directions (*p*<0.05). The parameter material had the highest influence on FS (*p*<0.001).

	Freeprint temp (Detax, Ettlingen, Germany)			a) 1-day storage in distilled water at 37°C; b) additionally followed by thermocycling between 5 (±2) and 55°C (±2) for 10,000 cycles, dwell time: 30 s; transfer time: 5 s.	
Kim 2016	N = 54 crowns UV polymerizing plastic cartridge resin (Visijet FTX Green; 3Dsystems):	μ-SLA	None	Marginal discrepancy: buccal, mesial marginal, lingual marginal and distal marginal: One array (OA) group Three arrays (TA) group Six arrays (SA) group	Marginal discrepancy: TA with best result (61.2 ± 37.3 μm), while SA with poorest result (92.5 ± 54.1 μm). All 3 groups showed significant differences by pairwise comparisons (p<0.001). The greatest discrepancy was in the buccal area for all groups.
Kim 2020a	Toronto all-on-4 Biocompatible photopolymer (Raydent C&B; Ray). the printed prosthesis were polymerized in 3 different ways: a) alone (P group), b) with support (PS group), c) on stone model (PM group)	SLA	None	Geometric accuracy and marginal and internal gap	PM group had the lowest mean discrepancy. The highest discrepancy was in occlusal area, especially in P group. PM group exhibited significantly smaller marginal gaps.
Kim 2020b	N= 21 crowns Photopolymer material (RAYDent C&B; Ray Co., Ltd., Hwaseong-si, Korea)	DLP	None	Accuracy (silicone replica method) and marginal and internal gaps	RMS values ranged from 41.00 to 126.60 μm, and the mean was 60.12 μm. Mean values of marginal, internal and total gaps: 132.96 ±139.23, 137.86 ± 103.09 and 135.68 ± 120.30 μm. Significant mean differences: marginal 132.96 μm and occlusal area 255.88 μm. Marginal gap of fabricated interim crowns based on CBCT STL data was within the acceptable clinical range.
Li 2020	Complete denture denture base material (FREEPRINT denture, Detax, Ettlingen, Germany).	DLP	None	Roughness evaluation (Sa) with profilometer, calculation of Sa parameter, SEM. groups: thermal cycling(5,000 thermal cycles at 5 °C - 55 °C, 70s per cycle) (aged) and without thermal cycling (non-aged). Subgroups: a) no surface treatment – control b) wetting with MMA + air-drying 120'' c)grounding with P600 silicon carbide abrasive paper d)125 μm aluminum oxide abrasive distance 10mm pressure 0.2MPa 10''	Roughness: for non-aged groups, Sa (4.13 ± 1.43 μm) was significantly higher (p < 0.05) as for aged group, samples displayed the roughest surfaces (7.15 ± 1.67 μm), with significantly higher mean Sa (p < 0.05).
Liu 2018	N =20 crowns polylactic acid	FDM and DLP	Milling and traditional handmade wax	internal adaption(3D analysis)	FDM: Axial: 0.1299 ± 0.0311 mm and Occlusal: 0.764 ± 0366 mm. DLP: Axial: 0.0373 ± 0.0126 mm and Occlusal: 0.808 ± 0245 mm. Occlusal gap of DLP did not satisfy the assumption of normality (*p*=0 .02). Marginal and axial gaps did not satisfy the assumption of equality of variance (*p*<0 .05).

Mahmood 2019	n=30 crowns polymermaterial (Castable V2, Formlabs, Somerville, MA, USA).	SLA	Conventional method (manual layering technique) and milling: wax blank (CAD/CAM wax blanks, YETI Dentalpro- dukte, Engen, Germany)	Fit checking measurement (impression replica method) in 11 points.	AM samples had smaller mean cement gaps compared to conventional or subtractive ($p \leq 0.001$) in the axial area, and to the milled ones ($p=0.002$) in the occlusal area. Among crowns with smaller gaps, AM copings had significantly smaller mean gaps compared to milled ones in the marginal and axial areas ($p \leq 0.001$).
Mai 2017	N= 12 crowns biocompatible photopolymer (VeroGlaze MED620; Stratasys)	PJ	Molding method: autopolymerizing acrylic resin (Alike; GC Europe) Milling: PMMA and methacrylic acid ester-based cross-linked resin blocks (Ceramill TEMP; Amann Girrbach)	Fitting evaluated in proximal, marginal, internal axial and occlusal regions (silicone-replica techniques)	RMS: 99 ± 19 µm. Absolute marginal discrepancy was smallest in PJ group at 99 ±19 mm.
Molinero-Mourelle 2018	n= 15 crowns Polyalactid acid (PLA)	FDM	FDM: PMMA samples	Marginal fit evaluation with a profile projector (Toupview Serial No. C1604280431) at 6 points.	PLA marginal fit of provisional restorations was clinically acceptable and the results were comparable to those observed with PMMA samples.
Muta 2020	N = 10 crowns PVA models for indirect resin composite (Gradia, GC, Tokyo, Japan)	FDM	Conventional method with self-curing : acrylic resin (Curegrace, Tokuyama Dental, Tokyo, Japan)	Dimensional accuracy and RMS differences of intaglio surface (3D digital analysis), internal crowns adaption (silicone-fitting test) and surface roughness.	RMS: 310 ± 50µm. Marginal discrepancy: within 100 µm. Surface roughness: 5.6 ± 0.72 and 3.25 ± 0.68 µm.
Oguz 2021	N = 11 complete dentures 3D printable resin (E- Denture; EnvisionTEC)	UV-light curing	Milling: prepolymerized PMMA blocks Compression molding: PMMA resin (Integra Heat Cure Acrylic; Birlesik Grup Dental, Ankara, Turkey) Injiection molding: PMMA resin (Ivobase Hybrid; Ivoclar Vivadent AG, Schaan, Liechtenstein)	Scanning with µ-CT and volumetric gap evaluation between denture base and cast using six region of interest for maxilla (anterior and posterior ridge crest, labial and buccal vestibule, palate, and posterior palatal seal) and 3 for mandible (intermolar, molar, and retromolar) in addition to overall gap measurements for edentulous arches.	Interactions between fabrication method and location had significant effects on mean volumetric gap measurements for both edentulous arches (p=0.0001). Significant differences detected among fabrication methods for locations and for overall volumetric gap measurements (p = 0.0001). The highest gap measurements were at palate in the maxilla.
Osman 2017	Crowns (building angles: 90-120-135-150-180-210-225-240-270) NextDent C&B resin	DLP (RapidShape D30)	None	dimentional accuracy using digital subtraction technique	The build angle influenced dimensional accuracy. The lowest RMSE was recorded for the 135-degree and 210-degree build angles. The overall deviation pattern was more favorable with the 135- in contrast with the 210-degree build angle.
Park 2016	N = 40 crowns and bridges PMMA (E-Dent; Envision TEC)	DLP	Milling: 4-axial milling machine, Pekkton milling blank (Pekkton Ivory; Cendres&Metaux) Conventional system: autoplymerizing PMMA resin (Jet; Lang Dental Mfg Co Inc)	Marginal and internal discrepancies with silicone replica method and digital microscope for internal space between abutment and interim restoration	Mean marginal discrepancy: 56.85 ± 22.24 µm. Fabrication method had significant effect on discrepancy at each measurement point ($p<0.001$). DLP was superior to the other fabrication methods but all methods were suitable and produced a marginal fit within the clinically acceptable range.

Peng 2019	N=16 crowns 3D-printed methacrylic oligomers (NextDent C&B MFH; NextDent by 3d system)	DLP	Milling: PMMA resin (ZCAD Temp Fix 98; Harvest Dental) Manually direct fabrication technique: Autoplymerized PMMA resin (Jet; Lang Dental	Silicone replica technique (non-cementation method) to determine internal discrepancy, microcomputed tomographic (μCT) scan assessment with 3D images and 2D images, marginal discrepancy measured (polyvinyl siloxane impression technique and stereomicroscope).	μCT 2D: 0.17 ± 0.04 mm. No significant effects reported.
Peng 2020	N = 12 crowns 3D printed methacrylic oligomers (NextDent C&B MFH; NextDent by 3D system, Soesterberg, Netherlands)	DLP	Milling: PMMA resin (ZCAD Temp Fix; Harvest Dental, Brea, CA) Manually fabrication technique: Bis-acrylic composite fabricated (Protemp Plus; 3M ESPE)	Internal fit evaluation (silicone replica technique and X-ray microcomputed tomography (μCT) technique), marginal discrepancy (vinyl polysiloxane (VPS) (Aquasil Ultra XLV) impression technique and optical coherence tomography (OCT) technique)	Silicone technique: 36.55 ± 4.22 mm^3; μCT 2D: 0.17 ± 0.04 mm; μCT 3D: 26.64 ± 3.07 mm^3. No significant effects reported.
Prechtel 2019	N= 16/group indirect inlays on extracted molars Essentium PEEK (ESS) (Essentium Inc., Pflugerville, USA), KetaSpire® PEEK MS-NT1 (KET) (Solvay Specialty Polymers USA, L.L.C., Alpharetta GA, USA), VESTAKEEP® i4 G (VES) (exp. material) (Evonik Industries AG, Essen, Germany) and VICTREX® PEEK 450G (VIC) (Victrex plc., Thornton Cleveleys, UK)	FLM (HTRD1.2, KUMOVIS, Munich, Germany)	Unprepared and unrestored teeth (positive control) and milling: JUVORA Dental Disc 2 (JUV) and direct resin composite fillings out of Tetric EvoCeram (TET).	Fracture load evaluation. N = 8/group treated in a chewing simulator combined with thermal cycling (1.2 million × 50 N; 12,000 × 5 °C/55 °C).	ESS had the lowest fracture load with a minimum of 956 N. Chewing simulation combined with thermal cycling did not cause any fractures. With respect to fracture types, differences between the groups were observed (p<0.001). All indirect restorations, regardless of the fatigue process, showed a significantly higher tooth fracture rate (75–100%) than TET. All 3Dprinted inlays remained intact after the fracture load test.
Prechtel 2020	N = 120 samples printed on horizontal or vertical directions Essentium PEEK (ESS) (Essentium Inc., Pflugerville, USA), KetaSpire PEEK MPS-NT1(KET) (Solvay Specialty Polymers USA, L.L.C., Alpharetta GA, USA), VICTREX PEEK 450G (VIC) (Victrex plc., Thornton Cleveleys, UK), VESTAKEEP i4 G (VES) (Evonik Industries AG, Essen, Germany)	FLM (HTRD1.1, KUMOVIS GmbH, Munich, Germany)	Milling: PEEK blanks from breCAM.BioHPP, Dentokeep, JUVORA Dental Disc 2 and Ultaire AKP	Martens hardness (HM) determined at baseline and longitudinally after thermocycling (5−55◦C, 10,000x) and autoclaving (134◦C, 2 bar).	Hardness: 185 ± 3.51, 179 ± 14.5 , 171 ± 33.2, 150 ± 17.8, 168 ± 10.4, 153 ± 19.1, 176 ± 20.0 and 102 ± 13.8 MPa. Material had the highest impact on HM followed by printing direction (p<0.001) and aging process (p=0.036). ESS showed the highest and VIC the lowest values initially and after thermocycling and autoclaving (p<0.001). VIC showed initially a comparable HM value with VES (p=0.290) and KET (p=0.104). KET and VES showed comparable HM values (p=0.403).
Prpić 2020	N = 10 rectangular specimen NextDent Base NDB = Monomer based on acrylic esters (Nextdent B.V.)	UV light curing (3DP)	Conventionally heat polymerized PMMA: ProBase Hot PBH (IvoclarVivadent AG), Paladon 65 PAL (Kulzer GmbH), Interacryl Hot IAH (Interdent d.o.o.) Injection molding: Polyamide Vertex ThersmoSens VTS = Polyamide (Vertex-Dental B.V.)	3-point flexural strength test (universal testing machine) and Brinell hardness	Flexural strength: 71.70 ± 7.38 MPa. 3D-printed samples had the lowest flexural strength. Hardness: 116.29 ± 6.28 MPa. The maximal and minimal surface hardness values were 123.19 and 106.0 MPa.

			Milling: IvoBase CAD IBC (IvoclarVivadent AG), Interdent CC disc PMMA IDP(Interdentd.o.), Polident CAD/CAM disc basic PDD (Polident d.o.o.)		
Reymus 2020	N= 60 fixed dental prosthesis (FDP) Experimental resin (EXP), NextDent C&B (CB), Freeprint temp (FT), and 3Delta temp (DT)	DLP (Rapidshape, GMBH)	Milling: PMMA, (TC) (TelioCAD, Ivoclar-Vivadent, Schaan, Liechtenstein) and conventional: interim material Luxatemp (LT).	Impact of 3D print material, build direction, post-curing, and artificial aging on fracture load	The highest values was for CB, DT and EXP showed the lowest values followed by FT ($p<0.001$). After artificial ageing there was a decrease in fracture load for EXP and DT ($p<0.001$). The highest impact on mechanical stability was exerted by material and post-curing unit ($\eta P2 = 0.233$), followed by material ($\eta P2 = 0.219$) and curing device ($\eta P2 = 0.108$) ($p < 0.001$).
Schönhoff 2021	N = 368 cubic (10x10x4 mm) and bar (2x3x15mm) specimens poluphenylene sulfone: Fil-A-Gehr PPSU Radel (Gehr) and Ultrason P 3010 NAT (BASF)	FFF	Extrusion technique: Radel R-5000 NT (Solvay) and PEEK Juvora (Juvora)	Flexural strength, baseline and after 5.000 and 10.000 TC (5°-55°C, 20s) with 3-point flexural strength in universal testing machine (crosshead speed of 1 mm/min) and martens hardness (HM) by pressing a Vickers diamond indenter (α=136°) with a max load of 9.807 N for 20’’ vertically. All specimens were tested longitudinally after aging by TC (5°-55°C, 20s) after 5000 TC, 10.000 TC, 10.000 TC + 36 days dry storage, and 20.000 TC.	Flexural strength: after 5000 TC the lowest values were for PPSU2-3D ($p<0.001$). In PPSU1-3D values at 10,000 TC were higher than initial flexural strength results ($p = 0.009$). Hardness: lowest for PPSU1-3D ($p < 0.001$).
Scotti 2020	3D-printed resin (PR) (NextDent C&B MFH; 3D Systems), autopolymerizing interim material (BA) (Protemp 4; 3M ESPE), and composite resin (Z350) (Filtek Z350XT; 3M ESPE)	SLA	None	Flexural strength (s) with 3-point bend test; Knoop hardness (H) and surface roughness (Ra) with a profilometer.	Z350 showed the highest values for s and H, followed by PR. BA showed the lowest results for both tests ($p<0.05$). Roughness: Z350 showed similar values to BA but lower than PR; PR showed similar roughness of BA.
Shim 2019	Bar specimen (80x10x4 mm) with 3 printing orientations (0, 45, and 90 degrees). PMMA NextDent Base; Vertex Dental)	SLA	None	Flexural strength and roughness	90° samples had the lowest error rates for length and 45° had higher error rates for thickness than other groups ($p<0.001$). Flexural strength increased in order 90°<45°<0° ($p<0.05$). The 45° samples had higher roughness ($p<0.001$).
Sim 2018	N = 8 crowns, bridges and inlay photoreactive liquid resin	DLP	None	Trueness	Trueness: 55.16 ± 2.70. Precision: 54.93 ± 8.44. 3D samples had the poorest accuracy with significant intergroup differences ($p<0.001$). Significant differences in trueness among model groups and types of preparation ($p<0.001$).
Tahayeri 2017	Samples bars (25 × 2 × 2 mm) commercial printable resin (NextDent C&B Vertex Dental) for provisional crowns and bridges.	SLA (FormLabs1+ printer)	Conventionally cured provisional materials (Integrity®, Dentsply; and Jet®, LangDental Inc.).	Accuracy (comparing width, length and thickness of samples for different printing orientation) and 3-point bending test.	Accuracy in relation to orientation: higher in thickness of 90° compared to 0° ($p<0.0001$) and 45° compared to 0° ($p < 0.001$) with 100 μm layer thickness.
Tasaka 2018	Denture base	UV light curing	Heat cured molding: heat-curing resin	Accuracy	The experimental denture base fabricated

	UV-curable acrylic resin (Vero Clear RGD835, Stratasys)		(Acron No.5, GC, Tokyo, Japan)		using AM was more accurate than the denture base fabricated with heat curing.
Tasaka 2021b	Maxillary and mandibular denture Ultravioletcured acrylic resin (UV)-cured acrylic resin (Vero Clear RGD835; Stratasys, Eden Prairie, MN, USA)	PJ (Objet260 Connex; Stratasys).	Heat curing	Accuracy	Significant displacement of artificial tooth between experimental maxillary denture AM compared to heat curing samples ($p<0.05$).
Wang 2021	N = 170 bar shape (18 x 6 x 2mm) samples PEEK (VESTAKEEP® i4G, Evonik Industries AG, Essen, Germany)	FFF	None	3-point bending test	Flexural strengths: maximal value obtained with 0.4 mm nozzle; 0.6 mm were the stiffest, with the least deformation, while samples with a 0.2 mm nozzle were flexible compared to others. The differences between the 3 groups were significant ($p<0.05$).
Wemken 2020	n=16 complete denture base Photopolymerizable resin (Denture Base LP, Formlabs)	SLA (Form 2, Formlabs)	injection moldin (IM) and milling (MIL) samples (Zenotec Select, Wieland Dental).	3D surface deviation of the total intaglio surface, the palate, the alveolar ridge, and the border seal region evaluated (RMSE) after 5000 hydrothermal cycles in water baths (5°-55°C, dwell time 30s each), and microwave sterilization in distilled water (6 cycles at 640 W for 6 min + 24h dry).	Trueness: SLA had the highest total RMSE of 96 ± 17 µm (+53/-84 µm) ($p \leq 0.001$), with increased negative deviations in the same region. Trueness after hydrothermal cycling: no differences between MIL and IM but measured for SLA (*p* =0 .001). Trueness after microwave sterilization: total RMSE and all regions of SLA were lower compared with MIL and IM (p =0.001). Solely SLA printed denture bases were dimensionally stable after microwave sterilization
Wemken 2021	N = 24 specimen 30 x10x1.5 mm Photopolymerizable resin containing aliphatic urethane dimethacrylate (V-print dentbase, VOCO, Cuxhaven, Germany)	DLP (SolFlex 170, VOCO, Cuxhaven, Germany)	Conventional (CB) and milling (SB)	4-point bending test, and fracture analysis performed after either pre-treatment by water storage (50h, 37°C), hydrothermal cycling (5000 cycles, 5°C and 55°C, 30s each), or microwave irradiation (6 cycles, 640W, 2min, wet)	Flexural strength post ageing: 94.0 ± 11.5, 78.8 ± 14.5 and 73.8 ± 15.0 MPa. Flexural strength: AB showed a resistance of 94.0 ± 11.5 MPa after water storage (comparable to CB). Strength of AB was reduced after hydrothermal cycling and microwave irradiation. AM leads to reduced flexural strength compared to pouring.
Wu 2021	N=16 crowns Dima print denture teeth (Kulzer North America South Bend, IN, Usa)	SLA	Milling (LuxaCrown, DMG, Hamburg, Germany) and manually manufactured (Lava Ultimate, 3M ESPE, St. Paul, MN, USA)	internal fit (silicone-checked method to measure internal gap) and marginal discrepancy (polyvinylsiloxane (PVS) replica method), optical coherence tomographic (OCT) scanning technique	Internal fit: 28.3 ± 9.3 axial, 101.9 ± 20.4 occlusal 108.7 ± 9.7 central pit. 3DP was significantly higher in gap distance at the occlusion than MAN and CAM ($p<0.05$). Marginal discrepancy: 120.8 ± 70.9 and 143.1 ± 39.9 µm. Considering absolute and horizontal marginal discrepancy, 3DP group had higher values than CAM and MAN ($p < 0.05$).

You 2020	N= 20 dentures (50µm and 100µm thickness) Resinliquid (ZMD-1000B; Dentis)	SLA	None	Trueness and accuracy evaluated with RMS formula.	Significant differences in trueness for intaglio and cameo surfaces ($p<0.05$). The cameo surface show a significant difference in precision ($p<0.001$). It is clinically more appropriate to set the layer thickness to 100 µm rather than 50 µm.

	Pubmed (12/05/2021)
Search	Query
#1	("additive manufacturing"[All Fields] OR "3D printing dentistry "[All Fields] OR "3D printing"[All Fields] OR (3D print* [title/abstract]) OR (additive manufact* [title/abstract]) OR "RP Technologies" [title/abstract] OR "Rapid Prototyping" [title/abstract] OR "three-dimensional printing" [title/abstract] OR "stereolithographic" [title/abstract] OR ("Printing, Three-Dimensional"[MeSH Terms]) OR ("Stereolithography"[MeSH Terms]) AND (("2011/05/05"[Date - Publication] : "2021/05/05"[Date - Publication]))) NOT (Systematic Review [Publication Type] OR Review [Publication Type] OR Meta-Analysis [Publication Type] OR Comment [Publication Type] OR Congress [Publication Type] OR Editorial [Publication Type] OR Case Reports [Publication Type] OR Clinical Conference [Publication Type] OR Comment [Publication Type] OR Consensus Development Conference [Publication Type])
#2	("Dental Prosthesis"[MeSH Terms] OR "Prosthodontics"[MeSH Terms] OR "Dentistry, Operative"[Mesh] OR "dental prosthesis"[All Fields] OR "crowns"[All Fields] OR "denture"[All Fields] OR "Prosthetic Dentistry"[All Fields] OR "Dental Materials"[Mesh] OR "Biomedical and Dental Materials"[Mesh] OR "Dental Materials"[All Fields] OR Dental Material* AND (("2011/05/05"[Date - Publication] : "2021/05/05"[Date - Publication]))) NOT (Systematic Review [Publication Type] OR Review [Publication Type] OR Meta-Analysis [Publication Type] OR Comment [Publication Type] OR Congress [Publication Type] OR Editorial [Publication Type] OR Case Reports [Publication Type] OR Clinical Conference [Publication Type] OR Comment [Publication Type] OR Consensus Development Conference [Publication Type])
#3	#1 AND #2 Filters: English, Italian